



TECHNISCHE UNIVERSITÄT MÜNCHEN

Fakultät für Medizin

# Exploring the pathogenic roles of enhanced c-REL function in cancer

**Eslam Katab (M.Sc.)**

Vollständiger Abdruck der von der Fakultät für Medizin der Technischen Universität München zur Erlangung des akademischen Grades eines

**Doktors der Naturwissenschaften (Dr. rer. nat.)**

genehmigten Dissertation.

**Vorsitz:** Prof. Dr. Percy A. Knolle

**Prüfer der Dissertation:**

1. Prof. Dr. Marc Schmidt-Supprian
2. Prof. Dr. Gabriele Multhoff

Die Dissertation wurde am 12.04.2022 bei der Technischen Universität München eingereicht und durch die Fakultät für Medizin am 07.06.2022 angenommen





*I dedicate this dissertation to  
my beloved wife, my parents, my brother, my sister  
and the whole family  
for their unconditional love and continuous support  
I genuinely love you and hope I can make you proud.*



## Table of Contents

<b>1</b>	<b>Summary</b> .....	<b>1</b>
<b>2</b>	<b>ZUSAMMENFASSUNG</b> .....	<b>2</b>
<b>3</b>	<b>Introduction</b> .....	<b>4</b>
	<b>3.1 Diffuse Large B-cell Lymphoma</b> .....	<b>4</b>
	3.1.1 Clinical diagnosis and classification.....	<b>4</b>
	3.1.2 Treatment.....	<b>5</b>
	<b>3.2 c-REL: a pivotal NF<math>\kappa</math>B subunit in DLBCL</b> .....	<b>6</b>
	3.2.1 Aberrant NF $\kappa$ B signaling in ABC DLBCL. ....	<b>8</b>
	3.2.2 c-REL gain and role in DLBCL.....	<b>9</b>
	3.2.3 c-REL role beyond lymphoma.....	<b>10</b>
	3.2.4 Post-translational modification of c-REL.....	<b>11</b>
	<b>3.3 Ubiquitination</b> .....	<b>12</b>
	3.3.1 The ubiquitin code.....	<b>13</b>
	3.3.2 Deubiquitinases (DUBs) .....	<b>14</b>
	3.3.3 OTU domain-containing protein 4 (OTUD4) .....	<b>15</b>
	<b>3.4 Aim of the study</b> .....	<b>17</b>
<b>4</b>	<b>Material</b> .....	<b>18</b>
	<b>4.1 Devices and Instruments</b> .....	<b>18</b>
	<b>4.2 Consumables</b> .....	<b>19</b>
	<b>4.3 Chemicals and reagents</b> .....	<b>19</b>
	<b>4.4 Commercial kits</b> .....	<b>21</b>
	<b>4.5 Enzymes</b> .....	<b>22</b>
	<b>4.6 Oligonucleotides</b> .....	<b>22</b>
	4.6.1 Cloning oligonucleotides.....	<b>22</b>
	4.6.2 Sequencing oligonucleotides.....	<b>24</b>
	4.6.3 shRNA sequence design and cloning.....	<b>25</b>
	4.6.4 Sequences of CRISPR sgRNA.....	<b>25</b>
	<b>4.7 Plasmids</b> .....	<b>26</b>
	<b>4.8 Bacteria</b> .....	<b>28</b>
	<b>4.9 Size-standards for DNA and proteins electrophoresis</b> .....	<b>28</b>
	<b>4.10 Primary antibodies</b> .....	<b>28</b>
	<b>4.11 Secondary antibodies</b> .....	<b>29</b>
	<b>4.12 Cell lines</b> .....	<b>29</b>



4.13 Cell culture media and supplements.....	30
4.14 Patient samples.....	30
4.15 Solutions and buffers.....	30
4.16 Software and databases.....	33
<b>5 Methods.....</b>	<b>34</b>
<b>5.1 Molecular cloning.....</b>	<b>34</b>
5.1.1 Polymerase Chain Reaction (PCR) .....	34
5.1.2 Agarose gel electrophoresis and gel purification.....	34
5.1.3 Restriction enzyme digestion and ligation.....	34
5.1.4 DNA mutagenesis.....	35
5.1.5 Bacterial transformation.....	35
5.1.6 Extraction of plasmid DNA from bacteria.....	35
5.1.7 Annealing of shRNA oligonucleotides.....	36
<b>5.2 Culture of eukaryotic cells and cell-based experiments.....</b>	<b>36</b>
5.2.1 Cell Culture.....	36
5.2.2 Freezing and thawing of cells.....	37
5.2.3 Harvesting cells.....	37
5.2.4 Plasmid DNA Transfection of cells.....	37
5.2.4.1 Calcium phosphate transfection.....	37
5.2.4.2 Transfection by Lipofectamine 2000.....	37
5.2.5 Production of lentiviral particles.....	38
5.2.6 Viral transduction of cells.....	38
5.2.7 Cycloheximide Chase assay.....	38
5.2.8 Flow cytometry .....	39
5.2.9 Fluorescence-activated cell sorting (FACS) .....	39
5.2.10 Immunofluorescence analysis.....	39
<b>5.3 Protein biochemistry.....</b>	<b>40</b>
5.3.1 Whole Cell Lysis and Protein Extraction.....	40
5.3.2 Cellular fractionation.....	40
5.3.3 SDS polyacrylamide gel electrophoresis (SDS-PAGE) .....	40
5.3.4 Silver staining.....	41
5.3.5 Protein Immunoblot (Western blotting) .....	41
5.3.6 Immunoprecipitation (IP) .....	42
5.3.7 Tandem Ubiquitin Binding Entities (TUBEs) Pull-down.....	42
5.3.8 In vivo ubiquitylation.....	43



5.4 Mass Spectrometry.....	43
5.4.1 Tandem Affinity purification for MS analysis.....	43
5.4.2 Ni-NTA Pull down of His-tagged Ubiquitome.....	44
5.4.3 Mass Spectrometric analysis.....	44
<b>6 Results .....</b>	<b>46</b>
<b>6.1 c-REL is post-translationally modified by ubiquitination.....</b>	<b>46</b>
6.1.1 MS-based approach to identify c-REL interactome.....	46
6.1.2 c-REL interaction with OTUD4.....	46
6.1.3 c-REL is ubiquitinated in DLBCL in the cytoplasm.....	49
<b>6.2 OTUD4 regulates c-REL ubiquitination and proteasomal degradation.....</b>	<b>50</b>
6.2.1 <i>OTUD4</i> downregulation enhances c-REL ubiquitination .....	50
6.2.2 <i>OTUD4</i> downregulation accelerates c-REL proteasomal degradation.....	52
6.2.3 OTUD4 deubiquitinates c-REL in the cytoplasm.....	53
6.2.4 OTUD4 catalytic activity is necessary for c-REL deubiquitination .....	55
<b>6.3 OTUD4 regulates nuclear levels of c-REL .....</b>	<b>55</b>
6.3.1 <i>OTUD4</i> downregulation destabilizes c-REL in DLBCL.....	55
6.3.2 <i>OTUD4 depletion diminishes c-REL nuclear localization in DLBCL....</i>	<i>57</i>
6.3.2 <i>OTUD4</i> downregulation decreases c-REL nuclear accumulation in PDAC.....	58
<b>6.4 OTUD4 negatively regulates NFκB in a DLBCL reporter cell line.....</b>	<b>59</b>
6.4.1 <i>OTUD4</i> downregulation enhances NFκB activity in DLBCL reporter cell line.....	59
<b>6.5 OTUD4 is essential for the expansion of cancer cells.....</b>	<b>61</b>
6.5.1 OTUD4 is critical for the competitive expansion of cancer cells.....	61
<b>6.6 OTUD4 as a prognostic marker.....</b>	<b>61</b>
6.6.1 OTUD4 expression correlates with c-REL in DLBCL.....	61
<b>7 Discussion .....</b>	<b>64</b>
7.1 c-REL is a target of the ubiquitin-proteasome system.....	64
7.2 c-REL-OTUD4 interaction.....	65
7.3 OTUD4-mediated stabilization and deubiquitination of c-REL.....	66



7.4	OTUD4-dependent regulation of c-REL nuclear localization.....	67
7.5	OTUD4 modulation of NFκB activity in DLBCL.....	68
7.6	The emerging role of OTUD4 in Cancer.....	69
7.7	Conclusion and outlook.....	71
8	Literature.....	72
9	List of figures and tables .....	80
11	Publications .....	81
12	Acknowledgement .....	82



## Abbreviations

°C	degree Celsius
AA	Amino acid
ABC	Activated B-cell-like
APS	Ammonium persulfate
ASCT	Autologous stem-cell transplantation
ATP	Adenosine 5'-triphosphate
BCR	B cell receptor
BES	N,N-Bis(2-hydroxyethyl)-2 aminoethanesulfonic acid
bp	Base pair
BrdU	5-Bromo-2'-deoxyuridine
C	Cytoplasmic
c-FLIP	Cellular FLICE inhibitor protein
C-terminal	Carboxy terminal
CAR	Chimeric antigen receptor
	Cyclophosphamide, doxorubicin, vincristine, and prednisone
CHOP	
CHX	Cycloheximide
ciAP	Cellular inhibitor of apoptosis protein
COO	Cell of origin
DEL	Double expresser lymphoma
DLBCL	Diffuse large B-cell lymphoma
DMEM	Dulbecco's Modified Eagle's Medium
DMSO	Dimethyl sulfoxide
DNA	deoxyribonucleic acid
dNTP	2'-desoxynukleosid-5'-triphosphat
DTT	dithiothreitol
DUB	Deubiquitinase
E. coli	Escherichia coli
EDTA	Ethylenediaminetetraacetic acid
EV	Empty vector
FACS	Fluorescence-activated cell sorting
FBS	Fetal bovine serum



FDA	Food and drug administration
FITC	Fluorescein isothiocyanate
Fw	Forward
G-2-P	Beta-Glycerolphosphate disodium salt hydrate
GCB	Germinal center B-cell-like
GFP	Green fluorescent protein
GSEA	gene set enrichment analysis
GST	glutathione S-transferase
HA	Hemagglutinin
HEPES	N-(2-Hydroxyethyl)piperazine-N`-2-ethane sulfonic acid
HGBCL- DH/TH	High-grade B-cell lymphoma known as a double or triple hit
His	Histidine
hr	Hour
HRP	Horseradish peroxidase
IHC	Immunohistochemistry
IκB	Inhibitor of κB
IKK	IκB kinase
IL	Interleukin
IMDM	Iscove's Modified Dulbecco's Media
IP	Immunoprecipitation
kilobase	Kb
LB	Luria-Bertani or Luria Broth
LE	Long exposure
LFQ	Label-free quantification
MEFs	Mouse embryonic fibroblasts
MINDYs	MIU-containing novel DUB family
MIU	Motif interacting with ubiquitin
mRNA	messenger RNA
MS	Mass spectrometry
N	Nuclear
N-terminal	Amino terminal
NaVa	Sodium orthovanadate (Na <sub>3</sub> VO <sub>4</sub> )
NES	Nuclear export sequence
NFκB	Nuclear factor kappa-light-chain-enhancer of activated B cells
NGS	Next-generation sequencing
NHL	Non-Hodgkin lymphoma
NIK	NFκB inducing kinase
NLS	Nuclear localization sequence
number	n
O-GlcNAcylation	O-linked β-N-acetyl-glucosamine
OTUD4	OTU domain-containing protein 4



OTUs	Ovarian tumor proteases
P/S	penicillin-streptomycin
PAGE	Polyacrylamide gel electrophoresis
PBS	Phosphate buffered saline
PDAC	Pancreatic ductal adenocarcinoma
PE	Phycoerythrin
PFA	Paraformaldehyde powder
PMBL	Primary mediastinal B-cell lymphoma
PMSF	phenylmethanesulfonylfluoride
PMSF	Phenylmethanesulfonylfluoride solution
PNK	Polynucleotide Kinase
PTM	Post-translational modifications
PVDF	Polyvinylidene fluoride
R-CHOP	Rituximab-CHOP
RBP	RNA binding protein
RE	Restriction endonuclease
RHD	Rel homology domain
RID	Rel inhibitory domain
RNA	ribonucleic acid
RPM	Revolution per minute
RPMI	Roswell Park Memorial Institute
Rv	Reverse
S.D.	Standard deviation
SDS	Dodecylsulfate-Na-salt
sgRNA	Single guide RNA
ShRNA	Short hairpin RNA
	Stable Isotope Labeling by/with Amino acids in Cell culture
SILAC	
SOC	Super optimal broth
TAD	Transcription activation domain
TAE	Tris-acetate-EDTA
	TNFR-associated factor family member-associated NFκB activator
TANK	
TBE	Tris-Borat-EDTA
TBK1	TANK-binding kinase 1
TLCK	Nα-Tosyl-L-lysine chloromethyl ketone hydrochloride
TLR	Toll-like receptor
TMED	N,N,N',N''-tetramethyl-ethylenediamine
TPCK	N-p-Tosyl-L-phenylalanine chloromethyl ketone
TRAIL	TNF-related apoptosis-inducing ligand
TRIS	tris(hydroxymethyl)aminomethane
TUBEs	Tandem Ubiquitin Binding Entities
Ub	Ubiquitin



UCHs	Ubiquitin C-terminal hydrolases
UPS	Ubiquitin-proteasome system
USPs	Ubiquitin-specific proteases
V	volt
W/V	Weight/Volume
WCE	Whole cell extract
WT	Wildtype
Y2H	Yeast two-hybrid



## 1 Summary

Multiple types of cancers show an aberrant, constitutive activation of the nuclear factor kappa-light-chain-enhancer of activated B cells (NF $\kappa$ B) signaling pathway. Within the family of NF $\kappa$ B transcription factors, c-REL plays a particularly important role in tumor development. Amplifications in the REL gene locus are frequently observed in human B-cell lymphomas, lymphoma cells express two alternatively spliced variants of the *REL* cDNA, and c-REL is able to transform lymphoid cells in vitro. c-REL expression and activation is regulated by transcriptional and post-translational mechanisms. Transcription-independent changes in the level of expression indicate an important role of post-translational mechanisms in the regulation of c-REL protein levels in B cells. Whether ubiquitination plays a role in the regulation of c-REL protein levels is not well studied.

This dissertation identifies c-REL as a substrate of the ubiquitin proteasome system (UPS) in B-cell lymphomas. Using mass spectrometry, the deubiquitinase (DUB) OTUD4 was identified as c-REL interacting protein. In vivo, c-REL deubiquitination occurred mainly in the cytoplasm and required an active catalytic site in OTUD4. Furthermore, biochemical and cell biological studies demonstrated the importance of OTUD4 for the stability and nuclear accumulation of c-REL. This OTUD4-mediated regulation of c-REL was conserved in diffuse large B-cell lymphoma (DLBCL) and pancreatic ductal adenocarcinoma (PDAC) cell lines. In addition, OTUD4 depletion impaired the expansion of DLBCL and PDAC cell lines. Finally, cytoplasmic OTUD4 and nuclear c-REL protein levels correlated in immunohistochemical studies of tumor tissue from DLBCL patients. Taken together, these results provide first evidence that a deubiquitinating enzyme can modulate NF $\kappa$ B activation in different tumor entities and identify OTUD4 as a possible new target in cancer therapy.

## 2 ZUSAMMENFASSUNG

Mehrere Krebsarten weisen eine aberrante, konstitutive Aktivierung des *nuclear factor 'kappa-light-chain-enhancer' of activated B-cells* (NF $\kappa$ B) Signalwegs auf. Innerhalb der Familie der NF $\kappa$ B Transkriptionsfaktoren ist c-REL für die Tumorentstehung von großer Bedeutung. In menschlichen B-Zell-Lymphomen werden häufig Amplifikationen im REL-Genlocus beobachtet, Lymphomzellen exprimieren zwei alternativ gespleißte Varianten der REL-cDNA und c-REL ist in der Lage, lymphoide Zellen in vitro zu transformieren. Die c-REL-Expression und -Aktivierung wird auf transkriptioneller und post-translationaler Ebene reguliert. Transkriptionsunabhängige Veränderungen im Expressionsniveau weisen auf eine bedeutende Rolle post-translationaler Mechanismen in der Regulation der c-REL Proteinmenge in B-Zellen hin.

Ob Ubiquitinierung eine Rolle in der Regulation der zellulären c-REL Level spielt, ist bislang kaum untersucht.

Diese Dissertation weist c-REL als Substrat des Ubiquitin-Proteasom-Systems (UPS) in B-Zell-Lymphomen nach. Mittels massenspektrometrischer Untersuchungen wurde OTUD4 als potentiell interagierende Deubiquitinase (DUB) von c-REL identifiziert. Die Deubiquitinierung von c-REL erfolgte in vivo hauptsächlich im Zytoplasma und setzte ein aktives katalytisches Zentrum in OTUD4 voraus. Mittels biochemischer und zellbiologischer Untersuchungen konnte die Bedeutung von OTUD4 für die Stabilität und nukleäre Akkumulation von c-REL aufgezeigt werden. Diese OTUD4-vermittelte Regulation von c-REL war in Zelllinien des diffus großzelligen B-Zell-Lymphoms (DLBCL) und des duktales Adenokarzinoms des Pankreas (PDAC) konserviert. Darüber hinaus beeinträchtigte die OTUD4-Depletion das Wachstum von DLBCL- und PDAC-Zelllinien. Schließlich korrelierten zytoplasmatische OTUD4- und nukleäre c-REL-Proteinmengen in immunhistochemischen Untersuchungen an Tumorgewebe aus DLBCL-Patienten. Zusammengefasst liefern diese Ergebnisse erste Hinweise darauf, dass ein deubiquitinierendes Enzym die NF $\kappa$ B-Aktivierung in verschiedenen Tumorentitäten



modulieren kann und identifizieren OTUD4 als möglichen neuen Angriffspunkt in der  
Krebstherapie

## 3 Introduction

### 3.1 Diffuse Large B-cell Lymphoma

Diffuse Large B-cell Lymphoma is the most aggressive subtype of Non-Hodgkin lymphoma (NHL). It accounts for 30 – 40 % of the newly diagnosed NHL patients. DLBCL is diagnosed at a median age of 65 years, with one-third of the patients older than 75 years (Sehn & Salles, 2021).

Although the causes of DLBCL are not well-known, epidemiological studies highlighted the complexity and multifactorial causality of the disease with potential risk factors entailing family history of NHL, genetic features, immune dysregulation, and environmental factors (Cerhan et al., 2014; Sehn & Salles, 2021).

#### 3.1.1 Clinical diagnosis and classification

The diagnosis of DLBCL is mainly dependent on the histological examination of an excised biopsy of a lymph node that shows diffuse proliferation of large malignant B-cells. These malignant cells stain positively for pan B-cell markers such as CD79a and CD20 (Liu & Barta, 2019; Sehn & Salles, 2021; Young et al., 2019). The advancement of genomic technologies revealed the complex heterogeneity of DLBCL that is thought of as biologically distinct tumor entities. Therefore, a more accurate classification of DLBCL based on the cell of origin (COO) or molecular features has been adopted (Liu & Barta, 2019; Susanibar-Adaniya & Barta, 2021; Young et al., 2019).

DLBCL is classified based on the COO into two dominant molecular groups: germinal center B-cell-like (GCB) and activated B-cell-like (ABC) (Fig. 1). The GCB type exhibits a signature of a germinal center B-cell characterized by elevated expression of both CD10 BCL6 and somatic hypermutations. Meanwhile, the ABC subtype resembles the expression profile of post-germinal or activated B cells reminiscent of constitutive activation of NF $\kappa$ B and the expression of BCL2 and IRF4. Ten to fifteen % of the cases don't fit into either group, hence called unclassified (Susanibar-Adaniya & Barta, 2021).

Genetic rearrangements of the proto-oncogene c-MYC and the anti-apoptotic BCL2 and or its transcriptional repressor BCL6 formed the basis of stratifying DLBCL patients relative to their molecular features. Eight to ten % of the de novo diagnoses

carrying MYC and BCL2 and/or BCL6 rearrangements had been recognized by WHO as a subset of high-grade B-cell lymphoma known as a double or triple hit (HGBCL-DH/TH). Immunohistochemistry (IHC) staining revealed that 30 % of DLBCL patients could have a double expresser lymphoma (DEL) characterized by simultaneous overexpression of both BCL2 and MYC. DEL patients showed a worse prognosis compared to patients with single or no overexpression of BCL2 and MYC (Jaffe et al., 2008; Sehn & Salles, 2021; Susanibar-Adaniya & Barta, 2021).

The use of next-generation sequencing (NGS) advanced technologies allowed Schmitz et al. to identify four prominent genetic subtypes of DLBCL: MCD, N1, BN2, and EZB subtypes (Fig. 1). By analyzing 574 pre-treatment DLBCL biopsy samples, the MCD subtype was defined by the co-occurrence of the CD79 and MYD88 (L265P) mutations, the N1 subtype by frequent NOTCH1 mutations, the BN2 subtype had NOTCH2 mutations and BCL6 fusions, and the EZB subtype showed EZH2 and BCL2 translocations. Both MCD and N1 correlated with the ABC type of DLBCL and had a poor prognosis (Schmitz et al., 2018; Sehn & Salles, 2021; Young et al., 2019).

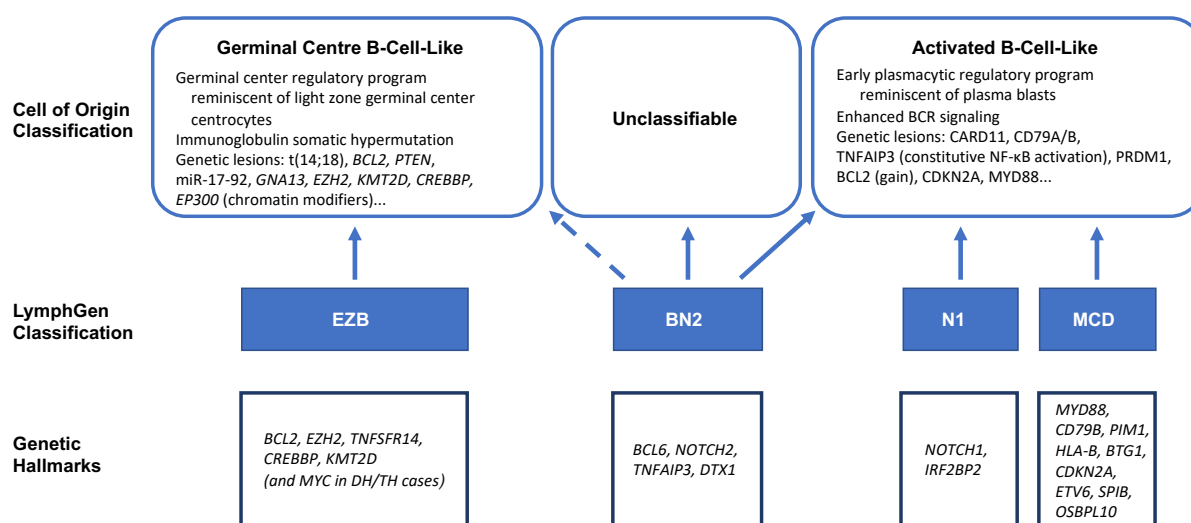


**Fig.1 Classification of DLBCL Subtypes.** A scheme of the different classification systems of DLBCL subtypes and the related genetic hallmarks of each subtype. Self-designed Figure adopted from (Sehn & Salles, 2021).

### 3.1.2 Treatment

Chemotherapy was the frontline therapy for DLBCL patients for more than 40 years. The patients were treated with eight cycles of the cyclophosphamide,



doxorubicin, vincristine, and prednisone (CHOP) regimen. Intensive CHOP-like regimens followed by autologous stem-cell transplantation (ASCT) enhanced the survival rate in high-risk patients. However, the increased toxicity limited the use of these therapeutic programs in elderly patients (Feugier et al., 2005; Sehn & Salles, 2021).

The immunotherapy era has revolutionized the treatment landscape of B-NHL, and chemoimmunotherapy has become the standard of care. The introduction of rituximab, a monoclonal CD20 targeting antibody, prolonged the survival in most NHL patients. However, up to 50% of those patients relapsed after complete remission or initial response to rituximab-CHOP (R-CHOP) (Crump et al., 2017; Feugier et al., 2005).

The increased resistance to the standard therapies created a need for innovative treatments. CD19 is a novel potential target that's homogeneously expressed on the surface of malignant cells in DLBCL patients. Its expression remains preserved even after anti-CD20 targeted therapy. There are several agents in clinical trials targeting CD19, such as the bispecific T-cell engagers blinatumomab and chimeric antigen receptor (CAR) T-cell products, including lisocaptogene maraleucel. The food and drug administration (FDA) approved using the anti-CD79b antibody-drug conjugate polatuzumab vedotin with bendamustine and rituximab (Pola-BR) and the combination of anti-CD19 monoclonal antibody tafasitamab and the immunomodulatory agent lenalidomide for relapsed or refractory disease (Abramson et al., 2020; Cheson et al., 2021; Sehn & Salles, 2021).

Research on tumor biology and genomics has improved the clinical management of lymphoma owing to the stratification of the patients based on their mutational landscape and molecular phenotype. This subclassification allowed the patients to benefit from the modern therapeutic drugs such as monoclonal antibodies and small molecule inhibitors. However, other promising agents as Obinutuzumab and bortezomib are failing Phase II/III trials because of the poorly understood underlying mechanisms. Hence, further mechanistic studies are still needed to better improve the patient's response to the newly emerging medications (Coccaro et al., 2020).



### 3.2 c-REL: a pivotal NF $\kappa$ B subunit in DLBCL

The nuclear factor  $\kappa$ -light-chain-enhancer of activated B cells (NF $\kappa$ B) represents a central modulator of the immune response. It was first identified as a protein found to bind conserved DNA sequences near the immunoglobulin (Ig)  $\kappa$  light-chain gene inside the nucleus of activated B cells, hence coined its name. Since its discovery 35 years ago, the role of NF $\kappa$ B in both innate and adaptive immunity was progressively established. (Hayden et al., 2006; Zhang et al., 2017).

NF $\kappa$ B stands for a universal transcription factor complex activated by a wide variety of stimuli, inducing the expression of a diverse set of genes in almost all mammalian cell types. Yet, the NF $\kappa$ B-induced gene expression is dependent on the specificity of the stimulus and the distinct cell type. Accordingly, NF $\kappa$ B activation has contributed to many biological processes, including cell activation, survival, and differentiation (Sen & Smale, 2010; Smale, 2011).

Mammalian NF $\kappa$ B is a family of five transcription factors: RELA(p65), RELB, c-REL, p50, and p52. The latter p50 and p52 are the proteolytic cleavage products of their precursors p105 and p100, respectively. All five members share an amino-terminal Rel homology domain (RHD) responsible for homo- and heterodimerization, DNA binding, and nuclear translocation. In addition to the RHD, c-REL, RELA, and RELB have a transcription activation domain (TAD) that positively regulates gene expression. The lack of TADs in p50 and p52 can result in transcriptional repression; therefore, they need to associate with either a TAD-containing NF $\kappa$ B member or a coactivator recruiting protein (Gilmore, 2006; Hayden & Ghosh, 2008).

In resting or unstimulated cells, NF $\kappa$ B dimers are inactive, sequestered in the cytoplasm in a complex with any of the inhibitor of  $\kappa$ B (I $\kappa$ B) proteins, including the precursors p100 and p105. Upon appropriate stimuli, NF $\kappa$ B activation can be subdivided into two distinct branches: The canonical or classical pathway triggers the activation of the I $\kappa$ B kinase (IKK) complex composed of IKK $\alpha$ , IKK $\beta$ , and the regulatory scaffold protein NEMO. The Activated IKK complex induces phosphorylation and subsequent K48 polyubiquitination of the I $\kappa$ B $\alpha$  inhibitory protein. Proteasomal degradation of I $\kappa$ B $\alpha$  leads to the release of the NF $\kappa$ B dimers,



mainly RELA:p50 and c-REL:p50, and their subsequent translocation into the nucleus activating target genes. In contrast, in the non-canonical or alternative NF $\kappa$ B pathway, the activated IKK $\alpha$  dimer together with NF $\kappa$ B inducing kinase (NIK) phosphorylates and promotes partial proteolysis of p100 to p52, which forms a heterodimer with RELB (Hayden et al., 2006; Hayden & Ghosh, 2008).

### 3.2.1 Aberrant NF $\kappa$ B signaling in ABC DLBCL

NF $\kappa$ B activation plays a fundamental role in immune homeostasis. It is essential for normal lymphocyte development, activation, and survival as a tightly regulated signaling pathway. NF $\kappa$ B regulates lymphocyte division by inducing the cell cycle regulators c-myc, cyclin D1, cyclin D2, and c-myb. It also induces survival factors such as the BCL2 family members A1 and BCL-XL, inhibitors of the cellular inhibitor of apoptosis protein (cIAP) family, and cellular FLICE inhibitor protein(c-FLIP). Furthermore, NF $\kappa$ B-induced proliferation and survival factors indirectly promote lymphocyte proliferation and survival, including IL-2, IL-6, or CD40L. Therefore, aberrant NF $\kappa$ B activity has been identified as a critical event in lymphoma pathogenesis (Jost & Ruland, 2007; Kennedy & Klein, 2018; Young et al., 2019).

NF $\kappa$ B's first connection to lymphoma oncogenesis arose from avian reticuloendotheliosis virus experiments. Those studies identified the viral homologue of the human c-REL (v-Rel) as a causative agent of aggressive lymphoma and leukemia in animals. NF $\kappa$ B's aberrant activation is detected in more than 80% of ABC-DLBCL patients. In this aggressive subtype, gene expression profiling revealed a distinct signature of many upregulated NF $\kappa$ B target genes such as cyclin D2, BCL2 family members, and c-FLIP. Unlike GC-DLBCL, constitutive IKK activation in ABC-DLBCL cell lines resulted in degrading I $\kappa$ B $\alpha$  rapidly and enhanced NF $\kappa$ B DNA binding activity (Jost & Ruland, 2007; Nagel et al., 2014).

Moreover, an unbiased RNA interference screen unraveled an upstream signaling complex mediating NF $\kappa$ B's constitutive activation in ABC-DLBCL. This complex comprises CARMA1, BCL10, and MALT1, for short CBM, conveying active signaling from the B cell receptor (BCR) to NF $\kappa$ B. Further mutations affecting the BCR signaling



regulators CD79A and CD79B as well as their downstream effectors, including SYK, BLNK, PLCG2, PRKCB and CARD11 were identified in ABC-DLBCL cases. Along with other mutations in TLR-MyD88 signaling pathways, these mutations resulted in a dysregulated activity of the NF $\kappa$ B pathway. Besides, TNFAIP3/A20, a negative regulator of signaling events upstream of the IKK complex, is frequently inactivated in NF $\kappa$ B driven-lymphomas, as in ABC-DLBCL by point mutation or silenced (Jost & Ruland, 2007; Nagel et al., 2014).

Sustained NF $\kappa$ B activation is essential for the survival of ABC DLBCL cells. Therefore, inhibition of NF $\kappa$ B signaling can have a therapeutic potential in treating NF $\kappa$ B-driven DLBCL. Targeting the upstream IKK complex with the small inhibitor molecules PS-1145 and MLX105 was selectively toxic for ABC-DLBCL cell lines but not GC-DLBCL cells. The NF $\kappa$ B pathway involves several kinases offering druggable targets with small-molecule inhibitors. The clinical use of ibrutinib, a selective and irreversible BTK inhibitor, demonstrated specific toxicity in ABC -DLBCL patients (Kennedy & Klein, 2018).

### **3.2.2 c-REL gain and role in DLBCL**

c-REL is a transcription factor and a fundamental member of the NF $\kappa$ B family. Human c-REL is encoded by the REL gene located on chromosome 2 and is composed of 587 amino acids. Like other NF $\kappa$ B members, c-REL shares a conserved RHD at the first 300 amino acids of its N-terminus. This RHD regulates many functions as inhibitor interaction, dimerization, nuclear localization, and DNA binding. In addition, c-REL carries a TAD at its C-terminus with two subdomains known as TAD1 and TAD2 anchored at the amino acid sequences 425-490 and 518-587, respectively. c-REL also has an inhibitory domain, referred to as the Rel inhibitory domain (RID), at the amino acid region 323-422. In vitro, mutants lacking the RID showed increased transactivation and DNA-binding capacity (Kober-Hasslacher & Schmidt-Supprian, 2019; Leeman et al., 2008).

Of the NF $\kappa$ B family members, c-REL is most directly connected to tumorigenesis. Human and mouse c-Rel's retroviral expression in vitro malignantly transformed chicken spleen cells. Additionally, the REL gene locus is frequently gained and amplified in human B cell lymphoma. Importantly, two alternative spliced variants of



the REL cDNA were found in human B cell lymphoma. The first variant encoded a protein (619 amino acids) longer than the wild type due to an exonized Alu sequence inserted between exons 8 and 9. The second lymphoma-specific identified transcript lacked exon 9 and consequently encoded a 564 amino acid protein. Both versions showed enhanced transactivation relative to the wild-type REL in vitro (Gilmore et al., 2001; Leeman & Gilmore, 2008).

Under physiological conditions, c-REL is ubiquitously expressed in the hematopoietic lineage. In B cells, c-REL protein levels increase throughout development, reaching its highest level in GC B cells. However, in a recent study, this increment in c-REL protein levels was not correlated with its *REL* mRNA, indicating that post-translational modifications may regulate c-REL. When ectopically expressed, c-REL blocked the differentiation of B cells into plasma cells due to inhibition of Blimp1 expression. c-Rel-deficient mice exhibited normal bone marrow development; however, several peripheral immune defects, including lower B cell numbers in the marginal zone, germinal center's impaired formation, and diminished proliferation and activation of mitogen-stimulated mature B cells. Moreover, siRNA-mediated c-REL inhibition significantly reduced cell survival and cell cycle progression in mouse B cell lymphoma cell lines. In contrast, in a conditional c-Rel overexpressing transgenic mouse strain, specific gain of c-Rel expression in B cells resulted in GC B cells' expansion and enhanced nuclear translocation of c-Rel. Complementing these findings, human GC-DLBCL patients showed an elevated c-REL expression level. These studies highlight the tight and dynamic transcriptional regulation of c-REL expression across B cell development (Köntgen et al., 1995; Kober-Hasslacher et al., 2020; Roy et al., 2019; Tian & Liou, 2009).

### **3.2.3 c-REL role beyond lymphoma**

c-REL is commonly associated with hematological malignancies; however, growing evidence suggests its contribution to the progression of solid tumors. In many breast cancers, the frequent amplification of the *IKKε* encoding gene, hence its increased activity, enhanced the nuclear accumulation of c-REL. Similarly, in transgenic mice, the overexpression of c-Rel in breast tissues under the control of mammary-specific promoter led to the development of breast tumors after approximately 20 months in one-third of the mice. Moreover, both amplification and



deletion of the *REL* gene have been reported in two patient cohorts, pinpointing a functional role of c-REL in breast cancer pathogenesis (Gilmore & Gerondakis, 2011; Hunter et al., 2016).

c-REL's involvement in lung cancer was suggested by the amplification of the *REL* gene in around 10% of metastatic lung carcinomas. Short hairpin (shRNA)-mediated inhibition of c-REL reduced the growth of lung cancer cell lines. In a lung adenocarcinoma mouse model, the activation of Ras concomitant with p53 loss resulted in a slight increase in c-REL's nuclear accumulation (Gilmore & Gerondakis, 2011; Meylan et al., 2009).

The role of c-REL in pancreatic ductal adenocarcinoma (PDAC) remains elusive. A recent study revealed c-REL as a critical mediator of TNF-related apoptosis-inducing ligand (TRAIL)-induced apoptosis in pancreatic cancer and identified NFATc2 as a target gene. In cell-based experiments, the reduction in c-REL levels correlated with a decrease in the pancreatic cancer stem cell growth upon combinatorial therapy. c-REL nuclear positivity was seen in other solid cancer, as in an endometrial cancer cohort, 50% of the cases showed positive nuclear staining for c-REL (Gilmore & Gerondakis, 2011; Hunter et al., 2016).

It is noticeable that implication of the *REL* gene locus is not restricted only to human B cell lymphoma, but also in autoimmunity. Single nucleotide polymorphisms (SNPs) within the *REL* gene locus were associated with several immunological autoimmune diseases including psoriasis, rheumatoid arthritis, celiac disease, and ulcerative colitis. Deregulation of the GC reaction was not only found in human B cell lymphomas, but also implicated in autoimmunity. Moreover, patients with certain immune diseases are at a higher risk of developing lymphoma later in their lives (Anderson et al., 2009; Kober-Hasslacher & Schmidt-Supprian, 2019; Vinuesa et al., 2009).

#### **3.2.4 Post-translational modification of c-REL**

Several post-translational modifications of c-REL have been elucidated. Previous studies showed that c-REL is phosphorylated within its TAD at the C-terminus. In vitro phosphorylation experiments, NF $\kappa$ B inducing kinase (NIK) or IKK $\epsilon$  and TNFR-associated factor family member-associated NF $\kappa$ B activator (TANK)-binding kinase 1 (TBK1) were proposed as potential kinases of c-REL leading



to its enhanced transactivation and nuclear accumulation, respectively. Besides impacting c-REL's transactivation, phosphorylation enhanced its lymphoid chicken cell's transforming capacity in vitro (Durand et al., 2018; Kober-Hasslacher & Schmidt-Supprian, 2019).

c-REL was first reported as a target of the ubiquitin-proteasome system in an in vitro biochemical study suggesting that c-REL degradation is wired to a C-terminal sequence between residues 118 and 171. Recently, Peli1 was described as an E3 ligase that regulates K48 ubiquitination of c-Rel in mouse T cells, hence its subsequent proteasomal degradation. Furthermore, Peli1 deficiency led to nuclear accumulation of c-Rel, suggesting a connection between c-Rel ubiquitination and its nuclear localization (Chang et al., 2011; Chen et al., 1998).

A recent study established that c-REL can be activated by glycosylation at Serine 305 via the addition of O-linked  $\beta$ -N-acetyl-glucosamine (O-GlcNAcylation). Lastly, the peptidyl-prolyl isomerase Pin1 was shown to associate with c-REL and enhance its mediated transformation of primary lymphocytes. Pin1 inhibition diminished c-REL nuclear localization in human lymphoma cell lines and profoundly affected lymphoma cells proliferation (Fan et al., 2009; Ramakrishnan et al., 2013).

### **3.3 Ubiquitination**

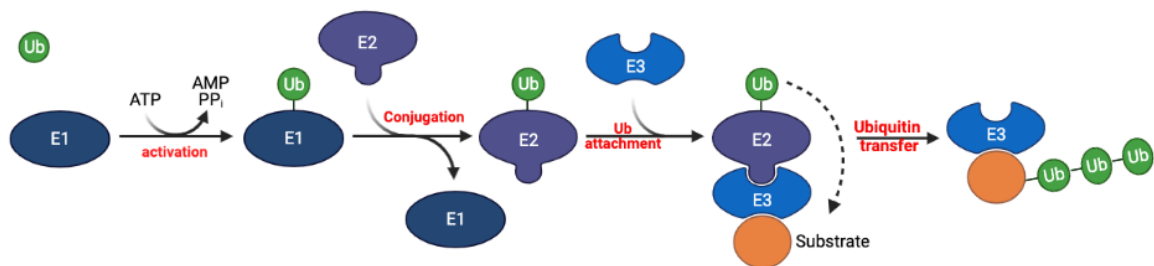
The human proteome shows a higher degree of complexity than the human genome. Although there are approximately 20000 to 25000 human coding genes, the total number of proteins in humans exceeds 1 million. This expansion and diversity of the human proteome are explained by two main mechanisms: mRNA splicing and post-translational modifications (PTMs).

PTMs involve the covalent attachment of a chemical group, sugar moiety, or a small protein to nascent or folded proteins' side chains or backbones. Such modifications influence protein's cellular localization and functionality, resulting in signal transduction and cellular activity regulation. PTMs include phosphorylation, glycosylation, nitrosylation, methylation, acetylation, lipidation, proteolysis, and ubiquitination (Leutert et al., 2021; Walsh et al., 2005).

### 3.3.1 The ubiquitin code

Ubiquitin is a highly conserved small protein composed of 76 amino acids. Ubiquitin's main features as a code are encrypted through its N-terminus and its seven lysine residues representing the attachment sites for chain assembly. The process by which ubiquitin is attached via its C-terminus to its substrate protein is called ubiquitination.

Ubiquitination is a crucial post-translational process that impacts the fate of the substrate protein. It is a multifaceted sequential process that requires the action of three different enzymes: E1 ubiquitin-activating enzyme, E2 ubiquitin-conjugating enzyme, and E3 ubiquitin ligating enzyme. Ubiquitination starts with activating the C-terminal glycine of ubiquitin in an ATP-dependent manner by an activating E1 enzyme. The activated ubiquitin is consequently transferred into an active cysteine residue of the conjugating E2 enzyme. Lastly, as depicted in Figure 2, the E3 enzyme ligates ubiquitin to a lysine residue of its substrate through an isopeptide bond (Akutsu et al., 2016; Hershko & Ciechanover, 1998).



Created in BioRender.com

**Fig. 2 The enzymatic process of ubiquitination.** Ubiquitination is a three-step enzymatic mediated process. The first step requires ATP-dependent activation of ubiquitin by an E1 ubiquitin-activating enzyme. In step two, the activated ubiquitin is transferred to the catalytic cysteine site of the E2 conjugating enzyme. The final step involves the attachment of the ubiquitin molecule to its corresponding substrate by the E3 ubiquitin ligase enzyme. The Figure was created on the BioRender.com website.



Proteins can be either monoubiquitinated when modified with a single molecule of ubiquitin or polyubiquitinated when ubiquitin polymers are introduced. In the latter case, the ubiquitin chain is formed by conjugating ubiquitin moieties through one of their lysine residues (K6, K11, K27, K29, K33, K48, K63) or the N-terminal methionine (M1). The topology of ubiquitin chains and other factors such as the timing and reversibility of the reaction affect the ubiquitination function.

Initially, the ubiquitin system was thought of as a tool that works along with the proteasome to degrade proteins. However, this view has been dramatically changed in the last decade due to the explosion of data on the complexity and fine-tuning regulation of the ubiquitin system. Ubiquitination has been described to control many cellular processes such as apoptosis, signal transduction, cell cycle regulation, DNA damage response, and immunity based on the linkage type. K48 ubiquitination constitutes the most predominant linkage type in cells. It accounts for more than 50% of all ubiquitin linkages and is responsible for the proteasomal degradation of its targeted protein. In contrast, K63-linked chains rank the second most abundant chain type and are involved in subcellular signaling and non-degradative functions (Komander & Rape, 2012; Swatek & Komander, 2016).

### **3.3.2 Deubiquitinases (DUBs)**

Ubiquitination is a precisely tunable PTM process. It is well controlled by the action of deubiquitinases (DUBs). DUBs are ubiquitin-specific proteases that prevent the ubiquitin signals from remaining constitutively on. The removal of ubiquitin from target proteins or the disassembly of polymeric ubiquitin chains by DUBs is an essential step in maintaining ubiquitin homeostasis in cells (Komander et al., 2009).

The number of DUBs discovered across different organisms varies widely, with its highest value in humans (~100 DUBs). The majority of human DUBs are cysteine proteases, and they belong to five distinct families: the ovarian tumor proteases (OTUs; 16 members), the ubiquitin-specific proteases (USPs; 54 members), the Josephin family (4 members), the ubiquitin C-terminal hydrolases (UCHs; 4 members) and the lately identified motif interacting with ubiquitin (MIU)-containing novel DUB family [MINDYs; 4 members]. Besides, human DUBs include one more Zn-dependent metalloprotease family called JAB1/MPN/MOV34 (JAMMs, also



known as MPN+; 16 members) DUBs (Clague et al., 2013; Mevissen & Komander, 2017).

DUBs exert their function through an active site (S1) within their catalytic domain, which recognizes the modified protein. They work either by directly binding the target protein and stripping the attached ubiquitin or identifying the ubiquitin chain itself and cleaving it. Moreover, some DUBs work indirectly on substrates recruited by macromolecular machines as the proteasome for deubiquitination. Herein, the DUB acts as a component of the molecular complex and does not select for its substrate (Komander et al., 2009; Mevissen & Komander, 2017).

The linkage specificity of the DUBs is defined by the existence of an extra S1' site within their catalytic domain. This S1' site binds proximal ubiquitin allowing only one linkage point of the distal ubiquitin to settle in the active site. Therefore, DUBs without S1' have no specificity, as seen in most members of the USP family. While many members of the OTU, JAMM, Josephin and MINDY family have an S1' site, consequently, exhibit a linkage specificity (Mevissen & Komander, 2017).

DUBs cleavage activity exists mainly in two forms: endo or exo-activities. DUBs with endo-cleavage activity remove ubiquitin from their substrate leaving behind an unanchored chain that generates monoubiquitin upon further processing. On the other side, the exo-cleavage acts on a polyubiquitin chain, facilitating the production of monoubiquitin through multiple cutting (Mevissen & Komander, 2017).

Like other components of the ubiquitin system, a variety of regulatory mechanisms tightly control DUBs. These mechanisms entail (a) regulation of DUBs' abundance by transcription, translation, and degradation, (b) subcellular localization of the DUB, and (c) regulating DUB's catalytic activity via PTM such as phosphorylation and ubiquitination and allosteric modulation. Since DUBs are involved in several biological processes, their deregulation has been linked to different diseases, including cancer, neurodegenerative and inflammatory diseases (Mevissen & Komander, 2017).

### **3.3.3 OTU domain-containing protein 4 (OTUD4)**

OTU domain-containing protein 4 (OTUD4) is a member of the subfamily OTU deubiquitinases. It has four different alternatively spliced isoforms, the longest of which is 1114 amino acids. The current understanding of OTUD4s' physiological



functions is limited. However, in the last few years, diverse functional roles of OTUD4 were deciphered. OTUD4 was initially shown to regulate the dorsoventral patterning in zebrafish (Tse et al., 2013).

By acting as a scaffold for USP7 and USP9X, OTUD4 was described as a positive regulator of alkylation damage response. It was found to stabilize ALKBH2 and ALKBH3 DNA demethylases, which are both critical for alkylation repair. This K48-mediated stabilization was however independent of its catalytic activity (Zhao et al., 2015).

As discussed earlier, phosphorylation is a PTM that can alter the catalytic function of DUBs. A new study demonstrated that phosphorylation of OTUD4 near its catalytic domain activated a K63 deubiquitinating specificity. This study revealed that OTUD4 negatively regulates NF $\kappa$ B by K63 deubiquitinating the Toll-like receptor (TLR)-associated factor MyD88. In addition, this work highlighted that OTUD4's catalytic activity was indispensable for its K63 specificity (Zhao et al., 2018).

OTUD4's role in innate immunity was further consolidated in the context of antiviral signaling.

A recent study unraveled that viral infection resulted in the upregulation of OTUD4 in an IRF3/7 dependent manner. Upregulated OTUD4 was discovered to stabilize MAVS by removing the K48-linked polyubiquitin chains, hence inducing an antiviral response (Liuyu et al., 2019).

In addition to its functions as deubiquitinase, OTUD4 was recently characterized as a RNA binding protein (RBP) with a suggested role in translational regulation. Das et al. showed that OTUD4 is a component of neuronal RNA granules under physiological conditions, while cellular stress induces its recruitment into cytoplasmic stress granules (Das et al., 2019).

In this thesis, I describe a new regulatory role of OTUD4 in NF $\kappa$ B signaling that is linked to its deubiquitinase activity. Moreover, I uncovered OTUD4 as a new vulnerability in DLBCL and PDAC tumor cell lines.



### 3.4 Aim of the study

In the c-Rel overexpression transgenic mouse model, GC B cells showed the highest accumulation of c-Rel protein levels compared to naïve B cells. However, c-Rel mRNA levels are lower in GC B cells compared to naïve B cells, suggesting a post-transcriptional regulation of c-Rel in B cells (Kober-Hasslacher et al., 2020).

This research project aimed to study the ubiquitin-related post-translational regulation of c-REL in the context of B cell lymphoma. For that purpose, an interactome mass spectrometric screen was performed to identify the ubiquitin modifying E3 ligases and DUB candidates. Having identified OTUD4 as a promising candidate, immunoprecipitation experiments validated its interaction with c-REL. The molecular mechanism by which OTUD4 regulates the stabilization and nuclear localization of c-REL in DLBCL and PDAC cells was deciphered using biochemical, and cell biology approaches. OTUD4's biological relevance in both DLBCL and PDAC cell lines was determined by shRNA-mediated knock-down experiments highlighting its importance for the competitive expansion of these cancer cells. Finally, the correlation between OTUD4 and c-REL was further investigated in primary patient samples.



## 4 Materials

### 4.1 Devices and Instruments

Device	Manufacturer
Analytic balance ABJ 220	Kern & Son
Aqualine water bath	Lauda-Brinkmann
Axiovert 40 CFL with HBO50	Carl Zeiss
Centrifuge 5417R with rotor F453011	Eppendorf
Centrifuge 5424 with rotor FA452411	Eppendorf
CytoFLEX LX Flow Cytometer	Beckman Coulter
E-Box VX2 Imager	Vilber
FACS Aria III	BD Biosciences
Fridges and lab freezers	Liebherr
Fusion-FX6.EDGE V.070	Vilber
HERAcell 150i CO <sub>2</sub> incubator	Thermo Fisher Scientific
HERAfreeze	Thermo Fisher Scientific
HERASafe KS safety cabinet	Thermo Fisher Scientific
Innova® 40 shaker for bacteria	New Brunswick Scientific
IX Inverted Fluorescence Microscope	Olympus
Invitrogen Chamber for Ready Gels	Invitrogen
LightCycler 480 System	Roche
LS4800 liquid nitrogen tank	Taylor-Wharton Lab Systems
LTQ Orbitrap Velos mass spectrometer	Thermo Fisher Scientific
Magnetic thermo stirrer RCT basic	IKA Laboratory Equipment
Mastercycler nexus	Eppendorf
Mini-PROTEAN Tetra cell SDS electrophoresis system	Bio-Rad Laboratories
Mini-Sub® Cell GT system for agarose electrophoresis	Bio-Rad Laboratories
MiSeq system	Illumina
Multifuge 3SR+	Thermo Fisher Scientific
NanoPhotometer	Implen
Neubauer chamber	Marienfeld
Novex Mini cell system for precast NuPAGE gels	Thermo Fisher Scientific
peqSTAR Thermocycler	Peqlab Biotechnology
Pipetman neo (P2N, P10N, P20N, P100N, P200N and P1000N)	Gilson
Polymax 1040 platform shaker	Heidolph Instruments
PowerPac Basic power supply	Bio-Rad Laboratories
PowerPac HC power supply	Bio-Rad Laboratories
Precision balance 572-37	Kern & Son
Scanner V750 Pro	Epson
SevenCompact pH/Ion pH-meter	Mettler-Toledo
Sorvall® RC-5B with rotors SS-24 and GS-3	Du Pont Instruments
SRX-101A developer	Konica-Minolta
Thermo block MBT250	Kleinfeld Labortechnik
Thermomixer compact	Eppendorf
Tube rotator	Fröbel Labortechnik



Tumbling roller mixer RM5	Neolab
---------------------------	--------

## 4.2 Consumables

Consumable	Manufacturer
3mm CHR paper (Whatman)	GE Healthcare
Cell culture flasks	Greiner Bio-One
Cell culture plates	Biochrom/Falcon
Cell scraper	Sarstedt
Clear qPCR sealers	Steinbrenner Laborsysteme
CL-XPosure™ Films	Thermo Fisher Scientific
Cryo tubes	Sarstedt
Eppendorf twin.tec PCR plates, semi-skirted, 96 well	Eppendorf
Graduated tubes	Greiner Bio-One
Hypodermic needles	Braun
Immobilon-P PVDF transfer membrane	Millipore
LightCycler 480 Multiwell Plate 96, white	Roche
LS columns	Miltenyi Biotec
Pipette tips	Sarstedt
SafeSeal tubes	Sarstedt
Serological pipettes	Greiner Bio-One
Syringe filters	TPP/Biochrom
Syringes	Braun
UVette routine pack	Eppendorf
x-well chamber slides on PCA detachable	Sarstedt

## 4.3 Chemicals and reagents

Chemical/reagent	Manufacturer
2-Mercaptoethanol	Sigma-Aldrich
2-Propanol	Carl Roth
3x FLAG Peptide	Sigma-Aldrich
5-Bromo-2'-deoxyuridine (BrdU)	Sigma-Aldrich
Acetic acid glacial	Carl Roth
Acetone	Carl Roth
Adenosine 5'-triphosphate (ATP)	Sigma-Aldrich
Agarose NEEO	Carl Roth
Albumin Fraction V (BSA)	Carl Roth
Ammonium persulfate (APS)	Sigma-Aldrich
Ampicillin sodium salt	Sigma-Aldrich
Anti-FLAG M2 Affinity Gel	Sigma-Aldrich
Anti-HA-Agarose	Sigma-Aldrich
Aprotinin from bovine lung	Sigma-Aldrich
Aqua ad injectabilia, sterile	B. Braun Melsungen
Bacto Agar	BD Diagnostics
Bacto Tryptone	BD Diagnostics
Bacto Yeast Extract	BD Diagnostics
BES buffered saline	Sigma-Aldrich
Beta-Glycerolphosphate disodium salt hydrate (G-2-P)	Sigma-Aldrich
Biotin	Sigma-Aldrich



Blasticidin S HCl	Thermo Fisher Scientific
Boric acid	Sigma-Aldrich
Brilliant Blue R 250	Carl Roth
Bromphenol Blue	Sigma-Aldrich
Calcium chloride dihydrate	Sigma-Aldrich.
Cycloheximide (CHX)	Sigma-Aldrich
Deoxycholic acid sodium salt	Sigma-Aldrich
Dimethyl sulfoxide (DMSO)	Carl Roth
Di-Sodium hydrogen phosphate dihydrate	Merck
DL-Dithiothreitol	Sigma-Aldrich
DNA Loading Dye (6x)	Thermo Fisher Scientific
dNTP Mix, 10 mM each	Thermo Fisher Scientific
Dodecylsulfate-Na-salt (in pellets, SDS))	SERVA
Ethanol	Merck
Ethylenediaminetetraacetic acid (EDTA)	Sigma-Aldrich
FACS Flow	BD Biosciences
GelRed Nucleic Acid Gel Stain	Biotium
Glucose	Sigma-Aldrich
Glutathione Sepharose 4B	GE Healthcare
Glycerol	Sigma-Aldrich
Glycin	Carl Roth
Hexadimethrine bromide (polybrene)	Sigma-Aldrich
Hexanucleotide Mix, 10x conc.	Roche
Hydrochloric acid 32%	Carl Roth
Hydrochloric acid fuming 37%	Carl Roth
Imidazole	Sigma-Aldrich
Kanamycin sulfate	Sigma-Aldrich
Leupeptin	Sigma-Aldrich
L-Glutathione reduced	Sigma-Aldrich
Lipofectamine 2000 Reagent	Thermo Fischer Scientific
LightCycler 480 SYBR Green I Master	Roche
Magnesium chloride anhydrous	Sigma-Aldrich
Magnesium sulfate anhydrous	Sigma-Aldrich
Methanol	J. T. Baker
MG132	Tocris
N-(2-Hydroxyethyl)piperazine-N`-2-ethane sulfonic acid (HEPES)	SERVA
N $\alpha$ -Tosyl-L-lysine chloromethyl ketone hydrochloride (TLCK)	Sigma-Aldrich
Ni-NTA Agarose	Qiagen
N,N,N',N``-tetramethyl-ethylenediamine (TMED)	Sigma-Aldrich
N-p-Tosyl-L-phenylalanine chloromethyl ketone (TPCK)	Sigma-Aldrich
Nonidet P-40 substitute (10%)	Roche
NuPAGE MES SDS Running buffer (20x)	Thermo Fisher Scientific
Okadaic Acid <i>Prorocentrum sp.</i>	Calbiochem
Paraformaldehyde powder (PFA)	Sigma-Aldrich
PBS Dulbecco, powder	Biochrom
Phenylmethanesulfonylfluoride solution (PMSF)	Sigma-Aldrich
Ponceau S solution	Sigma-Aldrich
Potassium chloride	Sigma-Aldrich
Protein A Sepharose CL-4B	GE Healthcare



Protein G Agarose, Fast Flow	Sigma-Aldrich
Protein G Sepharose 4 Fast Flow	GE Healthcare
Puromycin	Thermo Fisher Scientific
RNaseOUT Recombinant Ribonuclease Inhibitor	Thermo Fisher Scientific
Rotiphorese NF-Acrylamide/Bis-solution 40% (29:1)	Carl Roth
SERVA DNA Stain Clear G	SERVA Electrophoresis
Silver nitrate	Sigma-Aldrich
Skim Milk Powder	Sigma-Aldrich
SlowFade Gold antifade Reagent with DAPI	Thermo Fisher Scientific
SOC Medium	New England Biolabs
Sodium acetate	Merck
Sodium azide	Merck
Sodium carbonate	Merck
Sodium chloride	Carl Roth
Sodium dihydrogen phosphate monohydrate	Merck
Sodium fluoride	Sigma-Aldrich
Sodium hydroxide solution 45%	Carl Roth
Sodium orthovanadate	Sigma-Aldrich
Sodium phosphate dibasic	Sigma-Aldrich
Sodium tetraborate	Sigma-Aldrich
Sodium thiosulfate pentahydrate	Sigma-Aldrich
Strep-Tactin Superflow	IBA Lifesciences
SuperSignal West Pico Chemiluminescent Substrate	Thermo Fisher Scientific
SuperSignal West Femto Maximum Sensitivity Substrate	Thermo Fisher Scientific
Thymidine	Sigma-Aldrich
Trichloroacetic acid solution	Sigma-Aldrich
TRIS	Carl Roth
Triton X-100	Sigma-Aldrich
Trypsin inhibitor from soybean	Sigma-Aldrich
Tween 20	Sigma-Aldrich
UltraPure TBE buffer (10x)	Thermo Fisher Scientific
Water	Sigma-Aldrich

#### 4.4 Commercial kits

Kit	Manufacturer
DC Protein Assay	Bio-Rad
DNeasy Blood and Tissue Kit	Qiagen
GeneJET Gel Extraction Kit	Thermo Fisher Scientific
NucleoBond Xtra Midi	MACHEREY-NAGEL
NE-PER™ Nuclear and Cytoplasmic Extraction Reagents	Thermo Fisher Scientific
peqGOLD Plasmid Miniprep Kit	Peqlab
QIAquick PCR Purification Kit	Qiagen
QIAshredder	Qiagen
Rapid DNA Dephos & Ligation Kit	Roche
RNeasy Mini Kit	Qiagen



## 4.5 Enzymes

Enzyme	Manufacturer
AgeI (BshTI)	Thermo Fisher Scientific
BamHI	Thermo Fisher. Scientific
BsmBI	New England Biolabs
Bsu15I (ClaI)	Thermo Fisher. Scientific
Cfr9I (XmaI)	Thermo Fisher. Scientific
DNase I	New England Biolabs
DpnI	Thermo Fisher Scientific
Eco105I (SnaBI)	Thermo Fisher. Scientific
EcoRI	Thermo Fisher Scientific
HindIII	Thermo Fisher Scientific
Lambda Protein Phosphatase	New England Biolabs
NheI	Thermo Fisher Scientific
NotI	Thermo Fisher Scientific
Pfu Ultra II DNA Polymerase	Agilent Technologies
Sall	Thermo Fisher Scientific
SgsI (AscI)	Thermo Fisher Scientific
T4 DNA Ligase	Thermo Fisher Scientific
T4 Polynucleotide Kinase	New England Biolabs
XbaI	Thermo Fisher Scientific
XhoI	Thermo Fisher Scientific

## 4.6 Oligonucleotides

All oligonucleotides were purchased from Eurofins Genomics, Ebersberg, Germany.

### 4.6.1 Cloning oligonucleotides

Oligonucleotide	Sequence (5'-3')
OTUD4	CGG AAG CTT GCC ACC ATG GCC TGT ATT CAC TAT
Iso#3_HindIII_KZ_Fw	CTT CG
OTUD4_XhoI_RV	CGG CTC GAG TCA AGT GTG CTG TCC CCT ATG G
OTUD4 Iso#3_AgeI_FW	CGG ACC GGT ATG GAG GCT GCC GTC GGC
OTUD4_SnaBI_RV	CGG TAC GTA TCA AGT GTG CTG TCC CCT ATG
OTUD4 Iso#3_XmaI_FW	CGG CCC GGG ATG GCC TGT ATT CAC TAT C
OTUD4_BamHI_RV	CGG GGA TCC TCA AGT GTG CTG TCC CCT ATG
OTUD4 Iso#3_BamHI_FW	CGG GGA TCC ATG GCC TGT ATT CAC TAT C
OTUD4_ClaI_RV	CGG ATC GAT TCA AGT GTG CTG TCC CCT ATG
OTUD4_XhoI_RV	CGG CTC GAG TCA AGT GTG CTG TCC CCT ATG
OTUD4 Iso#3_XhoI_FW	CGG CTC GAG ATG GCC TGT ATT CAC TAT C



OTUD4 XhoI_Rv_c-Flag	CGG CTC GAG TCA CTT GTC GTC ATC GTC TTT GTA GTC AGT GTG CTG TCC CCT ATG
OTUD4 Iso#3_ AscI_ FW	GGC CCG CGC GGG ATG GCC TGT ATT CAC TAT CTT
OTUD4 NotI_RV	GCG GCC GC TCA AGT GTG CTG TCC CCT ATG
OTUD4 Iso#4_AgeI_ FW	CGG ACC GGT ATG GAG GCT GCC GTC GGC
OTUD4 Iso#4_ AscI_ FW	GCG GGC GCG CCG ATG GAG GCT GCC GTC GGC
OTUD4 Iso#4_AgeI_N-Flag_Fw	CGG ACC GGT ATG GAT TAC AAG GAT GAC GAC GAT AAG GAG GCT GCC GTC GGC
OTUD4 Iso4_BamHI_KZ_FW	CGG GGA TCC GCC ACC ATG GAG GCT GCC GTC GGC GTC CC
OTUD4 Iso#4_XhoI_FW	CGG CTC GAG ATG GAG GCT GCC GTC GGC GTC CC
OTUD4 Iso#4_BamHI_FW	CGG GGA TCC ATG GAG GCT GCC GTC GGC GTC CC
OTUD4 S202A FW	GAT GAA GAT AAC AGT GAA ATA GCC GAT TCA GAG GAT GAC AGT TGC
OTUD4 S202A RV	GCA ACT GTC ATC CTC TGA ATC GGC TAT TTC ACT GTT ATC TTC ATC
OTUD6B Iso#3_BamHI_FW	CGG GGA TCC ATG GAG GCG GTA TTG AC
OTUD6B Iso#3_EcoRI_RV	CGG GAA TTC TTA GCT GCA ATT TTC AG
c-Rel_HindIII_Fw	CGG AAG CTT GCC ACC ATG GCC TCC GGT GCG TAT AAC
c-Rel_XhoI_RV	CGG CTC GAG TTA TAC TTG AAA AAA TTC ATA TG
c-Rel_BamHI_Fw	CGG GGA TCC ATG GCC TCC GGT GCG TAT AAC CC
c-Rel_EcoRI_RV	CGG GAA TTC AAA AAA TTC ATA TGG AAA G
c-REL_AgeI_N-Flag_Fw	CGG ACC GGT ATG GAT TAC AAG GAT GAC GAC GAT AAG GCC TCC GGT GCG TAT
c-REL_BamHI_KZ_FW	CGG GGA TCC GCC ACC ATG GCC TCC GGT GCG TAT AAC CC
c-REL ClaI RV	CGG ATC GAT TTA TAC TTG AAA AAA TTC
c-REL K111R FW	AAT TTG GGT ATT CGA TGT GTG AGG AAA AAA GAA GTA AAA GAA GCT



c-REL K111R RV	AGC TTC TTT TAC TTC TTT TTT CCT CAC ACA TCG AAT ACC CAA ATT
c-REL K112R FW	TTG GGT ATT CGA TGT GTG AAG AGA AAA GAA GTA AAA GAA GCT ATT
c-REL K112R RV	AAT AGC TTC TTT TAC TTC TTT TCT CTT CAC ACATCG AAT ACC CAA
c-REL K113R FW	GGG TAT TCG ATG TGT GAA GAA AAG AGA AGT AAA AGA AGC TAT TAT
c-REL K113R RV	ATA ATA GCT TCT TTT ACT TCT CTT TTC TTC ACA CAT CGA ATA CCC
c-REL K193R FW	GGA TTT GTC GTG TAA ACA GGA ATT GTG GAA GTG TCA GAG GAG GAG
c-REL K193R RV	CTC CTC CTC TGA CAC TTC CAC AAT TCC TGT TTA CAC GAC AAA TCC
c-REL K292R FW	ACT TAC GGC AAT AAA GCA AAG CGA CAA AAG ACA ACT CTG CTT TTC
c-REL K292R RV	GAA AAG CAG AGT TGT CTT TTG TCG CTT TGC TTT ATT GCC GTA AGT
c-REL K112R-K113R FW	GGG TAT TCG ATG TGT GAG GAG AAG AGA AGT AAA AGA AGC TAT TAT TAC
c-REL K112R-K113R RV	GTA ATA ATA GCT TCT TTT ACT TCT CTT CTC CTC ACA CAT CGA ATA CCC

#### 4.6.2 Sequencing oligonucleotides

Standard sequencing primers were provided by Eurofins Genomics, Ebersberg, Germany. Sequences of additional primers used for sequencing in this study are listed below.

Oligonucleotide	Sequence (5'-3')
lentiCRISPRv2	GAC TAT CAT ATG CTT ACC GT
OTUD4 primer Seq. 2	TGA AGA ACA ATG GGA ACT C
OTUD4 primer Seq. 3	TCA CAG TCT CAG AAA TTC
OTUD4 primer Seq. 4	ACA TGT GTC TTT GTC AAA TC
OTUD4 primer Seq. 5	GCA GGA TGT ACC CAA AGG
OTUD4 primer Seq. 6	CTG TCT AAA GAT TGT GGT TC
OTUD4 primer Seq. 7	ACA TGT GAG AAG TGA GGA G



pTRIPZ_Seq_fw	GTC GAG GTA GGC GTG T
pTRIPZ_Seq_rv	GCG GGC CGC TGT CCT GAG

### 4.6.3 shRNA sequence design and cloning

Short hairpin RNA (shRNA)s sequences were designed using the GPP Web Portal developed by the Broad Institute (<https://portals.broadinstitute.org/gpp/public/>).

Conceptual design:

Forward Oligo:

5'-CCGG-Target sequence-CTCGAG-Reverse complement target sequence-TTTTTG-3'

Reverse Oligo:

5'-AATTCAAAA- Target sequence-CTCGAG-Reverse complement target sequence-3'

shRNA designation	Target Sequence (5'-3')
Scr shRNA	CCTAAGGTTAAGTCGCCCTCG
OTUD4 shRNA #1	TGCTGTATGAGAAGGTATTTA
OTUD4 shRNA #2	GAATCCAAGCAAGCCAATAAA
OTUD4 shRNA #3	CTGTATCCCAAGCTCATTTAA
c-REL shRNA #2	TGTTGTCTCGAACCCAATTTA
c-REL shRNA #3	CCCTGATGAACATGGTAATTT
c-REL shRNA #4	CTCCAAATACTGCAGAATTAA
c-REL shRNA #5	AGAGGAGGAGATGAAATATTT

The designed sequences were ordered from Eurofins Genomics. The annealed shRNAs were ligated into the pLKO.1 dsRed TRC cloning vector.

### 4.6.4 Sequences of CRISPR sgRNA

Single guide RNA (sgRNA) sequences were obtained from the published article Wang *et al.*, 2015. They were cloned into a Cas9-containing one vector system either lentiCRISPRv2 or its Doxycycline-inducible version TLCV2. To clone the guide sequence into the lentiCRISPR v2 or TLCV2, two oligos for each target sequence were synthesized according to the following form:



sgRNA	Target Sequence (5'-3')
Scr sgRNA	CGCTTCCGCGGCCCGTTCAA



OTUD4 sgRNA #1	TCTTCAATACAGGAATGGGT
OTUD4 sgRNA #2	ACAACAGATGTGGATTACAG
OTUD4 sgRNA #3	GCTGGTAAAGAAGGCACCGC
c-REL sgRNA #1	ATTGGGTTTCGAGACAACAGG
c-REL sgRNA #2	TAATTGAACAACCCAGGCAG
c-REL sgRNA #3	GTTGGAAAAGACTGCAGAGA

#### 4.7 Plasmids

Plasmid	Origin
pcDNA3.1(+)-zeo	Thermo Fisher Scientific
pcDNA c-REL	E. Katab, this study
pcDNA OTUD4 Iso#3	E. Katab, this study
pcDNA OTUD4 Iso#4	E. Katab, this study
pcDNA CD79A	E. Katab, this study
pcDNA CD79B	E. Katab, this study
pcDNA3.1-N-FLAG	Bassermann's Lab
pcDNA3.1-N-FLAG OTUD4 Iso#3	E. Katab, this study
pcDNA3.1-N-FLAG OTUD4 Iso#4	E. Katab, this study
pcDNA3.1-N-FLAG OTUD4 Iso#4 K78R	E. Katab, this study
pcDNA3.1-N-FLAG OTUD4 Iso#4 S202A	E. Katab, this study
pcDNA3.1-N-FLAG OTUD4 Iso#4 S517A	E. Katab, this study
pcDNA3.1-N-FLAG OTUD4 Iso#4 S517D	E. Katab, this study
pcDNA3.1-N-FLAG OTUD6B Iso#3	C. Richter, this study
pcDNA3.1-N-FLAG CD79A	E. Katab, this study
pcDNA3.1-N-FLAG CD79B	E. Katab, this study
pcDNA3.1-N-Strep-Strep-FLAG	Bassermann's Lab
pcDNA3.1-N-Strep-Strep-FLAG c-REL	E. Katab, this study
pcDNA3.1-N-Strep-Strep-FLAG c-REL K111R	E. Katab, this study
pcDNA3.1-N-Strep-Strep-FLAG c-REL K112R	E. Katab, this study
pcDNA3.1-N-Strep-Strep-FLAG c-REL K113R	E. Katab, this study
pcDNA3.1-N-Strep-Strep-FLAG c-REL K193R	E. Katab, this study
pcDNA3.1-N-Strep-Strep-FLAG c-REL K293R	E. Katab, this study
pTRIPZ N-Flag RFP	R. Spallek, this study
pTRIPZ N-Flag c-REL	E. Katab, this study



pTRIPZ N-Flag OTUD4 Iso#4	E. Katab, this study
pMD2.G	Addgene (#12259), D. Trono
psPAX2	Addgene (#12260), D. Trono
Flag-HA-OTUD4	Addgene (#22594), W. Harper
lentiCRISPR v2	Addgene (#52961), F. Zhang
lentiCRISPR v2 Scr	E. Katab, this study
lentiCRISPR v2 OTUD4 #1	E. Katab, this study
lentiCRISPR v2 OTUD4 #2	E. Katab, this study
lentiCRISPR v2 OTUD4 #3	E. Katab, this study
lentiCRISPR v2 c-REL #1	E. Katab, this study
lentiCRISPR v2 c-REL #2	E. Katab, this study
lentiCRISPR v2 c-REL #3	E. Katab, this study
TLCV2	K. Sleiman, Addgene (#87360), A. Karpf
TLCV2 Scr	E. Katab, this study
TLCV2 OTUD4 #1	E. Katab, this study
TLCV2 OTUD4 #2	E. Katab, this study
TLCV2 OTUD4 #3	E. Katab, this study
TLCV2 c-REL #1	E. Katab, this study
TLCV2 c-REL #2	E. Katab, this study
TLCV2 c-REL #3	E. Katab, this study
pLKO.1 TRC cloning vector dsRed	M. Heider, this study
pLKO.1 dsRed Scramble Sh	M. Heider, this study
pLKO.1 dsRed OTUD4 Sh#1	E. Katab, this study
pLKO.1 dsRed OTUD4 Sh#2	E. Katab, this study
pLKO.1 dsRed OTUD4 Sh#3	E. Katab, this study
pLKO.1 dsRed c-REL Sh#2	E. Katab, this study
pLKO.1 dsRed c-REL Sh#3	E. Katab, this study
pLKO.1 dsRed c-REL Sh#4	E. Katab, this study
pLKO.1 dsRed c-REL Sh#5	E. Katab, this study
pRK5-HA-Ubiquitin-WT	Addgene (#17608), T. Dawson
pLenti-His-Ubiquitin-Blasticidin	R. Spallek, this study



#### 4.8 Bacteria

Bacterial strain	Supplier
NEB 5-alpha competent <i>E. coli</i>	New England Biolabs

#### 3.9 Size-standards for DNA and proteins electrophoresis

Size-standard	Manufacturer
GeneRuler 1 kb DNA Ladder	Thermo Fisher Scientific
PageRuler Plus Prestained Protein Ladder	Thermo Fisher Scientific

#### 4.10 Primary antibodies

Antibody target (antibody clone)	Species of origin	Western Blot experiments Dilutions	Manufacturer (Catalog#)
$\alpha/\beta$ -tubulin	Rabbit	1:1000	Cell Signaling Technology (#2148)
ANTI-FLAG®	Rabbit	1:1000	Sigma-Aldrich (#F7425)
ANTI-FLAG® M2	Mouse	1:1000	Sigma-Aldrich (F3165-1MG)
CARD11(1D12)	Rabbit	1:1000	Cell Signaling Technology (#4435)
c-REL	Goat	1:1000	R&D Systems (#AF2699)
c-REL	Rabbit	1:1000	Cell Signaling Technology (#4727)
CUL1 (2H4C9)	Mouse	1:500	Sigma-Aldrich (#32-2400)
GAPDH	Mouse	1:1000	Santa Cruz (#sc-47724)
GST	Mouse	1:1000	Santa Cruz (#sc-138)
HA-Tag (C29F4)	Rabbit	1:1000	Cell Signaling Technology (#3724)
I $\kappa$ B $\alpha$ (L35A5)	Mouse	1:1000	Cell Signaling Technology(#4814)
IKK $\alpha$	Rabbit	1:1000	Cell Signaling Technology(#2682)
Lamin B2 (E1S1Q)	Rabbit	1:1000	Cell Signaling Technology(#13823)
MyD88 (E9K4E)	Mouse	1:1000	Cell Signaling Technology(#50010)
NF $\kappa$ B1 p105/p50	Rabbit	1:1000	Cell Signaling Technology(#3035)
NF $\kappa$ B 2 p100/p52	Rabbit	1:1000	Cell Signaling Technology(#4882)
NF $\kappa$ B p65 (D14E12) XP®	Rabbit	1:1000	Cell Signaling Technology(#8242)
OTUD4	Rabbit	1:1000	Sigma-Aldrich (#HPA036623)



OTUD6B	Rabbit	1:1000	Abcam (#ab127714)
Syk (D3Z1E) XP®	Rabbit	1:1000	Cell Signaling Technology(#13198)
Phospho-IRAK4 (Thr345/Ser346) (D6D7)	Rabbit	1:1000	Cell Signaling Technology(#11927)
Phospho-IkBα (Ser32/36) (5A5)	Mouse	1:1000	Cell Signaling Technology(#9246)
PKC βII (C-18)	Rabbit	1:500	Santa Cruz (#sc-210)
PLK1 (PL6/PL2)	Mouse	1:500	Thermo Fisher(# 33-1700)
RelB (D7D7W)	Rabbit	1:1000	Cell Signaling Technology(#10544)
Ubiquitin FK2	Mouse	1:1000	Enzo (#BML-PW8810-0100)

#### 4.11 Secondary antibodies

Antibody	Dilution (Application)	Manufacturer (Catalog#)
Donkey anti-Goat IgG Alexa Fluor 594	1:1000 (Immunofluorescence)	Thermo Fisher(#A-11058)
Donkey anti-Rabbit IgG Alexa Fluor 488	1:1000 (Immunofluorescence)	Thermo Fisher(#A-21206)

#### 4.12 Cell lines

##### Human Diffuse Large B-cell Lymphoma (DLBCL) Cell lines

Cell line	DLBCL Classification	Mutations	Source
BJAB	GC-DLBCL	HGNC, TP53	Prof. D. Krappmann
OCI-LY3	ABC-DLBCL	CARD11, MyD88, Bcl6	Prof. D. Krappmann
HBL-1	ABC-DLBCL	CD79B, MyD88	Prof. D. Krappmann
TMD8	ABC-DLBCL	CD79B, MyD88, PKCB	Prof. D. Krappmann

##### Other human Cell lines

Cell line	Origin	Source
HEK293T	Human Embryonic Kidney cell line	ATCC (CRL-3216)
MIA PaCa-2	Human Pancreatic Ductal Adeno Carcinoma cell line	ATCC CRL-1420
PANC-1	Human Pancreatic Ductal Adeno Carcinoma cell line	Prof. H. Algül

#### 4.13 Cell culture media and supplements

Product	Manufacturer
Dulbecco's Modified Eagle's Medium (DMEM)	Life Technologies
Fetal Bovine Serum superior	Biochrom Merck
Iscove's Modified Dulbecco's Media (IMDM)	Life Technologies
L-Glutamine 200mM (100X)	Biochrom Merck
Newborn Calf Serum	Biochrom Merck
Opti-MEM I, reduced serum media	Life Technologies
Phosphate buffered saline (PBS), 10X, sterile	Life Technologies
Penicillin/ Streptomycin (100X)	Life Technologies
RPMI 1640 GlutaMAX medium	Life Technologies
Trypan Blue Stain (0,4%)	Life Technologies
Trypsin-EDTA (10X) solution	Biochrom Merck

#### 4.14 Patient samples

Dr. med. vet. Katja Steiger, Institute of Pathology, Technical University of Munich.

#### 4.15 Solutions and buffers

NB. All listed buffers were prepared in distilled water, except when indicated otherwise.

Buffer or solution	Composition
FACS Buffer	Dulbeccos PBS (1x) 5% Fetal Bovine Serum
Freezing medium	Fetal Bovine Serum 10% DMSO
IF Buffer	Dulbeccos PBS (1x) 0.5% Tween 20
Inhibitors	1 mM DTT 10 mM G-2-P 1 µg/mL leupeptin 0.1 mM PMSF 0.1 mM Na <sub>3</sub> VO <sub>4</sub> 5 µg/mL TLCK 10 µg/mL TPCK



Laemmli Buffer (5x)	300 mM Tris (pH 6.8) 50% glycerol 10% SDS 5% $\beta$ -mercaptoethanol 0.05% bromophenol blue
Luria-Bertani (LB) medium (1x)	1% Bacto Tryptone 0.5% Bacto Yeast Extract 170 mM NaCl
Luria-Bertani (LB)-agar plates	LB medium 1.5% Bacto Agar
Lysis Buffer (150 mM NaCl)	50 mM Tris (pH 7.5) 150 mM NaCl 0.1% NP40 5 mM EDTA 5 mM MgCl <sub>2</sub> 5% Glycerol
SDS Running Buffer (10x)	250 mM Tris (pH 7.5) 1.92 M glycine 1% SDS
Silver Staining Solution A	50% methanol 12% acetic acid 0.0185% formaldehyde
Silver Staining Solution B	50% ethanol
Silver Staining Solution C	0.2% (w/v) sodium thiosulfate pentahydrate
Silver Staining Solution D	0.0278% formaldehyde 0.2% (w/v) silver nitrate
Silver Staining Solution E	6% (w/v) sodium carbonate 0.004% (w/v) sodium thiosulfate pentahydrate 0.0185% formaldehyde
Silver Staining Solution F	50% methanol 12% acetic acid
Stripping Buffer	62.5 mM Tris (pH 6.8) 0.867% $\beta$ -mercaptoethanol



	2% SDS
SDS-Transfer Buffer (1x):	48 mM Tris 39 mM glycine 20% methanol (v/v)
Washing Buffer	Dulbecco PBS (1x) 0.1% Tween 20
SOC Medium (1x):	2% Bacto Tryptone (w/v) 0.5% Bacto Yeast Extract (w/v) 10 mM NaCl 2.5 mM KCl 10 mM MgCl <sub>2</sub> 10 mM MgSO <sub>4</sub> 20 mM glucose
DNA Loading Dye (6x):	30% glycerol (v/v) 0.25% Bromphenol Blue (w/v) 0.25% xylene cyanol (w/v)
Ponceau Staining Solution (1x):	0.1% Ponceau S (w/v) 5% acetic acid glacial (v/v)
SDS-Page Separating Gel Buffer (1x):	Dulbecco PBS (1x) 1.5 mM Tris (pH 8.8)
SDS-Page Stacking Gel Buffer (1x):	Dulbecco PBS (1x) 0.5 mM Tris (pH 6.8)
TAE Buffer (1x):	40 mM Tris 20 mM glacial acetic acid 1 mM EDTA
Ubiquitination-Denaturing Buffer (1x):	Lysis Buffer (150 mM NaCl) 5 mM EDTA 10 % SDS
Ubiquitination-Quenching Buffer (1x):	Lysis Buffer (150 mM NaCl) 1 % Triton X-100 (v/v)



#### 4.16 Software and databases

Software or database	Manufacturer
BLAST Basic local alignment search tool	NCBI
GPP Web Portal	Broad Institute
SnapGene Viewer v5.0	Insightful Science
GraphPad Prism v8.0	Graph Pad Software
Mendeley	Elsevier
EvolutionCapt-v18.05	Vilber



## 5 Methods

### 5.1 Molecular cloning

Expression plasmids coding for different isoforms of human proteins of interest and mutants were prepared using restriction enzyme-based cloning techniques. First, the DNA sequence of interest (insert) was amplified by a PCR reaction from a suitable template DNA (see 5.1.1). The insert as well as appropriate vector plasmid DNA were digested either with the same restriction endonuclease (RE) or RE generating compatible ends. Following purification over gel electrophoresis end-compatible vector and insert DNA constructs were ligated (see 5.1.3). The resultant plasmid was then used to transform bacteria where it was amplified (see 5.1.5). At last, the abundantly produced plasmid was extracted and purified using commercial kits (see 5.1.6). To create a single amino acid mutation, a given DNA sequence was modified by PCR-based mutagenesis (see 5.1.4).

#### 5.1.1 Polymerase Chain Reaction (PCR)

DNA fragments of interest were amplified by PCR. On ice, a 50  $\mu$ L reaction mixture was prepared as follows; 100 ng template DNA, 0.2  $\mu$ M forward (Fw) and reverse (Rv) primers (see 3.6.1), 0.4 mM dNTPs (0.1 mM of each of the four dNTPs, dATP, dGTP, dTTP, dCTP), 5  $\mu$ L PfuUltra II reaction buffer (10x), 1  $\mu$ L *PfuUltra* II fusion HS DNA polymerase, filled up with distilled water (dH<sub>2</sub>O) to 50  $\mu$ L. The PCR program included an initial denaturation step of 2 minutes at 95°C, 30 cycles of consecutive DNA denaturation (30 sec, 95°C), primer annealing (30 sec, Primer T<sub>m</sub> – 5°C) and DNA elongation (30 sec per kb DNA, 72°C). To ensure proper completion of DNA elongation, the program was ended with a further incubation step at 68°C for 2 minutes.

#### 5.1.2 Agarose gel electrophoresis and gel purification

PCR products were purified after size-separation by electrophoresis in 1% agarose gels containing SYBR Safe DNA Gel Stain (Invitrogen). DNA bands were visualized under UV light (360 nm), and parts of the gel containing bands of the expected size were excised using an extracting gel band punch (Biozyme). Using the manufacturer's protocol, DNA was extracted from the cut bands using GeneJet Gel Extraction Kit (Thermo Scientific).

#### 5.1.3 Restriction enzyme digestion and ligation

Both PCR product (insert) and vector were digested with restriction enzymes to create single-stranded overhangs (complementary sticky ends) or blunt ends that allow the cloning of the insert into its end-complementary vector. Either the whole gel-extracted DNA fragment or 1-2  $\mu$ g of plasmid DNA was digested with restriction enzymes (Thermo Fisher or NEB) at



a ratio of 1 unit of enzyme per  $\mu\text{g}$  of substrate DNA along with the corresponding 10x enzyme buffer and water to make up a total volume of 30  $\mu\text{l}$ . This digestion reaction was incubated at 37°C for 60 minutes, and the digested DNA products gel purified and extracted using the GeneJet Gel Extraction Kit (Thermo Scientific). Purified fragments of insert and vector DNA were ligated at a molar ratio of 1 (vector) to 3 (insert) using the Rapid DNA Dephos & Ligation Kit (Roche) following the manufacturer's protocol.

#### **5.1.4 DNA mutagenesis**

Site-directed mutagenesis was carried out to change a specific codon within a coding sequence, thereby altering the amino acid code. For this purpose, 45 bp long primer pairs were designed with desired base pair changes in the middle of the sequence. A PCR was set to amplify the whole plasmid containing the cDNA with a program similar to the one previously described in section 5.1.5 with some changes: the number of cycles was reduced to 16, annealing temperature was fixed to 55°C, and the DNA elongation temperature to 68°C. The amplified PCR product was digested for 60 minutes with 1  $\mu\text{L}$  DpnI enzyme at 37°C to get rid of the non-mutated parent DNA. The linear PCR product was introduced into bacteria (see 5.1.5) and processed according to section 5.1.6.

#### **5.1.5 Bacterial transformation**

Introduction of foreign DNA into bacteria (bacterial transformation) was performed by heat shock. For this, 20  $\mu\text{l}$  of the NEB® 5-alpha Competent E. coli (High Efficiency) strain bacterial suspension were mixed with 2  $\mu\text{l}$  of a ligation reaction (see 5.1.3), incubated on ice for 5 minutes and exposed to 45 seconds of a 42°C heat shock. The mix was allowed to cool down on ice for 5 minutes and was then transferred into 1 ml of super optimal broth with catabolite repression (S.O.C) medium and incubated in the thermomixer at 37°C for 30 minutes. Transformed bacteria were then plated on Luria Broth (LB) agar plates containing 100  $\mu\text{g}/\text{ml}$  of ampicillin and incubated overnight at 37°C. The next day, single colonies were picked, cultured in 5 ml or 200 ml 1% ampicillin containing LB media, and grown overnight in a shaking incubator at 37°C.

#### **5.1.6 Extraction of plasmid DNA from bacteria**

From the overnight bacterial culture, plasmid DNA was isolated using commercially available DNA extraction kits using protocols provided by the kit suppliers. The peqGOLD Plasmid Miniprep Kit (Peqlab Life Science) was used for extraction of DNA from 1 mL cultures. For purification from 200 mL bacterial cultures the NucleoBond® Xtra Midi Kit (Macherey-Nagel) was used. Resultant DNA pellets were air-dried for 30 minutes and



dissolved in appropriate volumes of RNA free H<sub>2</sub>O. The identity of the obtained plasmid DNA was confirmed by Sanger sequencing at Eurofins Genomics, Ebersberg, Germany.

### **5.1.7 Annealing of shRNA oligonucleotides**

shRNA oligonucleotides were annealed in a 50 µL reaction by mixing 1 µL of each oligonucleotide (100 µM stock concentration) with 5 µL Buffer G (Thermo Fisher Scientific) and filled up with distilled H<sub>2</sub>O to 50 µL. The mixture was incubated at 95°C for 5 minutes, then allowed to cool down, at 0.1°C per second, to room temperature. The annealed shRNA oligos were ligated into the pLKO.1 TRC vector plasmid prepared by digestion with AgeI and EcoRI in recommended buffers (see section 5.1.3).

## **5.2 Culture of eukaryotic cells and cell-based experiments**

### **5.2.1 Cell Culture**

All human origin cell lines used in this study were cultured in a humidified incubator at 37°C with 5% CO<sub>2</sub>. The adherent human embryonic kidney cell line HEK293T and the pancreatic ductal adenocarcinoma (PDAC) cell line MIA PaCa-2 were cultured in Dulbecco's modified Eagle's medium (DMEM) with GlutaMAX supplemented with 1 % penicillin-streptomycin (P/S) and 10 % newborn calf serum or 10 % fetal bovine serum, respectively. Both cell lines were grown on cell culture plates and split regularly at an 80-100 % confluency every second day. Splitting these cells was done by removal of old medium, washing the cells once with PBS, followed by trypsin treatment for a few minutes in the incubator to allow cells to detach. The detached cells were harvested in their corresponding medium followed by centrifugation at 1200 rpm for 3 minutes. After discarding the supernatant, pelleted cells were resuspended in fresh medium, and re-plated at a ratio of 1:10 – 1:2 depending on their proliferation rate.

Human Diffuse Large B cell lymphoma (DLBCL) cell lines BJAB and OCI-LY3 were cultured in RPMI 1640 medium supplemented with 1 % P/S and 10 % or 20 % heat-inactivated FBS, respectively. The other two DLBCL cell lines, HBL-1 and TMD8, were grown in RPMI 1640 medium supplemented with 1 % P/S and 15 % heat-inactivated FBS. The DLBCL cell lines were all suspension cultures and were grown in cell culture flasks. Based on their proliferation rate, they were split every 1-2 days at a ratio of 1:8 – 1:2. For some experiments, cell number was counted using a Neubauer counting chamber after mixing the cells at a ratio of 1:1 with Trypan blue that only stains damaged cells.



### **5.2.2 Freezing and thawing of cells**

To freeze cells for storage, cells in culture were harvested by centrifugation at 1200 rpm for 3 minutes. The cell pellet was resuspended in 1,5 ml of FBS supplemented with 10% DMSO (freezing medium) and transferred into cryogenic storage tubes. The tubes were gradually frozen in Mr. Frosty™ (Thermo Fisher), an isopropanol-based freezing container, at -80°C. For long-term storage, the completely frozen cells were then transferred into a liquid nitrogen tank.

To thaw frozen cells, the cryogenic tubes were put in a 37°C water bath until the contents thawed. The cells were then transferred rapidly into a falcon with 10 mL culture medium and spun down at 1200 rpm for 3 minutes. Finally, the cells were resuspended in their culture medium and cultured as described in section 5.2.1.

### **5.2.3 Harvesting cells**

For RNA extraction or protein biochemical experiments, cells were harvested in falcon tubes and frozen in 1.5 mL Eppendorf tubes at -80°C till further processing.

In the case of adherent cells, cells were treated with trypsin for a few minutes, collected in medium, and centrifuged at 1200 rpm for 3 minutes. The cell pellet was resuspended in 1 mL PBS, transferred into 1.5 mL Eppendorf tubes, and washed once before freezing at -80°C.

### **5.2.4 Plasmid DNA Transfection of cells**

#### **5.2.4.1 Calcium phosphate transfection**

The calcium phosphate method offered a cheap and efficient way for transient transfection of adherent cells. In this method, the calcium chloride solution containing the DNA is mixed slowly with sodium phosphate contained in the BES-buffer, resulting in DNA–calcium phosphate precipitate, which can be taken up by cells (Graham and van der Eb 1973, Kingston, Chen et al. 2003). To transfect HEK293T cells, a pre-cultured 10 cm plate with cell confluency of 60 - 80 % was prepared. A 1 mL transfection mixture was prepared by dissolving 10 µg of DNA in 450 µL dH<sub>2</sub>O with the addition of 50 µl CaCl<sub>2</sub> to a final concentration of 250 mM. Then, 500 µL 2x BES solution was added dropwise to the tube walls with rotation. The mixture was left at room temperature for 20 minutes and later dropped carefully onto the cells while swirling the plate. The medium was replaced by fresh medium after 4 hrs.

#### **5.2.4.2 Transfection by Lipofectamine 2000**

For an enhanced transfection of the HEK293T cells with the yield of high levels of recombinant protein expression, the lipid-based transfecting agent Lipofectamine® 2000



(Thermo Fisher) was used following the manufacturer's protocol. To transfect cells in a 10 cm plate, two 400  $\mu$ l solutions were prepared. Solution A was prepared by mixing 10  $\mu$ g of the DNA in Opti-MEM medium up to 400  $\mu$ l, while for solution B, 60  $\mu$ l of Lipofectamine® 2000 were mixed with 340  $\mu$ l Opti-MEM medium and incubated separately for 5 minutes at room temperature. The DNA - lipofectamine ratio was chosen to be 1:3. Later, solutions A and B were mixed carefully and incubated at room temperature for 20 minutes. The mixture was then added dropwise onto the cells, and the plates were mixed by swirling. Three hours later, the medium was replaced with fresh medium.

### **5.2.5 Production of lentiviral particles**

The transfection methods described in 4.2.4.1 and 4.2.4.2 allowed only for either transient expression or knockdown of a target protein. A lentiviral stable expression system was established to study the prolonged effects of overexpressing a protein or silencing it. The lentiviral particles were produced in HEK293T cells by transfecting a 10 cm plate with 15  $\mu$ g packaging plasmid (psPAX2), 5  $\mu$ g envelope plasmid (pMD2.G), and 20  $\mu$ g transfer plasmid (pLKO.1 dsRed plasmid for shRNA, lentiCRISPRv2 for sgRNA and pTRIPZ plasmid for cDNA) using the calcium phosphate method (see 4.2.4.1). After 4 hrs, the medium was replaced by 10 mL of fresh medium, and the transfected cells were incubated for 48 hrs. The viral supernatant was harvested on the 2<sup>nd</sup> day by passing the collected supernatant through a 0.45  $\mu$ m filter and directly used for infection or stored at -80°C.

### **5.2.6 Viral transduction of cells**

To infect the adherent cell lines with lentiviral particles, the cells were pre-seeded in a 6-well plate one day prior to infection. Cells with 80% confluency were infected by replacing 1 ml of the culture medium with 1 ml of the viral supernatant along with 8  $\mu$ g/mL polybrene. On the next day, the virus-containing supernatant was removed, and the cells were washed 3 times with PBS before plating them back into 10 cm culture plates with fresh media.

For the infection of suspension cells, 1 million cells were infected similarly in a 6-well plate with 1 ml of viral supernatant and 8  $\mu$ g/mL of polybrene. The infection rate was enhanced by centrifugation at 700 g for 30 minutes. Twenty-four hours later, the virus was discarded by spinning down the cells at 1200 rpm for 3 minutes, and the cells' pellet was resuspended in 10 ml of fresh medium and transferred into culture flasks.

### **5.2.7 Cycloheximide Chase assay**

Cycloheximide is a chemical molecule that specifically inhibits protein synthesis in eukaryotes; hence it can be used for studying the stability of target proteins. A stock solution of 100 mg/ml was always freshly prepared by dissolving Cycloheximide in absolute ethanol.



The cells were treated with 100 µg/ml of Cycloheximide for up to 8 hours and harvested at indicated time points. To test for the proteasome-mediated degradation of target proteins, 10 µM of the proteasome inhibitor MG132 was simultaneously added for 4 hrs.

### **5.2.8 Flow cytometry**

Flow cytometry is a cell-analysis technique that can measure the physical characteristics of single cells (e.g., relative size, relative granularity) and detect the relative intensity of fluorescently labelled cells. Cells infected with the plasmid pLKO.1 dsRed stably expressed the dsRed fluorescent protein relative to their infection rate. The EGFP HBL-1 NFκB reporter cells expressed EGFP relative to the NFκB activation status. The intensity of the dsRed or EGFP signal was measured by CytoFLEX LX (Beckman Coulter) in the PE or FITC channel respectively. The results were analysed using the FlowJo v10 software.

### **5.2.9 Fluorescence-activated cell sorting (FACS)**

FACS (Fluorescence-activated cell sorting) is an application of flow cytometry by which a homogenous population can be obtained from a mixture of cells based on the specific light scattering and fluorescent characteristics of each cell. To overcome the low infection rate, the pLKO.1 dsRed infected cells were enriched by only sorting out viable dsRed labelled cells. FACS experiments were done using FACS Aria II (BD Biosciences) at the Cell Analysis Unit of the core facility of the Centre for Translational Cancer Research (TranslaTUM), Klinikum rechts der Isar with the crucial help of Dr. Ritu Mishra. The sorted cells were transferred into culture flasks to allow for further growth and subsequent experiments.

### **5.2.10 Immunofluorescence analysis**

Immunofluorescence is a histochemical staining methodology to study target proteins' localization and relative expression in fixed cells or tissues. For immunofluorescence experiments, the cells were seeded on detachable multi-well cell culture chambers on PCA slides 3 days post-infection. The attached cells were carefully washed once with PBS and incubated with cold absolute methanol for 10 minutes at -20°C. Following incubation, the methanol was aspirated, and the cells were washed once with PBS. Then, the cells were blocked with IF buffer for 20 minutes at 4°C. After discarding the IF buffer, the cells were incubated with primary antibodies diluted in IF buffer (1:400) at room temperature. 1 hr later, the cells were washed 3 times with IF buffer for 5 minutes each. The secondary antibodies were then added at a similar dilution to the primary antibodies for 1 hour at room temperature. After washing 3 times with IF buffer, the cells were quickly washed once with dH<sub>2</sub>O. Finally, the slide was mounted with a drop of DAPI containing mounting medium (Thermo Fisher



Scientific) and covered with a coverslip. Images were acquired with an Inverted Fluorescence Microscope (Olympus) using TillVision imaging software.

## **5.3 Protein biochemistry**

### **5.3.1 Whole Cell Lysis and Protein Extraction**

To study the protein content of a cell and how different proteins interact with each other, the cell membrane has to be disrupted either mechanically or non-mechanically, enzymatically, or by chemical buffers. Here, frozen or freshly collected cell pellets were resuspended in an appropriate volume of the standard 150 mM NaCl lysis buffer containing protease and phosphatase inhibitors. After proper mixing, the samples were left on ice for 30 minutes and spun down at maximum speed at 4°C for 20 minutes. The supernatant containing the lysates was transferred into the new Eppendorf, and protein concentration was measured using the Bio-Rad DC protein assay (Lowry assay) as described in the manufacture's protocol. Then, the lysates were either denatured by boiling with 5x Laemmli buffer for 5 minutes, separated by SDS-PAGE (see 4.3.3), and blotted onto PVDF membranes (Millipore) or stored at -20°C.

### **5.3.2 Cellular fractionation**

Protein localization influences the execution of subcellular processes within defined cellular compartments. To purify target proteins from cytoplasmic and nuclear compartments, The Thermo Scientific™ NE-PERTM Nuclear and Cytoplasmic Extraction kit was used according to the manufacture's protocol. Freshly harvested cells were washed twice with PBS, and incubated on ice with the cytoplasmic extraction buffers (CER I & II) supplemented with protease and phosphatase inhibitors for 10 minutes. The cytoplasmic fraction was obtained by spinning down the lysed cells at max speed for 5 minutes and transferring the supernatant into a new Eppendorf. The precipitate containing the nuclear fraction was further resuspended in the ice-cold nuclear extraction buffer (NER) and incubated on ice for 40 minutes with vigorous vortexing for 15 sec every 10 minutes. After centrifugation for 10 minutes at max speed, the supernatant containing the nuclear fraction was transferred to another fresh Eppendorf. Both fractions were either directly separated on SDS-PAGE after denaturing by cooking with Laemmli buffer at 95°C or frozen at -20°C till further use.

### **5.3.3 SDS polyacrylamide gel electrophoresis (SDS-PAGE)**

SDS-PAGE is an electrophoresis method in which proteins are separated based on their molecular mass. Its principle is based on the use of SDS as an ionic detergent that denatures proteins and creates uniformly negatively charged linear chains. When loaded into



polyacrylamide gel, proteins migrate through the gel matrix, once an electric field is applied, towards the positively charged anode where small proteins migrate faster than larger ones. Gels with different percentages of acrylamide (6 & 10 %) were freshly prepared to allow the separation of proteins with different molecular weights. Gels were composed of two main parts: separating and stacking gels. The separating gel (375 mM Tris pH 8.8, 10% SDS, 10% APS and acrylamide) was first polymerized with 4  $\mu$ L of TEMED per 10 mL gel solution. Then, it was topped with the stacking gel (125 mM Tris pH 6.8, 10% SDS, 10% APS and 4.4% acrylamide) polymerized with 5  $\mu$ L of TEMED per 5 mL gel solution. 25  $\mu$ g of protein lysates containing Laemmli buffer were loaded onto the gel assembled in an electrophoresis chamber along with a standard protein ladder and allowed to run at 80 V for 20 minutes followed by 1,5 hr at 120 V in a 1x SDS running buffer. Later, the separated proteins were either transferred onto PVDF membranes (Millipore) for immunoblotting or visualized by silver staining.

#### **5.3.4 Silver staining**

After SDS-PAGE, proteins in the gel can be analysed by silver staining. Silver ions interact with negatively charged proteins and are reduced to elemental silver, which makes proteins visible. In this study, silver staining was used to analyze the number of purified proteins. The composition of the solutions used is listed in section 3.15. Proteins were separated by SDS-PAGE using gradient NuPAGE Bis-Tris ready gels (4-12%) and NuPAGE MES SDS Running buffer. Subsequently, the gel was fixed in solution A for 1 hour and then washed three times in solution B for 20 minutes. After incubation in solution C for 1 minute, the gel was washed three times with distilled water for 20 sec and then incubated further in solution D containing the silver ions for 20 minutes. Excess silver ions were washed away two times with distilled water for 20 sec, and subsequently, the gel was incubated in solution E until protein bands became visible. After washing the gel two times with distilled water for 2 minutes, the reaction was stopped by incubation with solution F for 10 minutes. Finally, the gel was washed in 50% methanol for 20 minutes and stored in water.

#### **5.3.5 Protein Immunoblot (Western blotting)**

Immunoblotting is a commonly used technique aimed at detecting target proteins with specific antibodies. The proteins separated by the SDS PAGE were blotted to polyvinylidene fluoride (PVDF) membranes pre-activated in absolute methanol. The gel-membrane assembly was placed into a wet blot chamber full of transfer buffer for electroblotting either at 60 V for 4 hr or at 30 V overnight. Equal levels of the blotted proteins were ensured by staining the membranes with Ponceau S staining. To block unspecific binding, membranes were



incubated in 5% milk for 30 minutes. Then, the membranes were incubated overnight on a roller mixer with primary antibodies diluted in 5% milk or 5% BSA (bovine serum albumin) at 4°C. After washing with washing buffer three times, the membranes were later incubated with horseradish peroxidase (HRP) conjugated secondary antibodies at 1:5000 dilution in 5% milk for one hour. After washing for 3 times 10 minutes each, the membranes were developed with the chemiluminescent reagents Super Signal West (Thermo Scientific) for upto 15 minutes. Visualization of the protein bands was done using the Fusion FX imaging system (VILBER), and the intensity of the signal was quantified by the accompanying software Evolution Capt V18.02c (VILBER).

### **5.3.6 Immunoprecipitation (IP)**

Immunoprecipitation is a process by which target proteins are precipitated with an antibody either specific for the protein itself or the tag attached to such protein. In this study, two different IPs approaches were used; c-REL endogenous IP or FLAG IP. In the case of c-REL endogenous IP, 100 µl lysates prepared from BJAB, HBL-1 and OCI-LY3 cell lines (see 4.3.1) were incubated with 1 µl of c-REL antibody or IgG control (Cell Signaling) for 1.5 hr at 4°C on a rotating well. 25µl of Protein A Sepharose (GE Healthcare) was added to the mixture and allowed to rotate further at 4°C for 30 minutes. The Sepharose beads were washed 4 times with 150 mM NaCl lysis buffer by centrifugation at 1200 rpm for 1 minute. They were boiled with 50 µl of Laemmli buffer for 10 minutes at 95°C, and 12 µl were loaded onto SDS-PAGE for immunoblotting.

On the other hand, FLAG IP was performed on lysates extracted from HEK293T cells expressing FLAG-tagged proteins. For this 100 µl lysates were incubated with anti-FLAG M2 affinity agarose (Sigma-Aldrich) pre-washed with 1 ml of the standard lysis buffer mentioned earlier. The lysate/anti-FLAG beads mixture was set on a rotating wheel overnight at 4°C. The next day, the beads were spun down at 1200 rpm for 1 minute and similarly washed in 1ml of lysis buffer for 4 times. Before immunoblotting, the beads were cooked for 10 minutes at 95°C with Laemmli buffer.

### **5.3.7 Tandem Ubiquitin Binding Entities (TUBEs) Pull-down**

Tandem Ubiquitin Binding Entities (TUBEs) are specifically engineered domains with a high affinity to polyubiquitin chains. GST-tagged TUBEs were used to detect if c-REL is endogenously ubiquitinated and at which cellular fraction. In this context, BJAB, TMD8, and HBL-1 cell lines were first fractionated using the Nuclear and Cytoplasmic Extraction kit (Thermo Scientific) as described in section 4.3.2. The resultant cytoplasmic and nuclear lysates were incubated with GST-TUBEs for 2 hr rotating at 4°C. After four consecutive



washes with 150 mM NaCl lysis buffer by centrifugation at 1200 rpm for 1 minute, the precipitated beads were boiled for 10 minutes with 5x Laemmli buffer followed by immunoblotting.

### **5.3.8 In vivo ubiquitylation**

In vivo ubiquitination/de-ubiquitination assays provide an efficient way for detecting the ubiquitination status of target proteins. Along with overexpressing the target protein (substrate), either overexpression or knockout of DUB will impact the ubiquitination levels of the tested substrate. For this purpose, HEK293T cells were transfected using CaCl<sub>2</sub> (see 4.2.4.1) with 1 µg of HA Ubiquitin, 5 µg of FLAG-tagged c-REL (substrate) and 5 µg of untagged OTUD4 isoforms (DUB). Four hours later, the medium was replaced with fresh new medium, and the cells were incubated overnight at 37°C. In the case of knockout experiments, the cells were infected three days before transfection. Twenty-four hours after transfection, the cells were harvested and lysed in 100 µl of 150 mM NaCl lysis buffer supplemented with inhibitors and incubated on ice for 30 minutes. After centrifugation at max speed for 20 minutes, the lysates were transferred into new Eppendorfs, denatured with 10 µl 10% SDS and 1 µl EDTA (0,5 M), and cooked at 95°C for 5 minutes. The samples were then cooled down to room temperature for 5 minutes before quenching with 900 µl of 1% Triton X-100. Later, the mixture was cooled on ice for 5 minutes, followed by the addition of 25µl pre-washed anti-FLAG M2 affinity agarose (Sigma-Aldrich) and processed for FLAG IP as described in section (5.3.6).

## **5.4 Mass Spectrometry**

### **5.4.1 Tandem Affinity purification for MS analysis**

To identify potential E3 ligases and DUBs involved in the post-translational regulation of c-REL, N-terminal FLAG Strep-Strep-tagged c-REL was immunoprecipitated from HEK293T cells, and the co-precipitated interacting proteins were analyzed by mass spectrometry.

In this study, c-REL was sequentially immunoprecipitated using strep-Tactin Superflow resin and anti-FLAG M2 affinity agarose. To this aim, five 15-cm culture plates of HEK293T cells were transfected using CaCl<sub>2</sub> as explained earlier, with 20 µg of N-terminal FLAG Strep Strep-tagged c-REL DNA plasmid. 24 hr later, the cells were harvested, lysed in standard 150 mM NaCl lysis buffer, and further sonication was performed to ensure proper lysis of less accessible cellular compartments. The lysate was then incubated with Strep-Tactin Superflow resin rotating at 4°C for 2 hr. After washing out the unbound proteins, bound proteins were eluted at room temperature two times, 10 minutes each with desthiobiotin



elution buffer. The eluate was subsequently incubated with anti-FLAG M2 affinity agarose for 1 hr at 4°C followed by two washing steps, once in lysis buffer followed by one in PBS.

Consequently, the c-REL protein was eluted with 250 µg/ml 3×Flag peptide for three consecutive times and the pooled eluate was precipitated overnight with TCA at 4°C. The next day, the protein was pelleted by spinning down in a cooled centrifuge for 10 minutes at max speed, and the obtained pellet was further washed similarly with 500 µl cold acetone. Discarding the acetone supernatant, the pellet was additionally vacuum dried, and the purification was controlled by resuspending 5% of the beads in 5x Laemmli buffer for silver staining. Mass spectrometric analysis of the remaining 95% of dried protein was done at the Department of Proteomics and Bioanalytics at TUM.

#### **5.4.2 Ni-NTA Pull down of His-tagged Ubiquitome**

The Ni-NTA Purification System is an elaborate method used for the purification of recombinant proteins that contain a polyhistidine (6xHis) tag. To study the Ubiquitination levels of c-REL upon *OTUD4* downregulation, BJAB cell line expressing His-tagged ubiquitin was infected with *OTUD4* shRNA or Scrambled shRNA as a control. After three days, 60 million infected cells were harvested, lysed in 12 ml of Guanidinium lysis buffer, and sonicated on ice with 3x 5s pulses at high intensity. 600 µl Ni-NTA agarose slurry (QIAGEN) per sample were prepared under denaturing conditions by washing twice with 4 ml of the Guanidinium lysis buffer and spinning down at 1200 rpm for 3 minutes. After resuspending in 4 ml of the lysis buffer, the slurry was bound to the lysates on a rotating wheel at room temperature for 30 minutes. Then, the slurry was washed twice with lysis buffer and twice with the denaturing washing buffer by centrifugation at 1200 rpm for 3 minutes each. Later, it was further washed with 8 ml of native washing buffer for four native washes. Finally, the slurry was washed with 1 ml of 50 mM Ammonium bicarbonate PH 8.0, and the precipitated nickel beads were frozen on dry ice and sent for MS analysis at the Department of Proteomics and Bioanalytics at TUM.

#### **5.4.3 Mass Spectrometric analysis**

Mass spectrometric analysis of purified c-REL and Nickle purified whole Ubiquitome was done at the TUM Department of Proteomics and Bioanalytics. Sample preparation and analysis of c-REL and Ni NTA ubiquitin IPs were done by Jana Zecha, a former Ph.D. student in the lab of Prof. Bernhard Küster.

Briefly, the purified proteins were digested with trypsin, creating short peptide fragments which were subsequently dried and re-dissolved in 0.1% formic acid (FA). Then, Liquid chromatography with tandem mass spectrometry (LC-MS/MS) was done by coupling a



nanoLC-Ultra system (Eksigent) to an LTQ Orbitrap mass spectrometer (ThermoFisher Scientific) as described in (Fernandez-Saiz et al., 2013). Peak identification of the relevant peptides and their corresponding proteins was done by MaxQuant software (v1.6.3.3) and the UniProt database.

## 6 Results

### 6.1 c-REL is post-translationally modified by ubiquitination

#### 6.1.1 MS-based approach to identify c-REL interactome

Recently, we showed that the variation of c-REL protein levels in different B cell compartments does not correlate with its mRNA levels, pointing to post-transcriptional regulation of c-REL (Kober-Hasslacher et al., 2020). Previous studies also indicated that c-REL is a target of the ubiquitin-proteasome system (UPS), and Peli1 was described to K48 ubiquitinate c-Rel in mouse T cells (Chang et al., 2011; Chen et al., 1998). Therefore, I sought to identify c-REL's post-translational modifying enzymes belonging to the ubiquitin machinery in the context of B cell lymphoma.

To map the possible interacting E3 ligases and DUBs regulating c-REL, an unbiased affinity purification screen of overexpressed c-REL in HEK293T cells was performed by Vanesa Fernández Sáiz by isolating c-REL protein complexes in presence of MedB-1 cell lysates provided by Maike Kober-Hasslacher. Purified c-REL samples were coupled with mass spectrometric analysis was done by Jana Zecha (Fig. 3A). The MS results revealed an initial list of 471 proteins which was cleaned up by removing interactors with label-free quantification (LFQ) ratio of less than 1, resulting in a list of 342 proteins. The identified interactome was validated by finding the well-known c-REL interactors such as RELA, RELB, NFKB1, and NFKB2. Additionally, several E3 ubiquitin ligases and DUBs in the c-REL interactome were found (Fig. 3B).

To look for the top hits obtained in the screen, an arbitrary cut-off of LFQ ratio  $> 9$ , creating a smaller list of only 62 proteins that had only one E3 ligase was considered; TRIM33, and one DUB; OTUD4, along with c-RELs' other known interactors of the NF $\kappa$ B family (Fig. 3C). This analysis suggested TRIM33 and OTUD4 as c-REL's most probable interacting candidates of the ubiquitin system.

#### 6.1.2 c-REL interaction with OTUD4

Ubiquitination is a reversible regulatory process that is conversely regulated by the action of DUBs. DUBs have been recognized lately as a promising class for drug

targeting in different diseases, especially cancer. Thus, identifying a specific DUB that modulates c-REL is of interest in drug discovery.

In Vanesa Fernández's interactome screen, I found OTUD4 as the DUB candidate with the highest score to interact with c-REL. Rolland et al. had previously reported in a proteome-scale map that OTUD4 interacts with c-REL (Rolland et al., 2014). Moreover, OTUD4 was described to regulate NF $\kappa$ B signaling by deubiquitinating MyD88 in mouse embryonic fibroblasts (MEFs) (Zhao et al., 2018). Accordingly, I sought to investigate if OTUD4 would function as a DUB of c-REL. I started by validating the c-REL-OTUD4 interaction, seen in the MS analysis, by immunoprecipitation experiments of overexpressed FLAG-tagged OTUD4

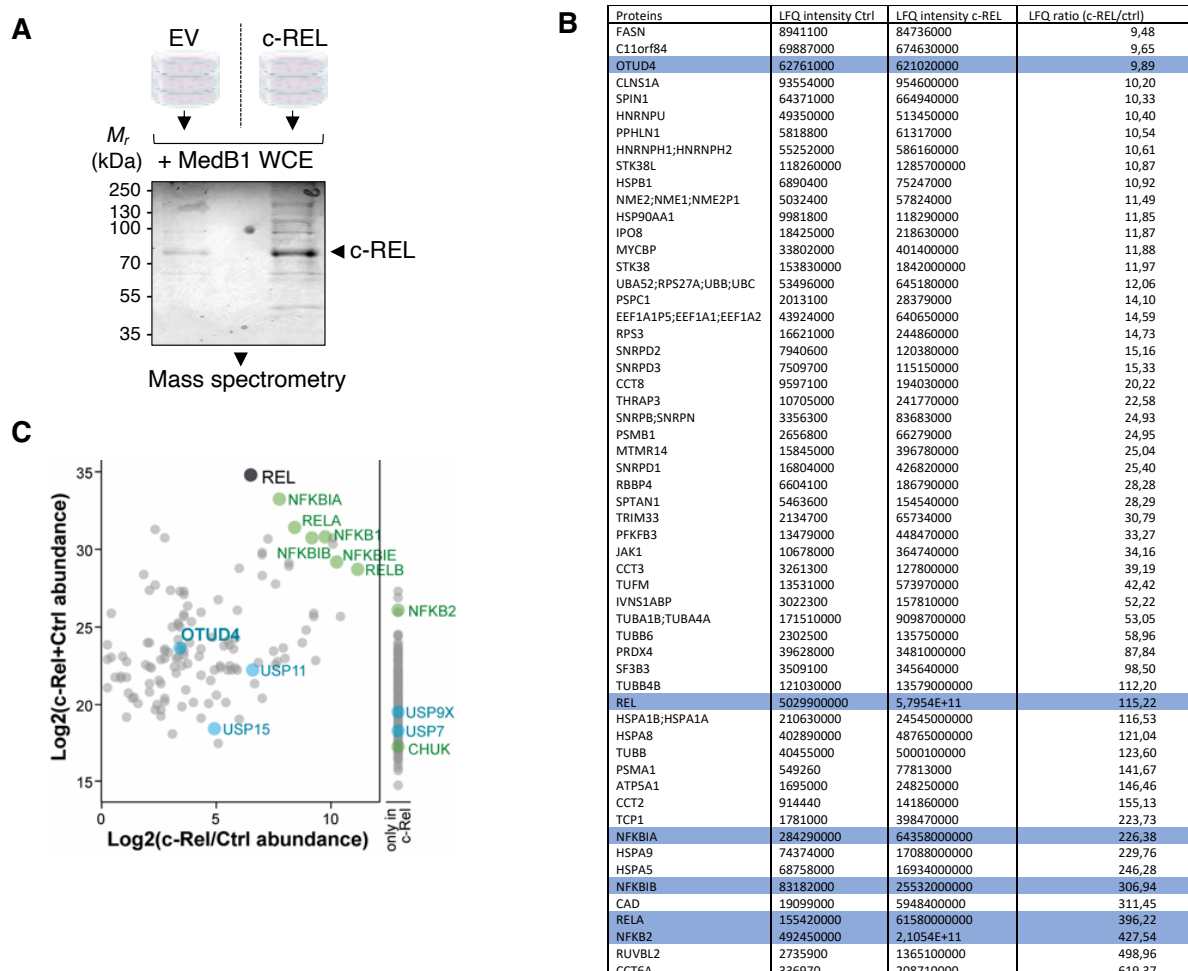


**Fig. 3 Mass spectrometric analysis of c-REL interactome. (A)** Silver staining of purified FLAG-tagged c-REL. N-terminal FLAG Strep Strep-tagged c-REL or empty vector (EV) were transiently overexpressed in HEK293T cells and sequentially immunoprecipitated from cell lysates, mixed with MedB-1 lysates, using strep-Tactin Superflow resin and anti-



FLAG M2 beads. The immunoprecipitated c-REL was eluted with 3×Flag peptide, and 1% of the elution was run on SDS-PAGE. Visualization of the purified proteins was done by silver staining of the gel. EV served as a negative control for non-specific binding, and the arrowhead points to a band of the c-REL expected size. **(B)** Mass spectrometric analysis of proteins co-immunoprecipitated with samples from A. List c-REL's potential interactors, including known NFκB interacting members and other identified proteins with an LFQ ratio of >9. LFQ intensities were calculated with MaxQuant software, and the ratios were obtained by dividing the LFQ intensities of FLAG Strep Strep- c-REL over the EV control. **(C)** Quantification of the deubiquitinases in the interactome of c-REL. Experiments in A were performed by Vanesa Fernandez Saiz and Maike Kober-Hasslacher while MS experiments and analysis were done by Jana Zecha at the Department of Proteomics and Bioanalytics (Prof. Bernhard Küster's lab).

or OTUD6B concomitantly with non-tagged c-REL. The immunoprecipitated OTUD4, not OTUD6B (used as a control DUB for the OTU domain-containing family), showed specific interaction with c-REL (Fig. 4A).

It was delineated that both c-REL and OTUD4 translocate between cytoplasmic and nuclear compartments (Kober-Hasslacher & Schmidt-Supprian, 2019; Zhao et al., 2015); consequently, I was prompted to analyze the c-REL-OTUD4 interaction in fractionated cell extracts. In line with our recent publication, overexpression of c-REL led to its nuclear accumulation (Kober-Hasslacher et al., 2020); however, OTUD4's overexpression appeared mainly in the cytoplasm. Unsurprisingly, I detected a clear interaction between c-REL and OTUD4 in the cytoplasmic fraction (Fig. 4B).

Although DUBs' interaction with their molecular targets is known to be weak, I further confirmed the endogenous interaction of OTUD4 with c-REL in DLBCL by endogenously immunoprecipitating c-REL from OCI-LY3 (an ABC-like DLBCL cell line) cells lysates (Fig.4C). Collectively, these results establish OTUD4 as a c-REL interacting DUB in B cell lymphoma.



These results support that c-REL is ubiquitinated in B cells, and its ubiquitination appears to be mainly in the cytoplasm.

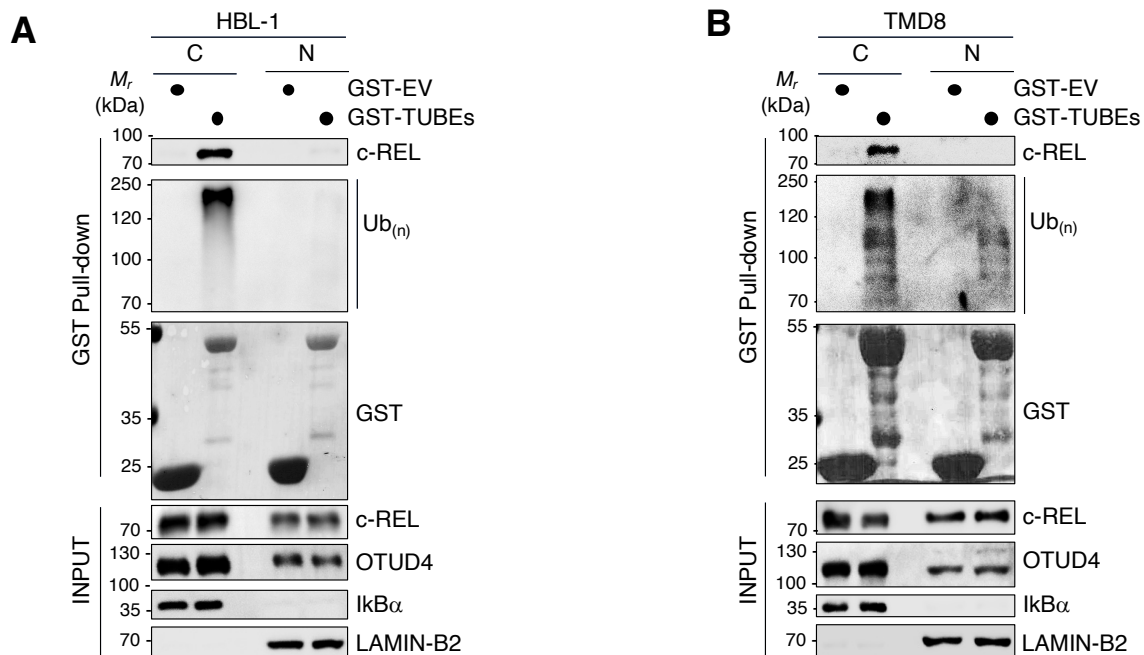


**Fig. 5 c-REL is ubiquitinated in DLBCL. (A and B)** Ubiquitin regulation of c-REL in DLBCL. Fractionated lysates from HBL-1 (A) and TMD8 (B) were incubated with GST or GST-TUBEs. Western blot of GST or GST-TUBEs pull-downs was performed, and ubiquitinated proteins were blotted against the depicted antibodies.

## 6.2 OTUD4 regulates c-REL ubiquitination and proteasomal degradation

### 6.2.1 *OTUD4* downregulation enhances c-REL ubiquitination

To investigate *OTUD4*'s function in ubiquitin regulation of c-REL, I generated a DLBCL BJAB cell line lentivirally transduced to stably express His(6x)-ubiquitin. I then silenced *OTUD4* using short hairpin RNA (shRNA) and performed a nickel pull-down of ubiquitinated protein in the presence (Scramble shRNA control) or absence of *OTUD4* (*OTUD4* shRNA). I observed the prominent appearance of a higher molecular weight band of c-REL upon *OTUD4* downregulation compared to the control sample. In addition, although at a lower level, I detected a molecularly lower c-REL band in *OTUD4*-silenced cells (Fig. 6A and 6B).

To quantify the amount of ubiquitinated c-REL peptides, I did a similar nickel pull-down experiment from SILAC labeled *OTUD4*-downregulated cells and unlabeled

control cells (Fig. 6C). MS-analysis, done by Jana Zecha, of the nickel beads revealed an abundance of c-REL ubiquitinated peptides in the absence of *OTUD4* along with other proteins known to be part of the NF $\kappa$ B signaling pathway (Fig. 6D).

Of note, peptides of MyD88 were not detected in *OTUD4*-silenced cells, although reported as an *OTUD4* substrate in MEFs (Zhao et al., 2018). These results suggest that *OTUD4* depletion increase the levels of c-REL ubiquitination in DLBCL.

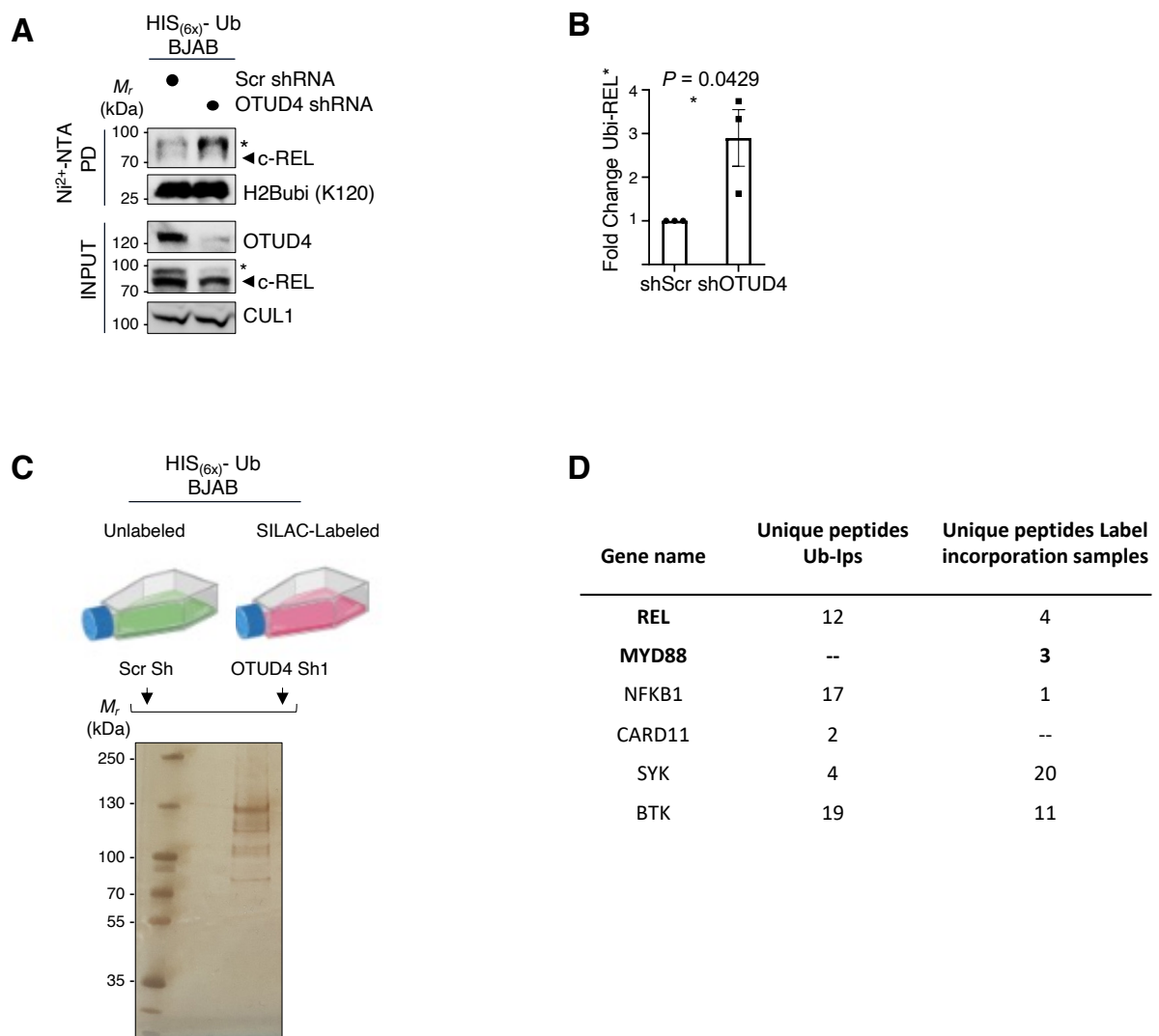


**Fig. 6** *OTUD4* depletion increases c-REL ubiquitination in DLBCL. **(A)** Ubiquitination of REL in the presence and absence of *OTUD4*. Pull-downs of REL from shRNA scramble or shRNA *OTUD4*-silenced DLBCL BJAB cells expressing His-tagged ubiquitin using Ni-NTA beads. Pulled-down proteins were blotted against ubiquitinated-histone 2B (ubiquitin-K120-H2B) as a positive control or against c-REL. The asterisk (\*) depicts a band of c-REL with lower mobility than expected (arrow). **(B)** Quantification of the slower migrating



band of c-REL (\*) bound to nickel beads in A. In 3 independent experiments, quantification of c-REL signal was done by normalizing the c-REL signal to the H2Bubi control signal. The error bar represents the mean  $\pm$  S.D, n = 3. Significance was analyzed by a parametric paired t-test. (C) Silver staining of the nickel-pulled ubiquitinated proteins. (D) List of ubiquitinated peptides found to be significantly ubiquitinated in *OTUD4*-silenced cells relative to the scramble control. MS experiments and analysis in D was done by Jana Zecha (TUM, Proteomics and Bioanalytics).

### 6.2.2 *OTUD4* downregulation accelerates c-REL proteasomal degradation

Next, I tested the stability of c-REL in different lymphoma cell lines. In the NF $\kappa$ B activated DLBCL cell line OCI-LY3, c-REL was rapidly degraded upon Cycloheximide treatment (Fig. 7A), while, in MedB-1, a primary mediastinal B-cell lymphoma (PMBL) cell line, it remained stable over a time course of eight hours (Fig. 7B).

I further tested c-REL stability in BJAB, a GC DLBCL cell line, cells and detected an apparent decrease of c-REL levels. This decrease was rescued by treating the cells with the proteasomal inhibitor MG132 for four hours (Fig. 7C). Since I observed an accumulation of ubiquitinated c-REL in His(6x)-ubiquitin expressing BJAB cells, I performed a similar stability assay upon *OTUD4* downregulation. I found a decrease of a higher molecular band of c-REL in control shRNA scramble expressing cells over a time period of 8 hours, which could be rescued with proteasomal inhibition. On the contrary, I noticed a stable lower band of c-REL that was not affected throughout the experiment, suggesting a c-REL isoform that is not degraded by the UPS. Interestingly, the MG132-rescued higher MW band of c-REL was absent in *OTUD4* silenced cells, whereas the stable lower band was diminished (Fig. 7D).

As a known substrate of OTUD4, MyD88 stabilization was affected in *OTUD4*-downregulated cells (Zhao et al., 2018). These results point to OTUD4 as a DUB that stabilizes c-REL in lymphoma.

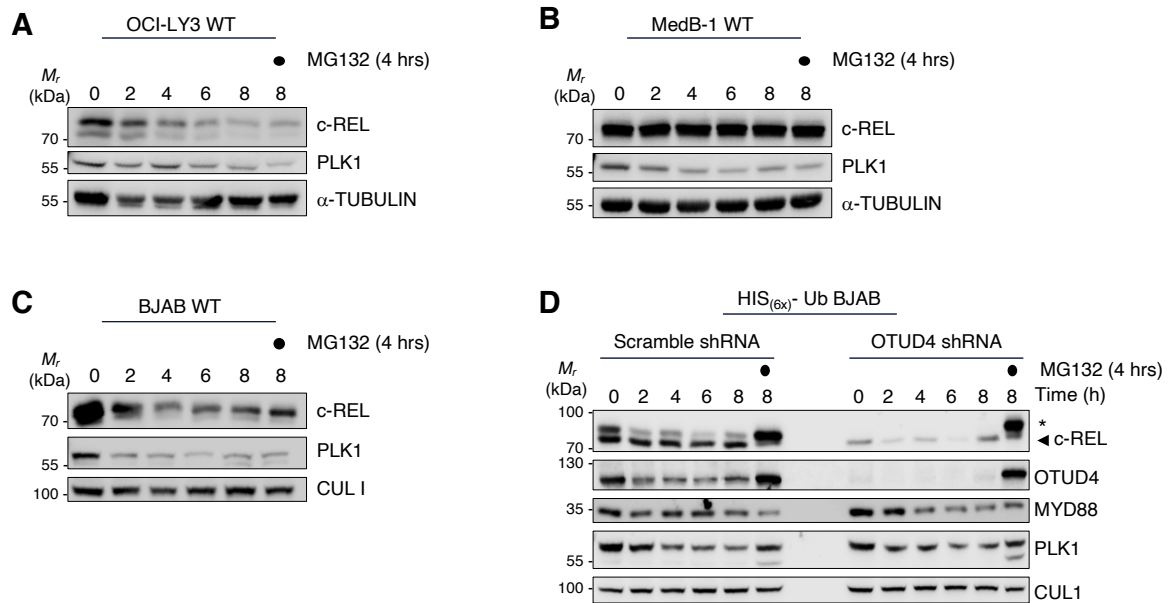


**Fig. 7 OTUD4 regulates the proteasomal degradation of c-REL. (A-D)** Cycloheximide time course of OCI-LY3 WT in A, MedB-1 WT in B, BJAB WT in C, and His(6x)- Ub BJAB in D. Samples were collected at the indicated time points and under 4h of proteasomal inhibition (MG132, 10 mM) when indicated. Cell extracts were blotted against shown antibodies. The asterisk (\*) depicts a higher MW band of c-REL (arrow). WT; wild type.

### 6.2.3 OTUD4 deubiquitinates c-REL in the cytoplasm

To validate OTUD4-mediated cleavage of ubiquitin signals from c-REL, I performed in vivo c-REL deubiquitination assays in fractionated HEK293T cells upon OTUD4 overexpression and downregulation. Overexpression of OTUD4 resulted in a clear decrease in the total ubiquitination signal of c-REL in the cytoplasmic fraction compared to the overexpression of the empty vector control (Fig. 8A and 8B). On the other hand, when I silenced *OTUD4* with shRNA and repeated the same experiment, I found that *OTUD4* downregulation increased the cytoplasmic c-REL total ubiquitination signal (Fig. 8C and 8D).

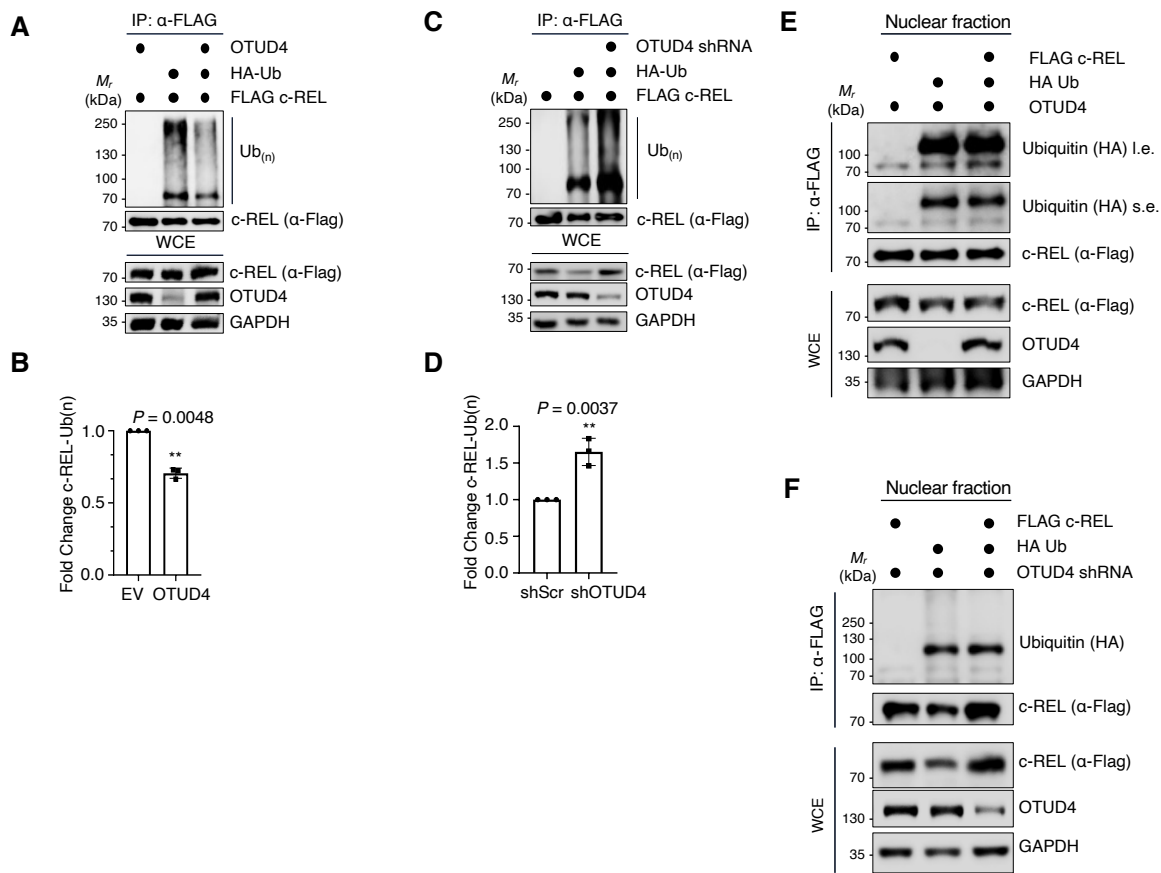


**Fig. 8 OTUD4 deubiquitinates c-REL in the cytoplasm.** (A) FLAG-tagged c-REL was co-overexpressed with HA-tagged ubiquitin and immunoprecipitated from cytoplasmic fraction under denaturing conditions in the presence of OTUD4 over-expression and blotted as shown. (B) Quantification of the ubiquitinated c-REL in A. The ubiquitination signal of immunoprecipitated c-REL quantified after normalization to the FLAG signal in 3 independent experiments. The error bar represents the mean  $\pm$  S.D,  $n = 3$ . Significance was analyzed by a parametric paired t-test. (C) Ubiquitination of c-REL upon *OTUD4* downregulation. As indicated, FLAG-tagged c-REL was co-overexpressed with HA-ubiquitin in HEK293T cells, and FLAG IPs were performed from cytoplasmic fractions under denaturing conditions upon control or *OTUD4* downregulation. As shown, samples of immunoprecipitated FLAG-c-REL were blotted against a FLAG or a ubiquitin antibody. (D) Quantification of the ubiquitination signal of immunoprecipitated c-REL in C. In 3 independent experiments, the signal of the ubiquitinated c-REL was normalized to the FLAG control signal. The error bar represents the mean  $\pm$  S.D,  $n = 3$ . Significance was analyzed by a parametric paired t-test. (E-F) The experiment was done similar to A and B, respectively, but the FLAG IPs were performed from nuclear fractions.



Neither OTUD4 overexpression nor its knockdown affected ubiquitination of c-REL in nuclear fractions (Fig. 8E and 8F). Taken together, these results indicate that OTUD4 modulates c-REL deubiquitination mainly in the cytoplasm.

#### **6.2.4 OTUD4 catalytic activity is necessary for c-REL deubiquitination**

OTUD4 catalytic activity was described as dispensable for its K48 mediated DUB activity, while the K63 function showed total dependence on the presence of the active site cysteine C45 (Das et al., 2019; Zhao et al., 2018).

To investigate whether OTUD4 active site is necessary for the modulation of c-REL stability and deubiquitination, I compared the full-length OTUD4 (isoform 4 NP\_001352986.1) versus a shorter isoform missing the first 65 N-terminal amino-acid residues and hence lacking the catalytic cysteine C45 (isoform 3 NP\_001096123.1) (Fig. 9A). Remarkably, the stabilization of the endogenous c-REL levels was observed only upon overexpression of OTUD4 isoform 4 (Fig. 9B and 9C). Accordingly, full-length OTUD4, but not OTUD4 isoform 3, decreased c-REL total ubiquitination levels (Fig. 9C). Together, my in vivo deubiquitination results suggest that the catalytic C45 present in OTUD4 isoform 4, but not in OTUD4 isoform 3, is responsible for the deubiquitination and stabilization of c-REL.

### **6.3 OTUD4 regulates nuclear levels of c-REL**

#### **6.3.1 *OTUD4* downregulation destabilizes c-REL in DLBCL**

To investigate OTUD4-mediated regulation of c-REL stability in DLBCL, I downregulated *OTUD4* in two different DLBCL cells lines representing the classical subtypes: GCB-like and ABC-like DLBCL. In the ABC-DLBCL cell line HBL-1, *OTUD4* was inactivated by CRISPR Cas9, while in the GCB-DLBCL BJAB cells, OTUD4 was silenced by shRNA. *OTUD4* downregulation in both cell lines distinctly caused a loss of endogenous c-REL relative to the non-targeting scrambled control (Fig. 10A-C). These results show that OTUD4 regulates the stability of endogenous c-REL in DLBCL.

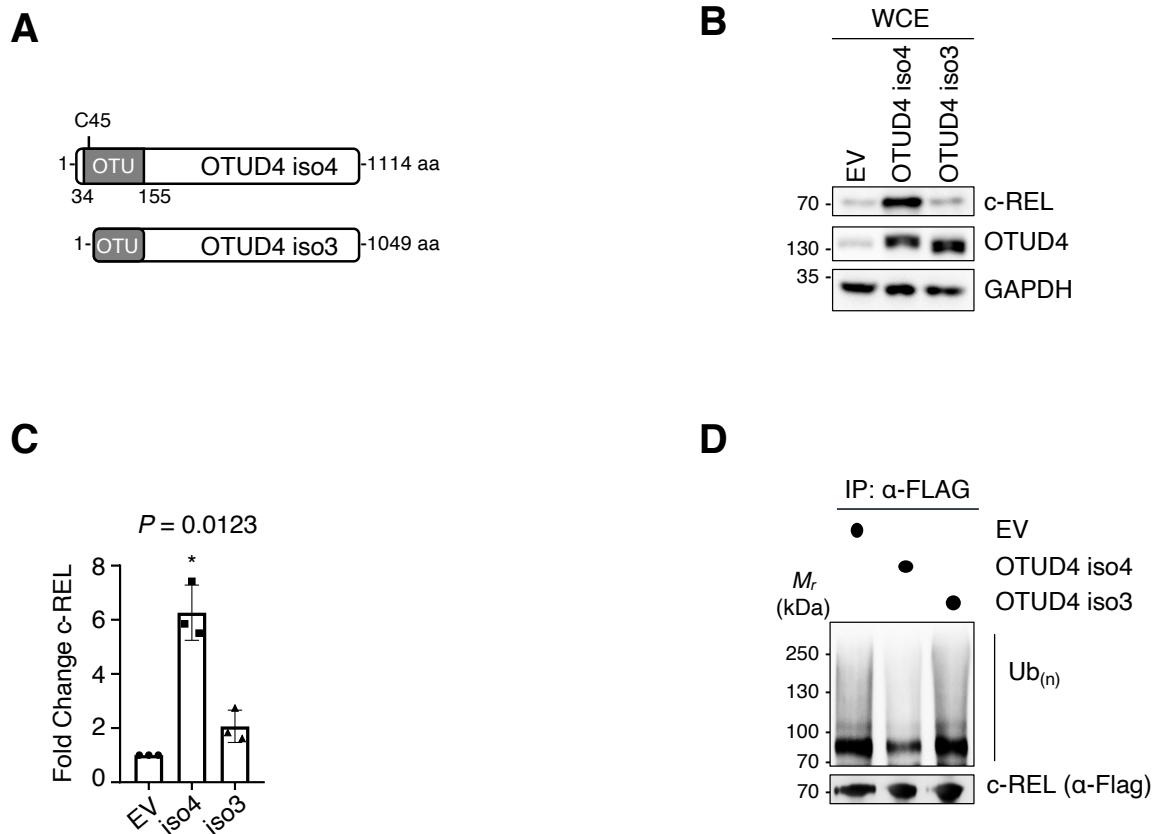


**Fig. 9 c-REL stabilization by OTUD4 isoforms.** (A) Schematic diagram of OTUD4 isoforms. aa; amino acids (B) whole cell extracts of HEK293T cells overexpressing empty vector (EV) or OTUD4 isoforms 4 and 3. Samples were blotted against the indicated antibodies. (C) Quantification of the c-REL levels in B. The c-REL signal representing the endogenous protein abundance was quantified by normalization to the signal of the GAPDH loading control in 3 independent experiments. The error bar represents the mean  $\pm$  S.D,  $n = 3$ . Significance was analyzed by a parametric paired t-test. (D) c-REL deubiquitination by OTUD4 isoforms. FLAG-tagged c-REL was immunoprecipitated from cytoplasmic fraction under denaturing conditions upon overexpression of OTUD4 isoforms and blotted as shown.

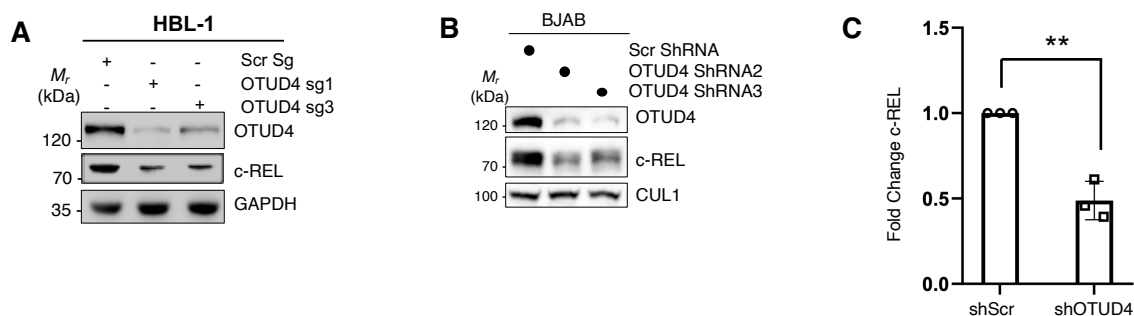


**Fig. 10 OTUD4 stabilizes c-REL in DLBCL.** (A) HBL-1 cells were infected with two different CRISPR sgRNAs targeting *OTUD4* and one Scrambled sgRNA control. Cells were harvested five days post-infection and lysed in standard lysis buffer. Lysates were blotted



against the indicated antibodies. **(B)** whole-cell extracts of *OTUD4*-silenced BJAB cells versus scrambled control. Samples were blotted against the indicated antibodies. **(C)** Quantification of the endogenous c-REL levels in B. The c-REL signal was normalized to the signal of CUL-1 loading control in 3 independent experiments. The error bar represents the mean  $\pm$  S.D,  $n = 3$ . Significance was analyzed by a parametric paired t-test.

### 6.3.2 *OTUD4* depletion diminishes c-REL nuclear localization in DLBCL

In line with the finding that c-REL nuclear accumulation in T cells was dependent on the E3 ligase Peli1 (Chang et al., 2011), I was prompted to test the consequence of *OTUD4* downregulation on the subcellular localization of c-REL. I did a CRISPR Cas9-mediated silencing of *OTUD4* in OCI-LY3 cells, fractionated the *OTUD4*-downregulated cells or the control, and assessed the levels of c-REL in both nuclear and cytoplasmic fractions.

Although the cytoplasmic c-REL was not affected, a massive decrease in c-REL nuclear levels was observed in the absence of *OTUD4* in western blot experiments (Fig. 11A and 11B). Immunofluorescence imaging of the same cells confirmed the western blot results and highlighted the co-localization of c-REL and *OTUD4* in the cytoplasm (Fig. 11C and 11D). Collectively, these data highlight the regulatory role of *OTUD4* in c-REL nuclear localization in DLBCL.

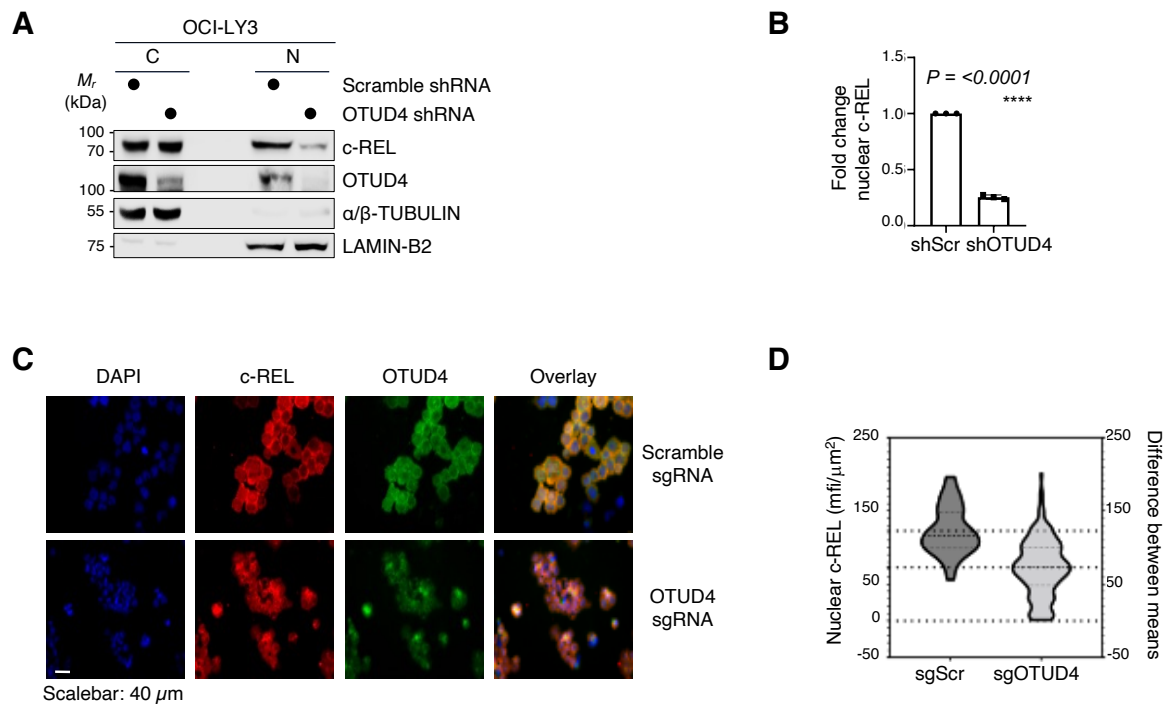


**Fig. 11 OTUD4 regulates the nuclear localization of c-REL in DLBCL.** (A) OTUD4-dependent nuclear localization of c-REL in DLBCL OCI-LY3 cells. Control or *OTUD4* depleted Cas9-expressing OCI-LY3 cells were fractionated into cytoplasmic (C) or nuclear (N) extracts and blotted against the depicted antibodies. (B) Quantification of the nuclear c-REL levels in A. In 3 independent experiments, the c-REL levels were normalized to the levels of the nuclear marker LAMIN-B2. The error bar represents the mean  $\pm$  S.D,  $n = 3$ . Significance was analyzed by a parametric paired t-test. (C) Representative immunofluorescence images of the same cells in A and stained with the antibodies for endogenous c-REL (red) and OTUD4 (green). DNA was stained with DAPI (blue). (D) Quantification of the nuclear signal of c-REL in C. Mean fluorescence intensity (MFI) per square micrometer of c-REL signal in the nucleus was measured. The difference between means is indicated in a violin diagram.

### 6.3.2 *OTUD4* downregulation decreases c-REL nuclear accumulation in PDAC

To validate the effects of *OTUD4* depletion on c-REL nuclear localization observed in DLBCL in another cancer entity, I used the pancreatic cancer cell line MIA PaCa-2 where c-REL was linked to apoptosis resistance (Geismann et al., 2014). I downregulated *OTUD4* by shRNA and fractionated the control or the *OTUD4*-silenced cells into cytoplasmic and nuclear fractions. Similar to the experiments in DLBCL cell lines, *OTUD4* depletion resulted in a noticeable reduction of c-REL nuclear levels while the cytoplasmic levels remained essentially unchanged (Fig. 12A and 12B). Confocal imaging asserted the western blot data and revealed the cytoplasmic occurrence of OTUD4 in PDAC cells (Fig. 12C and 12D).

In conclusion, this data present OTUD4 as a regulator of c-REL nuclear localization in PDAC.

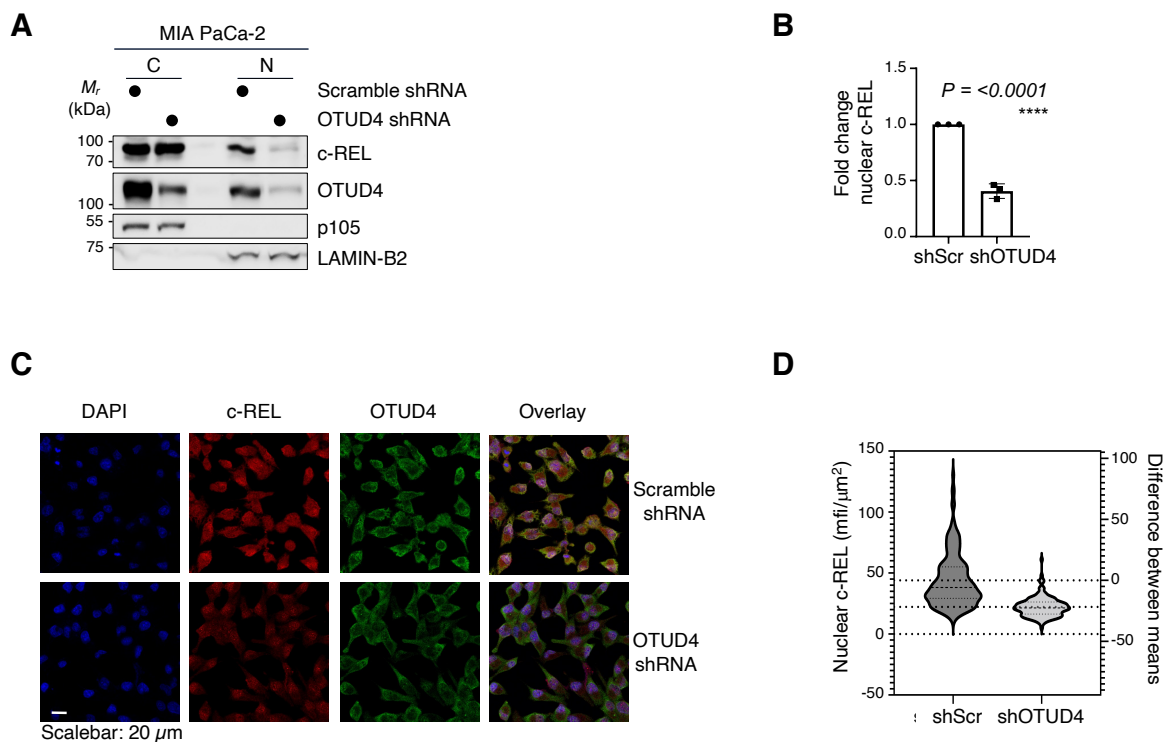


**Fig. 12 OTUD4 regulates c-REL nuclear localization in PDAC.** (A) OTUD4-dependent nuclear localization of c-REL in PDAC MIA PaCa-2 cells. Control or *OTUD4*-depleted cells were fractionated into cytoplasmic (C) or nuclear (N) extracts and blotted against the depicted antibodies. (B) Quantification of the endogenous nuclear c-REL levels in A. The c-REL levels were normalized to the levels of the nuclear marker LAMIN-B2 in 3 interdependent experiments. The error bar represents the mean  $\pm$  S.D,  $n = 3$ . Significance was analyzed by a parametric paired t-test. (C) Representative immunofluorescence images of the same cells in A cells and stained with the antibodies for endogenous c-REL (red) and OTUD4 (green). DNA was stained with DAPI (blue). (D) Quantification of the nuclear signal of c-REL in C. Mean fluorescence intensity (MFI) per square micrometer of c-REL signal in the nucleus was measured. The difference between means is indicated in a violin diagram.

## 6.4 OTUD4 negatively regulates NF $\kappa$ B in a DLBCL reporter cell line

### 6.4.1 *OTUD4* downregulation enhances NF $\kappa$ B activity in a DLBCL reporter cell line

c-REL nuclear localization is a cardinal consequence of NF $\kappa$ B activation mediated by continuous B cell receptor signaling (Kober-Hasslacher & Schmidt-Supprian, 2019). I showed earlier that OTUD4 regulates c-REL nuclear accumulation. While OTUD4 was reported to negatively modulate NF $\kappa$ B activity in MEFs by K63-deubiquitinating MyD88 (Zhao et al., 2018), I sought to investigate the effect of

silencing *OTUD4* on NF $\kappa$ B activation in ABC-like DLBCL using an EGFP-NF $\kappa$ B reporter HBL-1 cell line (provided by Prof. Daniel Krappmann, unpublished). I downregulated *OTUD4* in the reporter cells by two shRNAs, FACS-purified the *OTUD4*-depleted population, and analyzed the NF $\kappa$ B activity by measuring the EGFP intensity by flow cytometry. *OTUD4* depletion markedly increased NF $\kappa$ B activation in HBL-1 cells (Fig. 13 A-D). In line with the published literature, my preliminary results show that *OTUD4* negatively regulates NF $\kappa$ B reporter activity in HBL-1 ABC-like DLBCL cells. However, further experiments are needed to provide a supporting evidence.

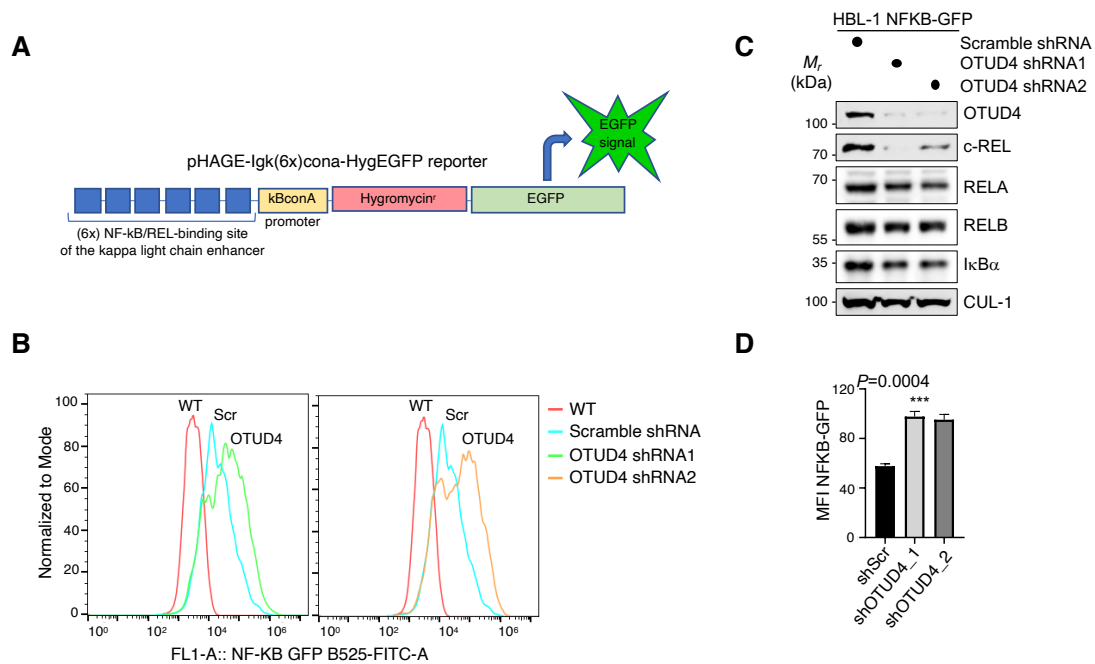


**Fig. 13 OTUD4 modulates NF $\kappa$ B transcription activity.** (A) Scheme of the NF $\kappa$ B reporter introduced in HBL-1 cell line provided by Prof. Daniel Krappmann. (B) Flow cytometry of NF $\kappa$ B reporter assay in HBL-1 cells expressing enhanced green fluorescent protein (EGFP) under a promoter dependent on NF $\kappa$ B transcriptional activity. The fluorescence of NF $\kappa$ B reporter-HBL-1 cells was measured after transfection with Scramble shRNA or two different *OTUD4* shRNAs to downregulate *OTUD4*. The Mean Fluorescence Intensity (MFI) was normalized to Mode. Wild-type (WT) HBL-1 cells (no NF $\kappa$ B reporter) were used as negative control. (C) Western-blot showing efficient *OTUD4* downregulation of cells used in B. Cell extracts were blotted against the indicated antibodies. (D) Quantification of MFI of the EGFP signal in B. The error bar represents the mean  $\pm$  S.D,  $n = 3$ . Significance was analyzed by a parametric paired t-test comparing each of *OTUD4* shRNAs to the scramble shRNA control.



## 6.5 OTUD4 is essential for the expansion of cancer cells

### 6.5.1 OTUD4 is critical for the competitive expansion of cancer cells

c-REL has been implicated in the pathogenesis of lymphoma as well as solid cancers. To assess the biological consequences of *OTUD4* downregulation in tumor cells, I silenced *OTUD4* using three different ds-Red expressing shRNAs constructs and analyzed the competitive expansion of DLBCL HBL-1 and BJAB cell lines by measuring the dsRed intensity by flow cytometry. Silencing of *OTUD4* clearly compromised the expansion of ABC-type HBL-1 cells and, albeit to a lesser extent, GCB-type BJAB cells (Fig. 14 A-D). The phenotype observed upon *OTUD4* downregulation in DLBCL was conserved in the PDAC MIA PaCa-2 cell line (Fig. 14 E-F). Therefore, my results suggest the indispensability of OTUD4 for the expansion of the investigated DLBCL and PDAC cell lines in vitro.

## 6.6 OTUD4 as a prognostic marker

### 6.6.1 OTUD4 expression correlates with c-REL in DLBCL

My in vitro experiments indicated a robust post-translational regulation of c-REL nuclear accumulation by OTUD4; hence I aimed to extrapolate such findings in human patients' samples. In a cohort of fifty-five DLBCL patients, Katja Steiger (TUM, Pathology) did an immunohistochemical staining of tumor tissues with both OTUD4 and c-REL antibodies and analyzed the correlation between the two proteins.

Interestingly, non-GC DLBCL patients with elevated c-REL levels showed a high expression of OTUD4, while those GC patients with low c-Rel expression had a low expression of OTUD4 as well (Fig. 15 A-B). As previously shown, *OTUD4* downregulation diminished c-REL nuclear accumulation in the DLBCL OCI-LY3 cell line; Katja further investigated if there is any correlation between the localization of OTUD4 and c-REL in patients' tissues. Intriguingly, she found a statistically significant correlation between cytoplasmic OTUD4 expression intensity and the nuclear levels of c-REL (Fig. 15C).

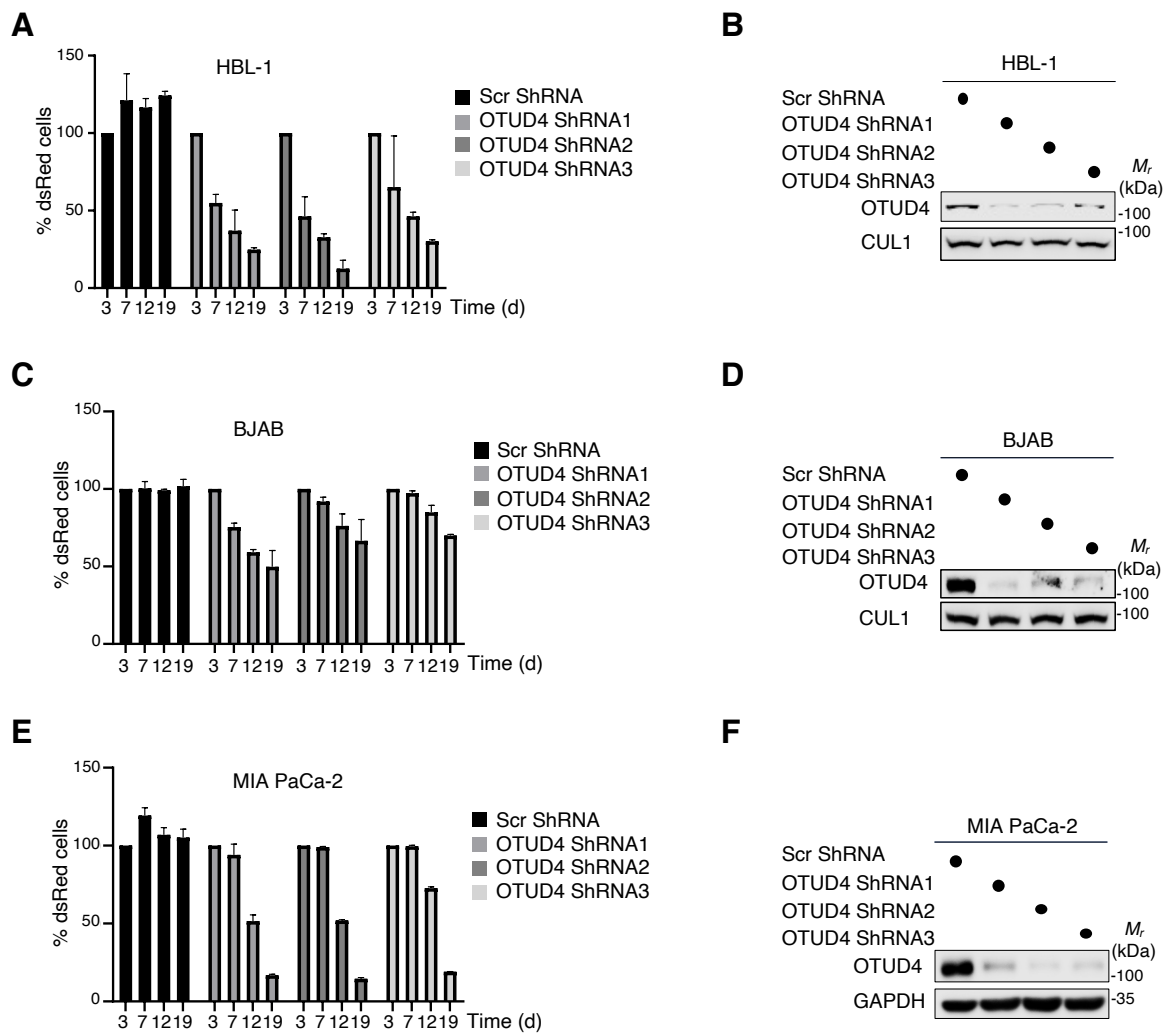


**Fig. 14 Loss of OTUD4 compromises the expansion of cancer cells.** (A) HBL-1 cells were infected with dsRed-expressing scramble shRNA or *OTUD4* shRNAs in a competitive co-culture with unmodified HBL-1 cells. Flow cytometric analysis of the dsRed-expressing population was done as a ratio of shRNA expressing, dsRED positive cells to uninfected cells at the indicated time points after infection. Results are presented in relation to day 3. The error bar represents the mean  $\pm$  S.D,  $n = 3$ . (B) Western blot showing efficient knockdown of *OTUD4*. (C-D) Experiments similar to A and B, performed in the BJAB cell line. (E-F) Experiments similar to A and B, performed in the MIA PaCa-2 cell line.

Furthermore, my analysis of *OTUD4* RNA expression in the GEPIA pipeline's (Tang et al., 2017) DLBCL dataset showed a statistically significant expression of *OTUD4* transcripts in the DLBCL patient compared to the healthy control group (Fig. 15D). Together, my results indicate a robust correlation between the cytoplasmic *OTUD4* expression and the nuclear c-REL levels in DLBCL patient samples.

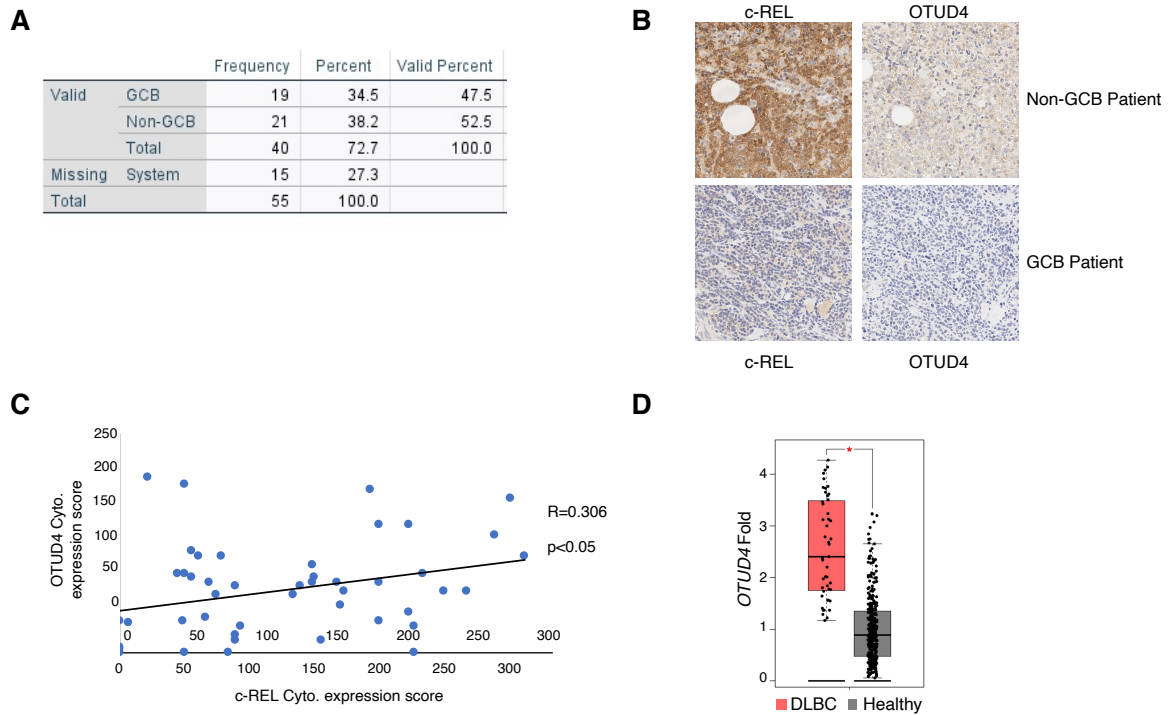


**Fig. 15 OTUD4 expression correlates with c-REL in DLBCL.** (A) A summary table of the fifty-five DLBCL patient's cohort shows the Hans classification. (B) Histological analysis of DLBCL patient tissues stained with c-REL and OTUD4 antibodies. (C) Correlation analysis between cytoplasmic OTUD4 intensity signal and nuclear c-REL signal. Analysis was done by SPSS software. (D) Gene expression analysis of *OTUD4* in DLBCL patients versus healthy volunteer group. The box plot is blotted as a log scale. Data retrieved from GEPIA pipeline. The experiments (A-C) were conducted by Katja Steiger (TUM, Pathology).

## 7 Discussion

### 7.1 c-REL is a target of the ubiquitin-proteasome system

As a transcription factor, c-REL has been established to play a crucial role in the developmental regulation of B cells. Moreover, its importance in lymphoma is underscored by the frequent gain or amplification of its gene locus (Kober-Hasslacher & Schmidt-Supprian, 2019).

Various post-translational modifications of c-REL were elucidated, including phosphorylation, ubiquitination, and glycosylation (Chang et al., 2011; Chen et al., 1998; Harris et al., 2006; Ramakrishnan et al., 2013; Sánchez-Valdepeñas et al., 2006). Since ubiquitination is a prominent post-translational process that regulates protein levels, this thesis sought to investigate the ubiquitin regulation of c-REL especially after a recent study showed that c-Rel protein levels are regulated by robust post-transcriptional mechanisms during terminal B cell differentiation (Kober-Hasslacher et al., 2020). A limited body of literature highlighted c-REL ubiquitination, with one study describing Peli1 as an E3 ligase that modulates c-REL ubiquitination and nuclear localization in T cells (Chang et al., 2011; Chen et al., 1998).

My study aimed to identify the ubiquitin modifying E3 ligases and DUBs interacting with c-REL in B cell lymphoma. Performing a mass spectrometric screen of affinity-purified c-REL mixed with lysates from the B cell lymphoma cell line MedB-1, the E3 ubiquitin ligase TRIM33 and the DUB OTUD4, among others, were identified as ubiquitin machinery components potentially interacting with c-REL. This result prompted my investigation of the ubiquitin regulation of c-REL in the context of B cell lymphoma.

GST-TUBEs Pulldown assays from the fractionated two DLBCL cell lines, HBL1 and TMD8, provided evidence of c-REL ubiquitination that appeared to be in the cytoplasmic fraction only. Although comparable levels of endogenously expressed c-REL were observed in the nuclear lysates, the GST-pulled ubiquitinated c-REL was detected mainly in the cytoplasm. Since these cell lines are representative models of the NF $\kappa$ B activated DLBCL subtype where c-REL nuclear localization occurs in response to the BCR activation, it remains to be elucidated whether c-REL nuclear accumulation is dependent on its ubiquitination in the cytoplasm in B cells.



Because c-REL does not have any known nuclear export sequence that results in sustaining NF $\kappa$ B activation (Fagerlund et al., 2008; Tam et al., 2001), it will be interesting to examine if induced nuclear ubiquitination of c-REL would shuttle it out of the nucleus and terminate its transcriptional activity.

## 7.2 c-REL-OTUD4 interaction

DUBs constitute an essential arm of the ubiquitin machinery that prevents the ubiquitin signal from being constitutively on. USP7 was the only reported DUB to directly deubiquitinate NF $\kappa$ B subunits in the nucleus, therefore mediating their DNA binding (Mitxitorena et al. 2020). However, no DUBs have been described to date to modulate c-REL ubiquitination.

In Vanesa Fernández's mass spectrometric screen, I identified OTUD4 as the topmost interacting DUB of c-REL. The involvement of OTUD4 in regulating NF $\kappa$ B signaling was first reported by Zhao et al. In their study, they unraveled that OTUD4 negatively regulated NF $\kappa$ B by deubiquitinating the TLR associated factor MyD88 (Zhao et al., 2018). Additionally, in a yeast two-hybrid (Y2H) screen, OTUD4 was identified to interact with c-REL (Rolland et al., 2014). The established connection between OTUD4 and NF $\kappa$ B signaling, along with The Y2H screen and Vanesa's mass spectrometric findings, encouraged me further to validate OTUD4 as a potential interacting candidate of c-REL.

I showed with biochemical immunoprecipitation experiments a specific interaction of OTUD4 with c-REL in the presence of negative control of the same DUB family. Despite the weak molecular interaction of DUBs with their substrates, I confirmed the endogenous interaction between c-REL and OTUD4 in DLBCL cells as well. I further tested the spatial interaction of OTUD4 with c-REL based on their reported dynamic translocation between the cytoplasm and nucleus (Kober-Hasslacher & Schmidt-Supprian, 2019; Zhao et al., 2015). While similar levels of FLAG-tagged c-REL were immunoprecipitated from both cytoplasmic and nuclear compartments, c-REL was bound to OTUD4 only in the cytoplasmic fraction. This finding goes in line with the literature indicating that OTUD4 is primarily cytoplasmic (Zhao et al., 2015), hence its interactions are supposed to occur mainly in the cytoplasm.

### 7.3 OTUD4-mediated stabilization and deubiquitination of c-REL

The ubiquitin-proteasome system (UPS) is an elaborate quality control system regulating the turnover of cellular proteins. Proteasomal degradation of proteins is a sequential process that starts with tagging the destined protein with ubiquitin molecules. Once ubiquitinated, the protein gets recognized by the large multicatalytic 26S proteasome that breaks it down into smaller peptides (Lecker et al., 2006).

After Cycloheximide-mediated inhibition of the nascent ribosomal protein synthesis, I showed that c-REL is proteasomally degraded in OCI-LY3 and BJAB cell lines representing the ABC-like and GCB-like subtypes of DLBCL, respectively. The proteasomal degradation of c-REL was validated by proteasomal inhibition MG132 rescuing the degradation of c-REL clearly in BJAB and to a lesser extent in OCI-LY3. The rate and the intensity of c-REL degradation in BJAB cells were markedly increased in upon *OTUD4* downregulation, suggesting a stability-mediated regulation by OTUD4. Surprisingly, in a similar stability time-course experiment of eight hours, c-REL remained stable in the Primary mediastinal B-cell lymphoma cell line MedB-1. The divergence of c-REL sensitivity to proteasomal degradation among different lymphoma cell lines requires further investigation. The existence of two different lymphoma splice variants of the *REL* transcript, with one found to have higher transactivation activity in vitro (Leeman et al., 2008; Leeman & Gilmore, 2008), may suggest that the resistance of c-REL to proteasomal degradation in the MedB-1 lymphoma cell line could be splicing-driven. Fine-tuning of c-REL levels by proteasomal degradation might exert an additional control for c-REL translocation and nuclear localization.

This study presents OTUD4 as the first DUB described to inhibit ubiquitination and proteasomal degradation of c-REL in B cell lymphoma. As a multifaceted DUB, OTUD4 was reported to possess K48 and K63 deubiquitinating activities. While OTUD4's K48 DUB activity appeared to be independent of the active catalytic site, the active cysteine C45 site was reported to be indispensable for OTUD4 to exert its K63 deubiquitinating function (Zhao et al., 2015, 2018). In this study, the active catalytic site of OTUD4 was found to be necessary for the stabilization and deubiquitination of c-REL. Such observations raise the question of investigating the different spliced variants of OTUD4 in lymphoma patients and whether these variants



would have an influence on c-REL stabilization and hence the prognosis of the disease. Additionally, the ubiquitin-chain specificity of the DUB activity of OTUD4 regulating c-REL deubiquitination remains to be discovered.

#### **7.4 OTUD4-dependent regulation of c-REL nuclear localization**

Stimulus-induced NF $\kappa$ B activation promotes the phosphorylation and the proteasomal degradation of the inhibitory I $\kappa$ B proteins. As a result, the NF $\kappa$ B members, sequestered in an inactive state in the cytoplasm by I $\kappa$ B complexes, form homo and heterodimers and translocate into the nucleus to start responsive transcriptional programs (Nagel et al., 2014).

C-REL carries a nuclear localization sequence at its Rel homology domain (RHD) (Gilmore & Gerondakis, 2011), however in most GC B cells, c-REL was found to be predominant in the cytoplasm (Barth et al., 2003). Post-translational modification including phosphorylation was reported to induce c-REL nuclear accumulation. The two kinases IKK $\epsilon$  and TBK1, were identified to phosphorylate c-REL at the C-terminus, leading to its dissociation from the I $\kappa$ B $\alpha$ -c-REL complex and localization into the nucleus. Nevertheless, this phosphorylation event did not impact c-REL transactivation potential (Harris et al., 2006).

Since phosphorylation has often been found to be an initial step preceding ubiquitination (Nguyen et al., 2013), it prompted me to think of the possible role of ubiquitination in c-REL nuclear localization. This notion was further underlined by a study in T-cells that revealed that the nuclear accumulation of c-REL was modulated by the ubiquitin E3 ligase Peli1 (Chang et al., 2011).

Here, I propose a model to regulate c-REL levels and its nuclear translocation beyond the I $\kappa$ Bs. In addition to I $\kappa$ Bs-mediated cytoplasmic retention, an emerging picture of additional complex mechanisms controlling and inducing constitutive c-REL activity in cancer. I described that c-REL deubiquitination in the cytoplasm by OTUD4 results in stabilizing c-REL from proteasomal degradation and allows for its further nuclear accumulation in lymphoma cell line. Inhibition of MyD88 excluded the possibility that c-REL destabilization is mediated by MyD88 as a published substrate of OTUD4 (data not shown).



The association of c-REL with solid cancer received attention over the recent years. Along with RELA, c-REL potentiated the Ras-mediated transformation of murine embryonic fibroblast (MEF) cells (Hanson et al., 2004). Moreover, Ras mutation was linked to the enhanced nuclear localization of c-REL in the lung cancer Ras-transformed mouse model (Meylan et al., 2009). This thesis showed that the OTUD4-mediated stabilization and nuclear accumulation of c-REL is conserved in the pancreatic carcinoma MIA PaCa-2 cell line as well. It remains to be addressed whether this regulatory mechanism of c-REL nuclear shuttling occurs as a downstream event to c-REL phosphorylation or constitutes a phosphorylation-independent ubiquitin-mediated regulation.

## 7.5 OTUD4 modulation of NF $\kappa$ B activity in DLBCL

The first connection between OTUD4 and NF $\kappa$ B was established by the study describing OTUD4 as the DUB of the TLR associated factor MyD88. It was shown that the phosphorylation of OTUD4 near its catalytic site activated a latent K63 DUB activity against MyD88. Since MyD88 is a critical scaffold protein that recruits downstream effector proteins important for NF $\kappa$ B signaling, they concluded that the K63 OTUD4-mediated deubiquitination in MEFs disrupted the recruitment of IRAK and TRAF6 proteins hence negatively regulating the NF $\kappa$ B signaling (Zhao et al., 2018).

Herein, I used the EGFP- NF $\kappa$ B reporter DLBCL cell line HBL-1 to examine how OTUD4 would modulate NF $\kappa$ B signaling in B cells. Flow cytometry analysis of *OTUD4*-depleted cells manifested an increased activation of the NF $\kappa$ B reporter compared to the control cells.

Nevertheless, the biochemical analysis of these cells confirmed the downregulation of *OTUD4* and highlighted the consequent decrease in the endogenous c-REL levels I have seen before in HBL-1 WT cells. In addition, there was a reduction in the levels of both I $\kappa$ B $\alpha$  and RELA. In line with the published literature (Zhao et al., 2018), my data confirmed the negative modulatory role of OTUD4 in NF $\kappa$ B signaling, although the cellular context is different. This speculated modulation in lymphoma is very preliminary and need to be further validated by imaging flow cytometry experiments where nuclear localization of RELA and c-REL



can be visualized by imaging and the expression levels can be quantified by flow cytometry simultaneously.

Since BCR-mediated activation of the canonical NF $\kappa$ B pathway would result in degradation of I $\kappa$ B $\alpha$  and an enhanced expression of both c-REL and RELA, it needs further investigation to understand whether c-REL and RELA would have repressive roles in the context of DLBCL. RELA was shown to act as a repressor inducing apoptosis when stimulated with UV-C and Daunorubicin (Campbell et al., 2004). In a recent study, c-REL was reported to act as a transcription repressor of RELA-mediated inflammatory genes (de Jesús & Ramakrishnan, 2020). Therefore, it remains open to address if c-REL and RELA would have antagonizing regulatory roles towards each other in the context of B cell lymphoma. It is still needed to assess whether any of them has a stronger transcriptional activity and would act as a suppressor of the other.

## 7.6 The emerging role of OTUD4 in Cancer

Diverse roles of OTUD4 were uncovered over recent years. OTUD4 was implicated in DNA damage responses by acting as a positive regulator of the alkylation repair demethylases ALKBH2 and ALKBH3 (Zhao et al., 2015). In addition, OTUD4 was proposed to act as RNA binding protein involved in stress granules formation (Das et al., 2019). Moreover, the role of OTUD4 in innate immune signaling was highlighted by deubiquitinating MyD88 (Zhao et al., 2018) and was also involved in antiviral immunity by deubiquitinating and stabilizing MAVS (Liuyu et al., 2019). In contrast, the role of OTUD4 in cancer is understudied.

c-REL is strongly linked to different human malignancies, including DLBCL and solid cancers. As discussed earlier, I established OTUD4 as the DUB of c-REL regulating its nuclear localization. Hence, in the last part of this thesis, I assessed the biological consequences of *OTUD4* downregulation on the expansion of different tumor cells lines. I tested the effect of *OTUD4* silencing on the competitive expansion of three different cell lines representing two distinct tumor entities: DLBCL and PDAC.

In DLBCL, *OTUD4* shRNA-mediated depletion compromised the expansion of the ABC DLBCL cell line HBL1 and, to a lesser extent, the GC DLBCL BJAB. The compromised expansion of HBL-1 and BJAB cells upon *OTUD4* depletion was



similarly obtained upon *REL* downregulation (data not shown). Similar results were observed when *OTUD4* was silenced in the PDAC cell line MIA PaCa-2, which is known to have activated NF $\kappa$ B signaling. It is still possible that the impact of *OTUD4* downregulation on the expansion of these cancer cells is mediated by yet to be deciphered substrates beyond c-REL.

There is a growing interest in exploiting DUBs as drug targets, given their possession of a well-defined catalytic site and their great diversity. However, the incomplete understanding of DUB biology hinders the development of DUB inhibitor drugs (Harrigan et al., 2018). As a first step of checking the validity of *OTUD4* as a drug target, the expression levels of *OTUD4* were checked in a cohort of fifty-five DLBCL patients subclassified by a pathologist according to the Hans classification system into GC and non-GC patients. Interestingly, this study provided a first observation that *OTUD4* levels correlated among the non-GC patients who showed elevated levels of c-REL as well, while those GC- samples with low c-REL levels had reduced expression of *OTUD4*. Intriguingly, a significant correlation was found between the cytoplasmic levels of *OTUD4* and c-REL nuclear staining. This patient-driven data consolidated the in vitro experiment findings suggesting a regulatory role of *OTUD4* in c-REL nuclear localization in lymphoma patients and a possible influence on the course of the disease.

However, further clinical investigations are still needed to understand the impact of *OTUD4* expression levels on the progression of the disease and response to current therapeutic interventions. Furthermore, *OTUD4* expression in larger cohorts of different B cell lymphoma malignancies would be of clinical benefit to establish *OTUD4* as a prognostic marker in lymphoma.



## 7.7 Conclusion and outlook

This thesis provided new insights into the ubiquitination of c-REL in DLBCL. Although attempts were made to characterize the ubiquitinated sites in c-REL in HEK293T cells by mass spectrometry, no lysine residues were identified. A new strategy to purify c-REL from lymphoma cell lines has been started, but the mass spectrometric analysis is still undergoing.

In addition, my study identified OTUD4 as a novel and critical component of the ubiquitin machinery regulating c-REL stabilization and nuclear localization. Moreover, these results introduced OTUD4 as a possible new vulnerability in DLBCL and PDAC. Nevertheless, further mechanistic exploration is required to understand how OTUD4 affects the expansion of those tumor cells.

To exploit OTUD4 as a therapeutic druggable target, additional work has to be executed to purify a physiologically active form of OTUD4 from human cells for structural studies and in vitro functional assays.

## 7 Literature

- Abramson, Jeremy S., Nilanjan Ghosh, and Sonali M. Smith. 2020. "ADCs, BiTEs, CARs, and Small Molecules: A New Era of Targeted Therapy in Non-Hodgkin Lymphoma." *American Society of Clinical Oncology Educational Book* (40):302–13.
- Akutsu, Masato, Ivan Dikic, and Anja Bremm. 2016. "Ubiquitin Chain Diversity at a Glance." *Journal of Cell Science* 129(5):875–80.
- Barth, Thomas F. E., José I. Martin-Subero, Stefan Joos, Christiane K. Menz, Cornelia Hasel, Gunhild Mechttersheimer, Reza M. Parwaresch, Peter Lichter, Reiner Siebert, and Peter Möller. 2003. "Gains of 2p Involving the REL Locus Correlate with Nuclear C-Rel Protein Accumulation in Neoplastic Cells of Classical Hodgkin Lymphoma." *Blood* 101(9):3681–86.
- Cerhan, James R., Anne Kricker, Ora Paltiel, Christopher R. Flowers, Sophia S. Wang, Alain Monnereau, Aaron Blair, Luigino Dal Maso, Eleanor V. Kane, Alexandra Nieters, James M. Foran, Lucia Miligi, Jacqueline Clavel, Leslie Bernstein, Nathaniel Rothman, Susan L. Slager, Joshua N. Sampson, Lindsay M. Morton, and Christine F. Skibola. 2014. "Medical History, Lifestyle, Family History, and Occupational Risk Factors for Diffuse Large B-Cell Lymphoma: The InterLymph Non-Hodgkin Lymphoma Subtypes Project." *Journal of the National Cancer Institute - Monographs* (48):15–25.
- Chang, Mikyoung, Wei Jin, Jae Hoon Chang, Yichuan Xiao, George C. Brittain, Jiayi Yu, Xiaofei Zhou, Yi Hong Wang, Xuhong Cheng, Pingwei Li, Brian A. Rabinovich, Patrick Hwu, and Shao Cong Sun. 2011. "The Ubiquitin Ligase Peli1 Negatively Regulates T Cell Activation and Prevents Autoimmunity." *Nature Immunology* 12(10):1002–9.
- Chen, Eying, Radmila Hrdlickova, Jiri Nehyba, Dan L. Longo, Henry R. Bose, and Chou Chi H. Lit. 1998. "Degradation of Proto-Oncoprotein c-Rel by the Ubiquitin-Proteasome Pathway." *Journal of Biological Chemistry* 273(52):35201–7.
- Cheson, Bruce D., Grzegorz Nowakowski, and Gilles Salles. 2021. "Diffuse Large B-Cell Lymphoma: New Targets and Novel Therapies." *Blood Cancer Journal* 11(4).
- Clague, Michael J., Igor Barsukov, Judy M. Coulson, Han Liu, Daniel J. Rigden, and Sylvie Urbé. 2013. "From Genes to Organism." *Physiol Rev* 93:1289–1315.
- Crump, Michael, Sattva S. Neelapu, Umar Farooq, Eric Van, Den Neste, John Kuruvilla, Jason Westin, Brian K. Link, Annette Hay, James R. Cerhan, Liting Zhu, Sami Boussetta, Lei Feng, Matthew J. Maurer, Lynn Navale, Jeff Wiezorek, William Y. Go, and Christian Gisselbrecht. 2017. "Outcomes in Refractory Diffuse Large B-Cell Lymphoma: Results from the International SCHOLAR-1 Study Key Points." *Blood*. 130(16):1800-1808.



- Das, Richa, Lukas Schwintzer, Stanislav Vinopal, Eva Aguado Roca, Marc Sylvester, Ana Maria Oprisoreanu, Susanne Schoch, Frank Bradke, and Meike Broemer. 2019. "New Roles for the De-Ubiquitylating Enzyme OTUD4 in an RNA-Protein Network and RNA Granules." *Journal of Cell Science* 132(12).
- de Jesús, Tristan James, and Parameswaran Ramakrishnan. 2020. "NF- $\kappa$ B c-Rel Dictates the Inflammatory Threshold by Acting as a Transcriptional Repressor." *IScience* 23(3).
- Du, Jiansen, Lin Fu, Yingli Sui, and Lingqiang Zhang. 2020. "The Function and Regulation of OTU Deubiquitinases." *Frontiers of Medicine* 14(5):542–63.
- Durand, Joel, Qing Zhang, and Albert Baldwin. 2018. "Roles for the IKK-Related Kinases TBK1 and IKK $\epsilon$  in Cancer." *Cells* 7(9):139.
- Fagerlund, Riku, Krister Melén, Xinmin Cao, and Ilkka Julkunen. 2008. "NF- $\kappa$ B P52, RelB and c-Rel Are Transported into the Nucleus via a Subset of Importin  $\alpha$  Molecules." *Cellular Signalling* 20(8):1442–51.
- Fan, Gaofeng, Yongjun Fan, Nupur Gupta, Isao Matsuura, Fang Liu, Zhen Zhou Xiao, Ping Lu Kun, and Céline Gélinas. 2009. "Peptidyl-Prolyl Isomerase Pin1 Markedly Enhances the Oncogenic Activity of the Rel Proteins in the Nuclear Factor- $\kappa$ B Family." *Cancer Research* 69(11):4589–97.
- Feugier, Pierre, A. Van Hoof, C. Sebban, P. Solal-Celigny, R. Bouabdallah, C. Fermé, B. Christian, E. Lepage, H. Tilly, F. Morschhauser, P. Gaulard, G. Salles, A. Bosly, C. Gisselbrecht, F. Reyes, and B. Coiffier. 2005. "Long-Term Results of the R-CHOP Study in the Treatment of Elderly Patients with Diffuse Large B-Cell Lymphoma: A Study by the Groupe d'étude Des Lymphomes de l'adulte." *Journal of Clinical Oncology* 23(18):4117–26.
- Geismann, C., F. Grohmann, S. Sebens, G. Wirths, A. Dreher, R. Häslar, P. Rosenstiel, C. Hauser, J. H. Egberts, A. Trauzold, G. Schneider, B. Sipos, S. Zeissig, S. Schreiber, H. Schäfer, and A. Arlt. 2014. "C-Rel Is a Critical Mediator of NF- $\kappa$ B-Dependent TRAIL Resistance of Pancreatic Cancer Cells." *Cell Death and Disease* 5(10).
- Gilmore, T. D. 2006. "Introduction to NF- $\kappa$ B: Players, Pathways, Perspectives." *Oncogene* 25(51):6680–84.
- Gilmore, Thomas D., Catherine Cormier, Jean-Jacques Jims, and Maria-Emily Gapuzan. 2001. *Malignant Transformation of Primary Chicken Spleen Cells by Human Transcription Factor C-Rel*. *Oncogene* 20(48):7098-103.
- Gilmore, Thomas D., and Steve Gerondakis. 2011. "The C-Rel Transcription Factor in Development and Disease." *Genes and Cancer* 2(7):695–711.



- Hanson, Julie L., Noel A. Hawke, David Kashatus, and Albert S. Baldwin. 2004. *The Nuclear Factor B Subunits RelA/P65 and c-Rel Potentiate but Are Not Required for Ras-Induced Cellular Transformation. Cancer Res* 64(20):7248-55.
- Harrigan, Jeanine A., Xavier Jacq, Niall M. Martin, and Stephen P. Jackson. 2018. "Deubiquitylating Enzymes and Drug Discovery: Emerging Opportunities." *Nature Reviews Drug Discovery* 17(1):57–77.
- Harris, Jennifer, Stéphanie Olié, Sonia Sharma, Qiang Sun, Rongtuan Lin, John Hiscott, and Nathalie Grandvaux. 2006. "Nuclear Accumulation of c-Rel Following C-Terminal Phosphorylation by TBK1/IKKε." *The Journal of Immunology* 177(4):2527–35.
- Hayden, M. S., A. P. West, and S. Ghosh. 2006. "NF-κB and the Immune Response." *Oncogene* 25(51):6758–80.
- Hayden, Matthew S., and Sankar Ghosh. 2008. "Shared Principles in NF-κB Signaling." *Cell* 132(3):344–62.
- Hershko, Avram, and Aaron Ciechanover. 1998. "The ubiquitin system." *Annu Rev Biochem* 67:425-79.
- Hilton, Laura K., Jeffrey Tang, Susana Ben-Neriah, Miguel Alcaide, Aixiang Jiang, Bruno M. Grande, Christopher K. Rushton, Merrill Boyle, Barbara Meissner, David W. Scott, and Ryan D. Morin. 2019. "Brief Report LYMPHOID NEOPLASIA The Double-Hit Signature Identifies Double-Hit Diffuse Large B-Cell Lymphoma with Genetic Events Cryptic to FISH." *Blood* 134(18):1528-1532.
- Hunter, Jill E., Jack Leslie, and Neil D. Perkins. 2016. "C-Rel and Its Many Roles in Cancer: An Old Story with New Twists." *British Journal of Cancer* 114(1):1–6.
- Jaffe, Elaine S., Elias Campo, Stefano Pileri, Steven H. Swerdlow, Stefano A. Pileri, Nancy Lee Harris, Harald Stein, Reiner Siebert, Ranjana Advani, Michele Ghielmini, Gilles A. Salles, and Andrew D. Zelenetz. 2016. "The 2016 revision of the World Health Organization classification of lymphoid neoplasms." *Blood* 127(20):2375-90.
- Jaynes, Patrick William, Prasanna Vasudevan Iyengar, Sarah Kit Leng Lui, Tuan Zea Tan, Natali Vasilevski, Sarah Christine Elizabeth Wright, Giuseppe Verdile, Anand D. Jeyasekharan, and Pieter Johan Adam Eichhorn. 2020. "OTUD4 Enhances TGFβ Signalling through Regulation of the TGFβ Receptor Complex." *Scientific Reports* 10(1).
- Jiang, Yong Hui, Jan Bressler, and Arthur L. Beaudet. 2004. "Epigenetics and Human Disease." *Annual Review of Genomics and Human Genetics* 5:479–510.



- Jost, Philipp J., and Jürgen Ruland. 2007. "Aberrant NF- $\kappa$ B Signaling in Lymphoma: Mechanisms, Consequences, and Therapeutic Implications." *Blood* 109(7):2700–2707.
- Köntgen, Frank, Raelene J. Grumont, Andreas Strasser, Donald Metcalf, Ruili Li, David Tarlinton, and Steve Gerondakis. 1995. "Mice Lacking the C-Rel Proto-Oncogene Exhibit Defects in Lymphocyte Proliferation, Humoral Immunity, and Interleukin-2 Expression." *Genes Dev* 9(16):1965–77.
- Kennedy, Ruth, and Ulf Klein. 2018. "Aberrant Activation of NF- $\kappa$ B Signalling in Aggressive Lymphoid Malignancies." *Cells* 7(11):189.
- Kober-Hasslacher, Maike, Hyunju Oh-Strauß, Dilip Kumar, Valeria Soberon, Carina Diehl, Maciej Lech, Thomas Engleitner, Eslam Katab, Vanesa Fernández-Sáiz, Guido Piontek, Hongwei Li, Björn Menze, Christoph Ziegenhain, Wolfgang Enard, Roland Rad, Jan P. Böttcher, Hans Joachim Anders, Martina Rudelius, and Marc Schmidt-Supprian. 2020. "C-Rel Gain in B Cells Drives Germinal Center Reactions and Autoantibody Production." *Journal of Clinical Investigation* 130(6):3270–86.
- Kober-Hasslacher, Maike, Hyunju Oh-Strauß, Dilip Kumar, Valeria Soberon, Carina Diehl, Maciej Lech, Thomas Engleitner, Eslam Katab, Vanesa Fernández-Sáiz, Guido Piontek, Hongwei Li, Björn Menze, Christoph Ziegenhain, Wolfgang Enard, Roland Rad, Jan P. Böttcher, Hans Joachim Anders, Martina Rudelius, and Marc Schmidt-Supprian. 2020. "C-Rel Gain in B Cells Drives Germinal Center Reactions and Autoantibody Production." *Journal of Clinical Investigation* 130(6):3270–86.
- Kober-Hasslacher, Maike, and Marc Schmidt-Supprian. 2019. "The Unsolved Puzzle of C-Rel in B Cell Lymphoma." *Cancers* 11(7).
- Komander, David, Michael J. Clague, and Sylvie Urbé. 2009. "Breaking the Chains: Structure and Function of the Deubiquitinases." *Nature Reviews Molecular Cell Biology* 10(8):550–63.
- Komander, David, and Michael Rape. 2012. "The Ubiquitin Code." *Annual Review of Biochemistry* 81:203–29.
- Lai, Keng Po, Jian Chen, and William Ka Fai Tse. 2020. "Role of Deubiquitinases in Human Cancers: Potential Targeted Therapy." *International Journal of Molecular Sciences* 21(7).
- Lecker, Stewart H., Alfred L. Goldberg, and William E. Mitch. 2006. "Protein Degradation by the Ubiquitin-Proteasome Pathway in Normal and Disease States." *Journal of the American Society of Nephrology* 17(7):1807–19.



- Leeman, J. R., M. A. Weniger, T. F. Barth, and T. D. Gilmore. 2008. "Deletion Analysis and Alternative Splicing Define a Transactivation Inhibitory Domain in Human Oncoprotein REL." *Oncogene* 27(53):6770–81.
- Leeman, Joshua R., and Thomas D. Gilmore. 2008. "Alternative Splicing in the NF- $\kappa$ B Signaling Pathway." *Gene* 423(2):97–107.
- Leutert, Mario, Samuel W. Entwisle, and Judit Villén. 2021. "Decoding Post-Translational Modification Crosstalk with Proteomics." *Molecular and Cellular Proteomics* 20:100129.
- Liu, Yang, and Stefan Klaus Barta. 2019. "Diffuse Large B-Cell Lymphoma: 2019 Update on Diagnosis, Risk Stratification, and Treatment." *American Journal of Hematology* 94(5):604–16.
- Liuyu, Tianzi, Keying Yu, Liya Ye, Zhidong Zhang, Man Zhang, Yujie Ren, Zeng Cai, Qiyun Zhu, Dandan Lin, and Bo Zhong. 2019. "Induction of OTUD4 by Viral Infection Promotes Antiviral Responses through Deubiquitinating and Stabilizing MAVS." *Cell Research* 29(1):67–79.
- Mevisen, Tycho E. T., and David Komander. 2017. "Mechanisms of Deubiquitinase Specificity and Regulation." *Annu Rev Biochem* 86:159–192.
- Mevisen, Tycho E. T., Manuela K. Hospenthal, Paul P. Geurink, Paul R. Elliott, Masato Akutsu, Nadia Arnaudo, Reggy Ekkebus, Yogesh Kulathu, Tobias Wauer, Farid El Oualid, Stefan M. V. Freund, Huib Ovaa, and David Komander. 2013. "XOTU Deubiquitinases Reveal Mechanisms of Linkage Specificity and Enable Ubiquitin Chain Restriction Analysis." *Cell* 154(1):169.
- Meylan, Etienne, Alison L. Dooley, David M. Feldser, Lynn Shen, Erin Turk, Chensi Ouyang, and Tyler Jacks. 2009. "Requirement for NF- $\kappa$ B Signalling in a Mouse Model of Lung Adenocarcinoma." *Nature* 462(7269):104–7.
- Nagel, D., M. Vincendeau, A. C. Eitelhuber, and D. Krappmann. 2014. "Mechanisms and Consequences of Constitutive NF- $\kappa$ B Activation in B-Cell Lymphoid Malignancies." *Oncogene* 33(50):5655–65.
- Nguyen, Lan K., Walter Kolch, and Boris N. Kholodenko. 2013. "When Ubiquitination Meets Phosphorylation: A Systems Biology Perspective of EGFR/MAPK Signalling." *Cell Communication and Signaling* 11(1):1–15.
- Pinto-Fernández, Adán, Simon Davis, Abigail B. Schofield, Hannah C. Scott, Ping Zhang, Eidarus Salah, Sebastian Mathea, Philip D. Charles, Andreas Damianou, Gareth Bond, Roman Fischer, and Benedikt M. Kessler. 2019. "Comprehensive Landscape of Active Deubiquitinating Enzymes Profiled by Advanced Chemoproteomics." *Front Chem* 7:592.

- Popovic, Doris, Domagoj Vucic, and Ivan Dikic. 2014. "Ubiquitination in Disease Pathogenesis and Treatment." *Nature Medicine* 20(11):1242–53.
- Ramakrishnan, Parameswaran, Peter M. Clark, Daniel E. Mason, Eric C. Peters, Linda C. Hsieh-Wilson, and David Baltimore. 2013. "Activation of the Transcriptional Function of the NF- $\kappa$ B Protein c-Rel by O-GlcNAc Glycosylation." *Science Signaling* 6(290).
- Reyes-Turcu, Francisca E., Karen H. Ventii, and Keith D. Wilkinson. 2009. "Regulation and Cellular Roles of Ubiquitin-Specific Deubiquitinating Enzymes." *Annual Review of Biochemistry* 78:363–97.
- Rolland, Thomas, Murat Taşan, Benoit Charloteaux, Samuel J. Pevzner, Quan Zhong, Nidhi Sahni, Song Yi, Irma Lemmens, Celia Fontanillo, Roberto Mosca, Atanas Kamburov, Susan D. Ghiassian, Xiping Yang, Lila Ghamsari, Dawit Balcha, Bridget E. Begg, Pascal Braun, Marc Brehme, Martin P. Broly, Anne Ruxandra Carvunis, Dan Convery-Zupan, Roser Corominas, Jasmin Coulombe-Huntington, Elizabeth Dann, Matija Dreze, Amélie Dricot, Changyu Fan, Eric Franzosa, Fana Gebreab, Bryan J. Gutierrez, Madeleine F. Hardy, Mike Jin, Shuli Kang, Ruth Kiros, Guan Ning Lin, Katja Luck, Andrew Macwilliams, Jörg Menche, Ryan R. Murray, Alexandre Palagi, Matthew M. Poulin, Xavier Rambout, John Rasla, Patrick Reichert, Viviana Romero, Elien Ruysinck, Julie M. Sahalie, Annemarie Scholz, Akash A. Shah, Amitabh Sharma, Yun Shen, Kerstin Spirohn, Stanley Tam, Alexander O. Tejada, Shelly A. Trigg, Jean Claude Twizere, Kerwin Vega, Jennifer Walsh, Michael E. Cusick, Yu Xia, Albert László Barabási, Lilia M. Iakoucheva, Patrick Aloy, Javier De Las Rivas, Jan Tavernier, Michael A. Calderwood, David E. Hill, Tong Hao, Frederick P. Roth, and Marc Vidal. 2014. "A Proteome-Scale Map of the Human Interactome Network." *Cell* 159(5):1212–26.
- Roy, Koushik, Simon Mitchell, Yi Liu, Sho Ohta, Yu sheng Lin, Marie Oliver Metzgi, Stephen L. Nutt, and Alexander Hoffmann. 2019. "A Regulatory Circuit Controlling the Dynamics of NF $\kappa$ B CRel Transitions B Cells from Proliferation to Plasma Cell Differentiation." *Immunity* 50(3):616-628.e6.
- Sánchez-Valdepeñas, Carmen, Angel G. Martín, Parameswaran Ramakrishnan, David Wallach, and Manuel Fresno. 2006. "NF- $\kappa$ B-Inducing Kinase Is Involved in the Activation of the CD28 Responsive Element through Phosphorylation of c-Rel and Regulation of Its Transactivating Activity." *The Journal of Immunology* 176(8):4666–74.
- Schmitz, Roland, George W. Wright, Da Wei Huang, Calvin A. Johnson, James D. Phelan, James Q. Wang, Sandrine Roulland, Monica Kasbekar, Ryan M. Young, Arthur L. Shaffer, Daniel J. Hodson, Wenming Xiao, Xin Yu, Yandan Yang, Hong Zhao, Weihong Xu, Xuelu Liu, Bin Zhou, Wei Du, Wing C. Chan, Elaine S. Jaffe, Randy D. Gascoyne, Joseph M. Connors, Elias Campo, Armando Lopez-Guillermo, Andreas Rosenwald, German Ott, Jan Delabie, Lisa M. Rimsza, Kevin

- Tay Kuang Wei, Andrew D. Zelenetz, John P. Leonard, Nancy L. Bartlett, Bao Tran, Jyoti Shetty, Yongmei Zhao, Dan R. Soppet, Stefania Pittaluga, Wyndham H. Wilson, and Louis M. Staudt. 2018. "Genetics and Pathogenesis of Diffuse Large B-Cell Lymphoma." *New England Journal of Medicine* 378(15):1396–1407.
- Schneider C, Pasqualucci L, Dalla-Favera R. 2011. "Molecular pathogenesis of diffuse large B-cell lymphoma." *Semin Diagn Pathol* 28(2):167-77.
- Schubert, Alexander F., Justine V Nguyen, Tyler G. Franklin, Paul P. Geurink, Cameron G. Roberts, Daniel J. Sanderson, Lauren N. Miller, Huib Ovaa, Kay Hofmann, Jonathan N. Pruneda, and David Komander. 2020. "Identification and Characterization of Diverse OTU Deubiquitinases in Bacteria." *The EMBO Journal* 39(15).
- Sehn, Laurie H., and Gilles Salles. 2021. "Diffuse Large B-Cell Lymphoma" *New England Journal of Medicine* 384(9):842–58.
- Sen, Ranjan, and Stephen T. Smale. 2010. "Selectivity of the NF- $\kappa$ B Response." *Cold Spring Harbor Perspectives in Biology* 2(4).
- Smale, Stephen T. 2011. "Hierarchies of NF- $\kappa$ B Target-Gene Regulation." *Nature Immunology* 12(8):689–94.
- Susanibar-Adaniya, Sandra, and Stefan K. Barta. 2021. "2021 Update on Diffuse Large B Cell Lymphoma: A Review of Current Data and Potential Applications on Risk Stratification and Management." *American Journal of Hematology* 96(5):617–29.
- Swatek, Kirby N., and David Komander. 2016. "Ubiquitin Modifications." *Cell Research* 26(4):399–422.
- Tam, Winnie F., Weihong Wang, and Ranjan Sen. 2001. "Cell-Specific Association and Shuttling of I $\kappa$ B $\alpha$  Provides a Mechanism for Nuclear NF- $\kappa$ B in B Lymphocytes." *Molecular and Cellular Biology* 21(14):4837–46.
- Tang, Zefang, Chenwei Li, Boxi Kang, Ge Gao, Cheng Li, and Zemin Zhang. 2017. "GEPIA: A Web Server for Cancer and Normal Gene Expression Profiling and Interactive Analyses." *Nucleic Acids Research* 45(W1):W98–102.
- Tian, Wenzhi, and Hsiou Chi Liou. 2009. "RNAi-Mediated c-Rel Silencing Leads to Apoptosis of B Cell Tumor Cells and Suppresses Antigenic Immune Response in Vivo." *PLoS ONE* 4(4).
- Tse, William Ka Fai, Yun Jin Jiang, and Chris Kong Chu Wong. 2013. "Zebrafish Transforming Growth Factor- $\beta$ -Stimulated Clone 22 Domain 3 (TSC22D3) Plays Critical Roles in Bmp-Dependent Dorsoventral Patterning via Two Deubiquitylating Enzymes Usp15 and Otud4." *Biochimica et Biophysica Acta - General Subjects* 1830(10):4584–93.



- Walsh, Christopher T., Sylvie Garneau-Tsodikova, and Gregory J. Gatto. 2005. "Protein Posttranslational Modifications: The Chemistry of Proteome Diversifications." *Angewandte Chemie - International Edition* 44(45):7342–72.
- Wang, Yanfeng, and Feng Wang. 2021. "Post-Translational Modifications of Deubiquitinating Enzymes: Expanding the Ubiquitin Code." *Front Pharmacol.* 12:685011.
- Yang Y, Staudt LM. 2015. "Protein ubiquitination in lymphoid malignancies." *Immunol Rev.* 263(1):240-56.
- Young, Ryan M., James D. Phelan, Wyndham H. Wilson, and Louis M. Staudt. 2019. "Pathogenic B-Cell Receptor Signaling in Lymphoid Malignancies: New Insights to Improve Treatment." *Immunological Reviews* 291(1):190–213.
- Zhang, Qian, Michael J. Lenardo, and David Baltimore. 2017. "30 Years of NF- $\kappa$ B: A Blossoming of Relevance to Human Pathobiology." *Cell* 168(1–2):37–57.
- Zhao, Yu, Mona C. Majid, Jennifer M. Soll, Joshua R. Brickner, Sebastian Dango, and Nima Mosammaparast. 2015. "Noncanonical Regulation of Alkylation Damage Resistance by the OTUD 4 Deubiquitinase." *The EMBO Journal* 34(12):1687–1703.
- Zhao, Yu, Miranda C. Mudge, Jennifer M. Soll, Rachel B. Rodrigues, Andrea K. Byrum, Elizabeth A. Schwarzkopf, Tara R. Bradstreet, Steven P. Gygi, Brian T. Edelson, and Nima Mosammaparast. 2018. "OTUD4 Is a Phospho-Activated K63 Deubiquitinase That Regulates MyD88-Dependent Signaling." *Molecular Cell* 69(3):505-516.
- Vinuesa, Carola G., Īaki Sanz, and Matthew C. Cook. 2009. "Dysregulation of Germinal Centres in Autoimmune Disease." *Nature Reviews Immunology* 9(12):845–57.
- Anderson, Lesley A., Shahinaz Gadalla, Lindsay M. Morton, Ola Landgren, Ruth Pfeiffer, Joan L. Warren, Sonja I. Berndt, Winnie Ricker, Ruth Parsons, and Eric A. Engels. 2009. "Population-Based Study of Autoimmune Conditions and the Risk of Specific Lymphoid Malignancies." *International Journal of Cancer* 125(2):398–405.
- Coccaro, Nicoletta, Luisa Anelli, Antonella Zagaria, Tommasina Perrone, Giorgina Specchia, and Francesco Albano. 2020. "Molecular Complexity of Diffuse Large B-Cell Lymphoma: Can It Be a Roadmap for Precision Medicine?" *Cancers* 12(1).
- Campbell KJ, Rocha S, Perkins ND. 2004. "Active repression of antiapoptotic gene expression by RelA(p65) NF-kappa B." *Mol Cell* 13(6):853-65.



## 8 List of figures

Figure 1: Classification of DLBCL Subtypes .....	5
Figure 2: The enzymatic process of ubiquitination .....	13
Figure 3: Mass spectrometric analysis of c-REL interactome. ....	47
Figure 4: OTUD4 interaction with c-REL. ....	49
Figure 5: 5 c-REL is ubiquitinated in DLBCL.....	50
Figure 6: <i>OTUD4</i> depletion increases c-REL ubiquitination in DLBCL.....	51
Figure 7: OTUD4 regulates the proteasomal degradation of c-REL.....	53
Figure 8: OTUD4 deubiquitinates c-REL in the cytoplasm.....	54
Figure 9: c-REL stabilization by OTUD4 isoforms.....	56
Figure 10: OTUD4 stabilizes c-REL in DLBCL. ....	56
Figure 11: OTUD4 regulates the nuclear localization of c-REL in DLBCL .....	58
Figure 12: OTUD4 regulates c-REL nuclear localization in PDAC .....	59
Figure 13: OTUD4 modulates NF $\kappa$ B transcription activity. ....	60
Figure 14: Loss of OTUD4 compromises the expansion of cancer cells.. ....	62
Figure 15: OTUD4 expression correlates with c-REL in DLBCL. ....	63



## 9 Publications

Kober-Hasslacher, Maike, Hyunju Oh-Strauß, Dilip Kumar, Valeria Soberon, Carina Diehl, Maciej Lech, Thomas Engleitner, **Eslam Katab**, Vanesa Fernández-Sáiz, Guido Piontek, Hongwei Li, Björn Menze, Christoph Ziegenhain, Wolfgang Enard, Roland Rad, Jan P. Böttcher, Hans Joachim Anders, Martina Rudelius, and Marc Schmidt-Supprian. 2020. “C-Rel Gain in B Cells Drives Germinal Center Reactions and Autoantibody Production.” *Journal of Clinical Investigation* 130(6):3270–86.

**Eslam Katab**, Anushree Jai Kumar, Jana Zecha, Maike Kober-Hasslacher, Daniel Kovacs, Katja Steiger, Ritu Mishra, Wilko Weichert, Bernhard Kuster, Florian Bassermann, Marc Schmidt-Supprian and Vanesa Fernández-Sáiz. “OTUD4 regulates the NFκB transcription factor c-REL and the expansion of cancer cells.” Manuscript Submitted.\*

\* This publication is based on the results obtained in this dissertation.



## 10 Acknowledgement

I would like to thank Dr. Vanesa Fernández Sáiz for giving me the chance to work on this very interesting research project and for her trust and encouragement to develop my own ideas and experiment them. Thank you, Vanesa, for being a friendly supportive mentor.

I would deeply thank Prof. Marc Schmidt-Supprian for supervising me along the way and challenging me with thoughtful questions that help me to grow intellectually. Thank you, Marc, for helping me and granting me access to your lab resources.

I would also thank Prof. Gabriele Multhoff for being my second supervisor and for discussing my progress at an annual meeting.

An extended thank you to Prof. Florian Bassermann for allowing me to use his lab facilities and resources and for the help I got from all his research group.

Thank you so much for our collaborators who kindly helped a lot with different experiments and recommendations.

I would deeply thank Prof. Josef Mautner for his tremendous support scientifically and psychologically. Thank you, so much dearest chief, for your kindness and the indispensable advice you gave me throughout the whole journey.

Thank you, Dinesh Adhikary, for being a faithful friend and always being there for me, especially during the tough times.

Last, but not least I am very grateful and beyond thankful for my dear family. Reem, my beloved wife, without your presence I would never be able to finish this thesis. Your love and support can't be described in words, no wonder you are my biggest blessing in life. Dad and Mom, since being a small kid, your incredible support is the cornerstone of everything I have achieved. Thank you so much for believing in me and I am and will be always indebted for your unconditional love and non-ending care. Thank you, Ahmed and Alaa, my lovely brother and sister, for care, support and your love. I wish I could make you proud.